

Lorentz Symmetry Breaking in a Cosmological Context

Thesis by

Moira I. Gresham

In Partial Fulfillment of the Requirements
for the Degree of
Doctor of Philosophy



California Institute of Technology
Pasadena, California

2010

(Defended May 6, 2010)

© 2010

Maira I. Gresham

All Rights Reserved

Acknowledgments

This thesis would not exist were it not for my collaborators Sean Carroll, Heywood Tam, Mark Wise, and Tim Dulaney. I especially thank Tim Dulaney for keeping me on task, for reading drafts of this thesis and of job applications, and for countless honest and productive conversations about physics; we have worked well together.

My adviser, Mark Wise, and my unofficial coadviser, Sean Carroll, have been great academic role models, mentors, advisers, and supporters. I feel very lucky to have had the opportunity to work with them both; through observing and working with them I have learned how to do physics.

I also learned a great deal in my time at Caltech through conversations with other excellent scientists in the Wise and Carroll research groups—especially Matt Johnson, Matt Buckley, and my former office-mates Lotty Ackermann and Mike Salem.

My first physics teacher, Jeff Butler of Cheney High School, and the Reed College physics and mathematics departments prepared me well for graduate studies in physics. I am especially grateful to have learned from and worked with David Griffiths, who is a model teacher and adviser. I am also grateful to the Churchill Foundation of the US for jump-starting my graduate career by sending me to Cambridge to study theoretical physics in Part III of the Mathematical Tripos.

My graduate work at Caltech was supported by a National Defense Science and Engineering Graduate fellowship and a National Science Foundation graduate research fellowship, as well as the DOE grant that supports the Wise research group.

On a more personal level, I am ever thankful for the seemingly unconditional love and support of my parents, Jim and Susanne and to my sister, Miranda, for tremendous moral support and for reminding me that I can do it. Finally, I thank my

best friend and life partner, Tim Doyle. In addition to his unwavering moral support, I am thankful for his enthusiasm for and honest critiques of my work throughout my graduate career.

Abstract

This thesis is comprised primarily of work from three independent papers, [1], [2], and [3], written in collaboration with Sean Carroll, Tim Dulaney, and Heywood Tam. The original motivation for the projects undertaken came from revisiting the standard assumption of spatial isotropy during inflation. Each project relates to the spontaneous breaking of Lorentz symmetry—in early Universe cosmology or in the context of effective field theory, in general. Chapter 1 is an introductory chapter that provides context for the thesis. Chapter 2 is an investigation of the stability of theories in which Lorentz invariance is spontaneously broken by fixed-norm vector “æther” fields. It is shown that models with generic kinetic terms are plagued either by ghosts or by tachyons, and are therefore physically unacceptable. Chapter 3 is an investigation of the phenomenological properties of the one low-energy effective theory of spontaneous Lorentz symmetry breaking found in the previous chapter to have a globally bounded Hamiltonian and a perturbatively stable vacuum—the theory in which the Lagrangian takes the form of a sigma model. In chapter 4 cosmological perturbations in a dynamical theory of inflation in which an Abelian gauge field couples directly to the inflaton are examined. The dominant effects of a small, persistent anisotropy on the primordial gravitational wave and curvature perturbation power spectra are found using the “in-in” formalism of perturbation theory. It is found that the primordial power spectra of cosmological perturbations gain significant direction dependence and that the fractional direction dependence of the tensor power spectrum is suppressed in comparison to that of the scalar power spectrum.

Contents

Acknowledgments	iii
Abstract	v
1 Introduction	1
1.1 The Big Picture	1
1.2 How This Thesis Emerged	6
1.3 Synopsis	7
1.4 CMB Temperature Correlations	8
1.5 From Primordial Perturbations to CMB Temperature Correlations . .	11
1.6 The Cosmic No-Hair Theorem	15
1.7 Æther	16
1.8 Hairy Inflation	17
1.9 Standard Slow-Roll Inflation	18
1.9.1 Background Equations	18
1.9.2 Perturbations from Single-Field Slow-Roll Inflation	21
2 Instabilities in the Æther	29
2.1 Introduction	29
2.2 Models	35
2.2.1 Validity of Effective Field Theory	38
2.3 Boundedness of the Hamiltonian	40
2.3.1 Timelike Vector Field	44
2.3.2 Spacelike Vector Field	46

2.3.3	Smooth Potential	47
2.3.4	Discussion	49
2.4	Linear Instabilities	50
2.4.1	Timelike Vector Field	51
2.4.2	Spacelike Vector Field	53
2.4.3	Stability is Not Frame Dependent	55
2.5	Negative Energy Modes	55
2.5.1	Spin-1 Energies	57
2.5.2	Spin-0 Energies	59
2.6	Maxwell and Scalar Theories	60
2.6.1	Maxwell Action	62
2.6.2	Scalar Action	65
2.7	Conclusions	67
2.A	Appendix: Solutions to the Linearized Equations of Motion	69
3	Sigma-Model Æther	74
3.1	Introduction	75
3.2	Excitations in the Presence of Gravity	77
3.3	Experimental Constraints	82
3.4	Cosmological Evolution	83
3.5	Extra Dimensions	85
3.6	Conclusions	87
4	Primordial Perturbations from Anisotropic Inflation	89
4.1	Introduction	89
4.2	Model and Background Solution	94
4.3	Perturbations: Setup and Strategy	101
4.3.1	Physical Scenario	102
4.3.2	Correlations Using “in-in” Formalism	103
4.3.3	Decomposition of Perturbations	104
4.3.4	Canonically Normalized Variables	105

4.3.5	Comparison with Data	106
4.4	Perturbations: Odd Sector	107
4.4.1	Preliminary Look at Stability	108
4.4.2	Diagonalized Action	110
4.4.3	Correlations Using Perturbation Theory	111
4.4.4	Discussion	116
4.5	Perturbations: Even Sector	118
4.5.1	Diagonalizing the Action	122
4.5.2	Correlations Using Perturbation Theory	123
4.6	Conclusions	128
4.A	Appendix: Parametrization of Perturbations	129
4.B	Appendix: Quadratic Action and Einstein's Equations	133
4.C	Appendix: Diagonalizing a Kinetic Term	135
4.D	Appendix: Estimates of Integrals	136
	Bibliography	139

List of Figures

1.1	Cosmological evolution timeline.	2
1.2	WMAP 7-year full-sky map of the cosmic microwave background. . . .	8
1.3	Spectrum of CMB multipole coefficients from 7-year WMAP data. . .	9
2.1	Hamiltonian density as a function of Goldstone field values	45
3.1	Æther rest frame mode phase velocities	79
3.2	Sigma-model æther Parameter space allowed by constraints from Čerenkov radiation and PPN	83
4.1	Log plot of anisotropy parameter as a function of e -foldings	100
4.2	Plot of primordial perturbation correlation integrand as a function of e -foldings	138

Chapter 1

Introduction

This thesis is comprised primarily of work from three independent papers, written in collaboration with Sean Carroll, Tim Dulaney, and Heywood Tam. The original motivation for the projects undertaken came from revisiting the standard assumption of spatial isotropy during inflation. Each project relates to the spontaneous breaking of Lorentz symmetry—in early Universe cosmology or in the context of effective field theory, in general. Here I motivate and introduce the three projects, presented in chapters 2, 3, and 4. At the end of this chapter I provide some more technical background that helps to contextualize the subsequent chapters.

1.1 The Big Picture

I like the way that physics tries to answer big questions. For example particle physicists answer “What are we made of?” by searching for the elementary constituents of matter and for mathematical structure within which these constituents and their interactions can be understood. Cosmologists approach “Where are we?” and “How did we come to be?” by using modern physics theory, astrophysical observations, logic, and intuition to construct a plausible and consistent picture of the Universe and its evolution.¹ The work in this thesis grew from thinking about what might have occurred very early on in our Universe’s history.

¹Recently, even the situation of our Universe within a hypothetical larger set of universes has been a topic of research.

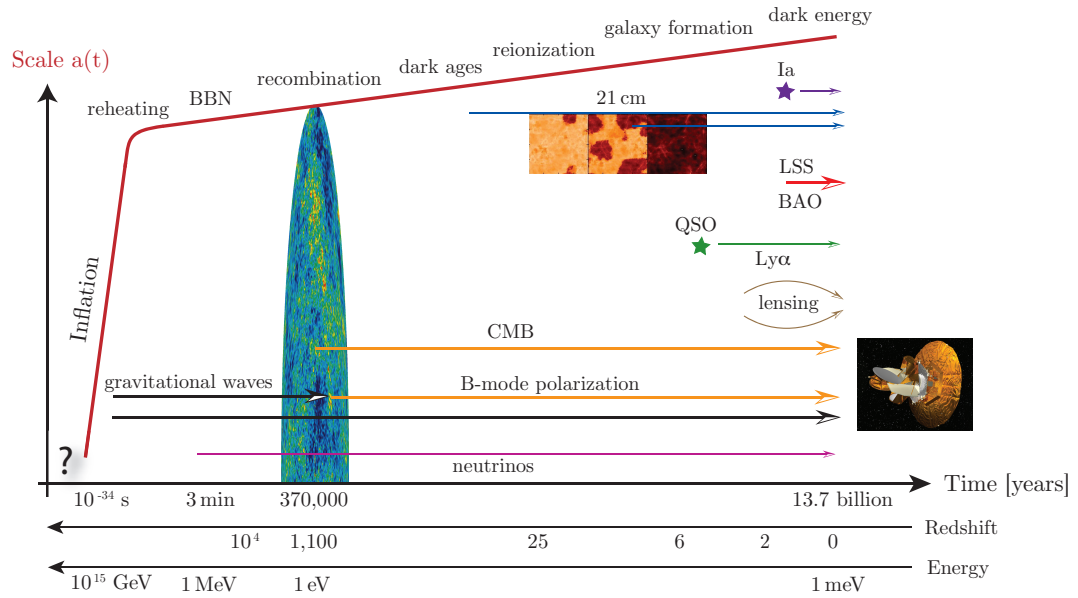


Figure 1.1: Image taken with permission from [4]. History of the Universe, including key events in the history of our Universe and some of the observable objects/features that have or could in principle provide(d) us with information about its evolution. *Acronyms:* BBN (Big Bang Nucleosynthesis), LSS (Large-Scale Structure), BAO (Baryon Acoustic Oscillations), QSO (Quasi-Stellar Objects; Quasars), $\text{Ly}\alpha$ (Lyman-alpha), CMB (Cosmic Microwave Background), Ia (Type Ia supernovae), 21 cm (hydrogen 21 cm-transition).

We already have a remarkably consistent and detailed picture and history of our Universe. A cartoon of this history is provided in Fig 1.1. In particular, it has been established that the Universe has been expanding (at various rates, indicated by the slope of the solid red line in Fig 1.1) for the entire traceable history of our Universe—about 14 billion years. In particular, we are quite confident that the Universe began² in a very hot, dense state. The name for this beginning is “the Big Bang”. We don’t really know how the Big Bang occurred, or what happened in the primordial era just after the Big Bang.

Returning to the cartoon history of our Universe, the vertical axis in Fig. 1.1 is the scale factor, which characterizes the expansion of the Universe. The horizontal axis is time—or equivalently decreasing temperature³ or decreasing redshift of light in the Universe; the Universe cools and the wavelength of light gets stretched (*i.e.*, light is redshifted⁴) as it expands. The labeled arrows indicate signals from the past that we might observe at earth today. For example, observations of light from distant type Ia supernovae have provided an important measure of the local expansion rate of the Universe.

For the purposes of motivating the work in this thesis, the important thing to notice in Fig. 1.1 is that one of the longest arrows comes from the Cosmic Microwave Background (CMB). CMB radiation is light that last scattered off of a plasma of photons, electrons, and protons when the Universe was at a temperature of about 1 eV; at this temperature almost all free electrons and protons combined into neutral hydrogen. This point in history is known as *recombination* (electrons and protons recombined into neutral hydrogen), and the place from which the CMB photons reach-

²“Began” might be a controversial word to use here. It could be that the Universe collapsed into a very hot, dense, state and then began expanding again, or the hot dense state may have been born from a parent universe.

³Temperature (T) is related to energy (E) by

$$T = E/k_B, \quad k_B = 8.62 \times 10^{-5} \frac{\text{eV}}{\text{K}}, \quad (1.1)$$

where k_B is Boltzmann’s constant, K is Kelvin and eV is electron-Volts.

⁴In the visual spectrum, red light has longer wavelength than green light, which has longer wavelength than blue light. Thus the name “redshifting” for light with longer wavelength and “blueshifting” for light with shorter wavelength.

ing us today came is known as the *surface of last scattering*.^{5,6} Before recombination the Universe was effectively opaque—filled with a plasma of electrons, protons, and photons, all scattering off of each other frequently. When the collision rates slowed down enough⁷ so that electrons and protons could combine into neutral hydrogen (“recombination”), the Universe became effectively transparent; light could free-stream without colliding much with other particles. So the farthest back we can effectively see is the distance that light has traveled from the time of recombination.

Arrows that reach farther back than the CMB arrow in Fig. 1.1 are from primordial gravitational waves or neutrinos; gravitons and neutrinos decoupled from the primordial plasma earlier than photons and so have been free-streaming for longer. We think that gravitational wave and neutrino backgrounds analogous to the CMB exist and we hope to eventually observe them (or “observe” their nonexistence), but we haven’t yet because our instruments are not sensitive enough. Thus the CMB is currently our best window to the very early Universe.⁸ The Wilkinson Microwave Anisotropy Probe (WMAP) is pictured at the end of the CMB arrow in Fig. 1.1. That is because WMAP has served as our eyes looking on the CMB window. As will be discussed in subsequent sections, WMAP has taken very high resolution pictures of the CMB that have moved us into an age of precision (early) cosmology. The Planck satellite is currently taking even higher resolution pictures of the CMB and should advance early Universe cosmology even further.

The spectrum of CMB photons is thermal, and very nearly uniform across the

⁵Though the CMB radiation last scattered throughout 3-dimensional space at roughly the same time, from our vantage point on earth we see a bubble of radiation—a 2-dimensional surface. The photons at that surface formed another surface back when they last scattered long ago.

⁶Think about the sky on a cloudy day. The light reaching our eyes from the sky last scattered off of water molecules forming the clouds in the atmosphere. We can’t see past the clouds because even though much of the light we’re seeing made its way from the sun through a jagged path within the clouds and out the other side, the light’s characteristics changed substantially during all of the collisions it had within the cloud, and what we see is light with those characteristics—not the characteristics of direct sunlight. The CMB light is analogous to light that last scattered off of the clouds.

⁷Due to expansion the plasma became less dense, hence less collisions per time.

⁸Figuring out what happened in the very early Universe is not only interesting as an answer to the “Where did we come from?” question, but physics at very high energy scales played an important role at this time, so we could also learn more about high energy physics by looking this far back in cosmic history.

entire sky. That CMB radiation is thermal is a profound fact; it seems to imply that the region from which CMB photons came at recombination must have been in thermal equilibrium; in particular the photons must have been in causal contact.⁹ The thermal spectrum and near uniformity of the CMB, along with its nearly scale-invariant spectrum¹⁰ of deviations from uniformity have led many to believe that the Universe must have undergone a period of rapid expansion during the first moments after the Big Bang. Without such a period of rapid expansion or some other nonstandard sequence of events, the uniformity of the CMB appears to be an extraordinary accident. If we trace back the evolution of the Universe assuming that just the kind of matter we observe today to dominate the energy density of the Universe determined the dynamics of our Universe's expansion, then the expansion of the Universe would have always been decelerating and CMB photons separated by about a degree on the sky or more couldn't have been in causal contact before or after the time of last scattering. So photons across the entire sky could not have reached thermal equilibrium, which means the uniform, thermal spectrum across the entire sky would be an extremely unlikely coincidence. This is known as the Horizon Problem. A period of accelerating expansion of the Universe could have allowed the CMB photons on our sky to reach thermal equilibrium before the time of last scattering and, in this sense, solves the Horizon Problem [5]. Such a period of accelerating expansion in the early Universe is known as *inflation*.

I, like many (including the authors of Fig. 1.1), find inflation to be compelling. As I'll touch on later in this introduction, not only does inflation solve the Horizon Problem, but it also provides an explanation of the small, nearly scale-invariant energy density anisotropies that seeded structure formation in the Universe and can account for the pattern of small temperature variation across the CMB sky. But until we develop technology good enough to measure, for example, primordial gravitational waves or neutrinos, the best evidence we have that inflation did or did not occur is our measurement of the CMB. It's *indirect* evidence.

⁹Photons come into equilibrium by interacting with each other. If they were never in causal contact, then they couldn't have interacted and thus couldn't have reached equilibrium.

¹⁰I'll discuss what's meant by "scale-invariant spectrum" in §1.9.2.

Cosmologists must often make do with indirect evidence due to the very nature of cosmology. Unlike physicists who are trying to uncover the laws of nature in our neighborhood, cosmologists cannot design and repeat experiments that in effect recreate events that we expect to occur. For example, particle physicists have the luxury of building big machines that smash particles together and then measuring what comes out in order to test whether Higgs bosons exist. Cosmologists do not have the luxury of recreating the Big Bang and then measuring what happens subsequently. On the other hand, in some sense both particle physicists and cosmologists run into the same basic problem; it's technologically impossible (whether in principle or just given practical constraints) to test certain theories directly. We must then get creative and clever; we must come up with theories that subsume experimentally verified theories and find ways to test such new theories indirectly, given our technological capabilities. Speculation is inevitably part of the creative process by which advancements in such cases are made.

Indeed, a problem that remains even if we're right that inflation did occur is *how* it occurred. By what mechanism did the Universe inflate?¹¹ It's productive to speculate about the multitude of theoretical mechanisms of inflation and then try to figure out ways to find astrophysical signatures (*e.g.*, signatures on the CMB) that support or rule out such mechanisms. It was out of this kind of creative process—speculating about the primordial Universe and how we might see its features through the window of the CMB—that this thesis emerged.

1.2 How This Thesis Emerged

The motivation for the work in this thesis came from the possibility that rotational symmetry (*i.e.*, isotropy) was broken during inflation. There are several reasons why this possibility had not been seriously considered until recently:

- We observe isotropy to be a very nearly exact local symmetry today. (Local

¹¹Remember: I mentioned above that ordinary matter (the kind of matter that we know is fueling the expansion of the Universe today) cannot give rise to inflation.

isotropy leads to conservation of angular momentum, for example, and allows for the classification of particles by their spin.)

- The CMB, at least at a glance, appears to be very nearly statistically isotropic. (More on this in §1.4.)
- Under straightforward assumptions about the nature of the fields involved during an inflationary epoch, statistical isotropy of the CMB and of the Universe on large scales is a consequence of inflation. (More on this in §1.6.)

But we should keep an open mind. Slightly anisotropic inflation is an interesting possibility. A generic signature of slight anisotropy during inflation on the CMB was postulated and studied in [6]. The work in this thesis emerged after thinking about particular models of inflation that could yield an anisotropic inflationary scenario leading to the generic signature put forth in [6].

1.3 Synopsis

Chapters 2 and 3 address stability issues in a popular class of models that give rise to the breaking of Lorentz Symmetry: *æther* models. Here, “æther” refers to a dynamical fixed-norm vector field. Spatial rotations being a subgroup of the Lorentz group, in particular *æther* models can give rise to the breaking of rotational invariance. The project out of which chapter 2 emerged transformed into one very different from the project we originally set out to do. From a study of the evolution of *æther* fields in an expanding Universe, we were eventually led to study more generally the effective field theory of spontaneously broken Lorentz symmetry in flat space. In the course of the original project, we found obstructions to the smooth evolution of initial data, and later realized that this was a symptom of much more general problems in these theories. Chapter 3 is a study of the one *æther* theory that we found to be well behaved. Chapter 2 is also interesting from a perspective independent of cosmology; it brings together three of the most powerful concepts in modern theoretical physics: gauge symmetries, spontaneous symmetry breaking, and effective field theory. In a

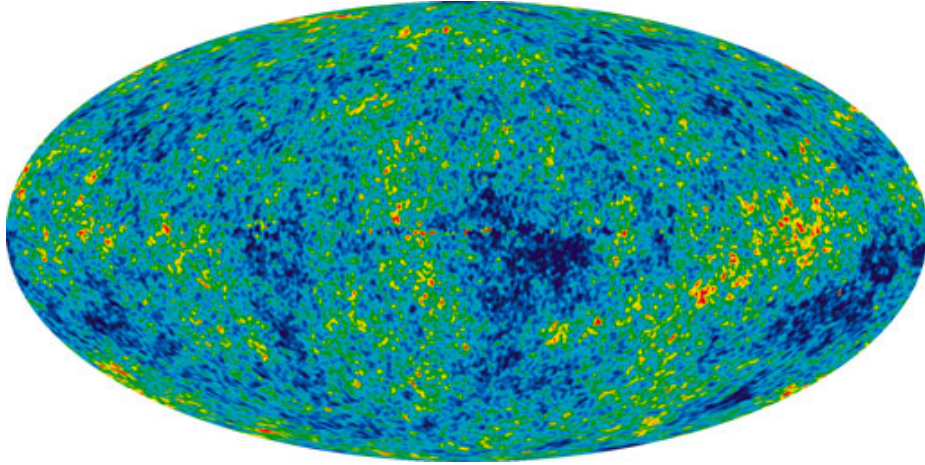


Figure 1.2: WMAP 7-year full-sky Mollweide projection map of the cosmic microwave background. WMAP measures temperature differences across the sky. The colors represent temperatures according to a linear scale, ranging from $-200 \mu\text{K}$ to $+200 \mu\text{K}$. The root mean square variation is on the order of tens of μK . From independent measurements, we know that the average temperature of the CMB is 2.725 K . That means the temperature across the entire sky varies, roughly speaking, by only about one part in 100,000. Credit: WMAP Science Team.

few words, usually we talk about *internal* symmetries being spontaneously broken; but what happens in theories in which *space-time* symmetry is spontaneously broken?

Chapter 4 is a study of a model that can give rise to anisotropy during inflation through a mechanism very different than that of æther theories. The model, first set forth in the context of anisotropic inflation in [7], is built on standard single field inflation, but includes a nonstandard coupling of the inflaton field to a $U(1)$ gauge field. We study the stability of the model and also (more importantly) the spectra of cosmological perturbations in the theory.

In the remainder of this chapter I shall review more carefully some more technical background needed to contextualize chapters 2, 3, and 4—especially chapter 4.

1.4 CMB Temperature Correlations

As mentioned in §1.1, the Cosmic Microwave Background (CMB) is light that has been more-or-less free-streaming toward us since the time at which the Universe had cooled (through expansion) to a temperature at which hydrogen ions and electrons

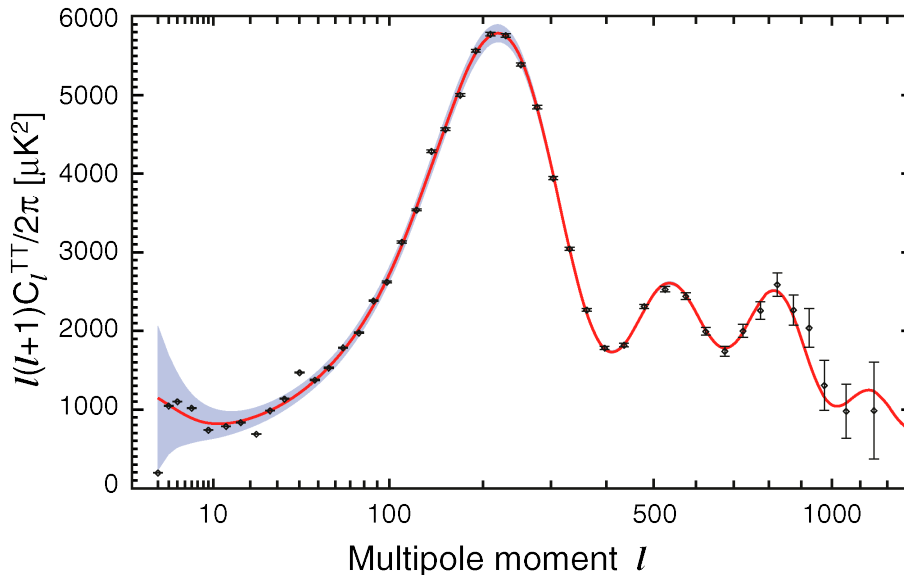


Figure 1.3: Spectrum of CMB multipole coefficients from 7-year WMAP data. (The C_l s plotted here are multiplied by \bar{T}^2 as compared to the definition in (1.6), *i.e.*, these are the temperature difference multipole moments, not the *fractional* temperature difference multipole moments.) Credit: WMAP Science Team.

recombined to form neutral hydrogen—about 370,000 years (about 10^{-5} times the age of the Universe) after the Big Bang. The CMB radiation has a very nearly uniform temperature across the sky, but there are small variations. See Fig. 1.2. A systematic way to look for patterns of those variations is to compute correlations between various points on the map of temperature differences that we’ve measured across the entire sky.¹²

It’s convenient to decompose the fractional temperature difference as a function of position on the sky, \hat{e} (where $\hat{e} \cdot \hat{e} = 1$), into spherical harmonics:

$$\frac{T(\hat{e}) - \bar{T}}{\bar{T}} = \frac{\Delta T(\hat{e})}{\bar{T}} = \sum_{l=0}^{\infty} \sum_{m=-l}^l a_{lm} Y_l^m(\hat{e}), \quad (1.2)$$

where \bar{T} is the average temperature of the CMB, and the spherical harmonic functions

¹²I primarily consulted [8] and [9] while writing the following two sections.

are normalized such that

$$\int d\hat{e} Y_{l'}^{m'*}(\hat{e}) Y_l^m(\hat{e}) = \frac{4\pi}{2l+1} \delta_{ll'} \delta_{mm'}. \quad (1.3)$$

In principle, the temperature difference depends not only on a direction in the sky, but also on the vantage point from which the measurement is made (in our case, the Earth). In other words, the a_{lm} s are implicitly functions of vantage point, \vec{x} . On the other hand, based on the Copernican principle we'd expect a given correlation function averaged across directions on the sky to be approximately equal to the same function averaged over different vantage points, but for a fixed direction. An averaging over vantage points is known as a *cosmic mean*. And the difference between a local measurement and the cosmic mean is known as *cosmic variance*. We can make generic predictions from inflation only for cosmic means. Thus, since our measurements are necessarily local, we're always limited by cosmic variance.

We expect the distribution of temperature perturbations to be random, but with a certain distribution. For example, if the distribution is Gaussian, then the pattern of fluctuations on the sky should be completely characterized by the two-point function,

$$\left\langle \frac{\Delta T(\hat{e}_1)}{\bar{T}} \frac{\Delta T(\hat{e}_2)}{\bar{T}} \right\rangle, \quad (1.4)$$

where $\langle \dots \rangle$ denotes the cosmic mean. If the distribution is non-Gaussian, then higher order correlation functions are needed to completely characterize the pattern of fluctuations.

The covariance of the two-point temperature correlation is defined as follows,

$$\begin{aligned} C_{ll',mm'} &\equiv \langle a_{l'm'}^* a_{lm} \rangle \\ &= \left(\frac{2l+1}{4\pi} \right) \left(\frac{2l'+1}{4\pi} \right) \int d\hat{e} d\hat{e}' Y_l^{m*}(\hat{e}) Y_{l'}^{m'}(\hat{e}') \left\langle \frac{\Delta T(\hat{e})}{\bar{T}} \frac{\Delta T(\hat{e}')}{\bar{T}} \right\rangle. \end{aligned} \quad (1.5)$$

In practice, we cannot measure the cosmic mean; the “covariance” we measure doesn't

have $\langle \dots \rangle$. However, for a statistically isotropic and homogeneous Universe,

$$C_{ll',mm'} = \delta_{mm'} \delta_{ll'} C_l \quad (1.6)$$

where the C_l are known as multipole moments. If the temperature variation is governed by a Gaussian distribution, then an observed C_l^{obs} is the average over $2l + 1$ independent a_{lm} s, squared, and it can be shown that the cosmic variance for a given C_l^{obs} is

$$\left\langle \left(\frac{C_l^{obs} - C_l}{C_l} \right)^2 \right\rangle = \frac{2}{2l + 1}. \quad (1.7)$$

The dipole moment, C_1 , for example, has a variance of 67%. This fact, and complications having to do with Earth's motion around the sun make any predictions we might have for the cosmic mean dipole moment practically incomparable with experiment.

The observed multipole moments (normalized by $l(l + 1)/2\pi$) as measured by WMAP are plotted in Fig. 1.3. From the detailed shape of the spectrum of multipole moments, cosmologists have been able to extract some of the most precise values for cosmological parameters to date—such as the Hubble rate, the age of the Universe, the curvature of space, the percent energy density in the Universe from dark matter, baryons, and dark energy, etc. One can read how such parameters are extracted in texts such as [9] or [8]. In the next section we'll get a feel for how the spectrum of energy density fluctuations before the surface of last scattering is ultimately related to the CMB spectrum.

1.5 From Primordial Perturbations to CMB Temperature Correlations

Inflation not only explains how our current horizon volume might have been in causal contact in our past, but it can also provide an explanation for the pattern of temperature fluctuations that we observe in the CMB. The key is that energy density fluctuations generated during inflation give rise to temperature fluctuations on the

CMB today because of effects such as, for instance, what's known as the Sachs-Wolfe effect: the relative redshifting of photons that emerge from regions with higher energy density compared to their neighbors. To trace the evolution of photons from the primordial era—the end of inflation for our purposes—given just the energy density perturbation spectrum at that time to the surface of last scattering, and then through time and space until they're reaching us today is a somewhat complicated task, but suffice it to say that given a spectrum of energy density perturbations at the end of inflation a pattern of temperature variations on the CMB sky can be predicted given established nuclear physics, thermodynamics, scattering theory, and general relativity. The remarkable thing is that a particular form of the energy density spectrum is *predicted* at the end of inflation, and this form of the energy density spectrum indeed leads to a CMB temperature power spectrum that matches well with the one we measure!

More specifically, the fractional deviation from the mean temperature of the CMB in a particular direction, \hat{e} , on the sky is given by

$$\frac{T(\hat{e}) - \bar{T}}{\bar{T}} = \frac{\Delta T(\hat{e})}{\bar{T}} = \int d\vec{k} \sum_l \left(\frac{2l+1}{4\pi} \right) (-i)^l \delta_\varepsilon(\vec{k}) P_l(\hat{k} \cdot \hat{e}) \Theta_l(k), \quad (1.8)$$

where $\delta_\varepsilon(\vec{k})$ is the Fourier transform of the primordial energy density perturbation, $(\varepsilon(\vec{x}) - \varepsilon_0)/\varepsilon_0$, P_l is a Legendre polynomial, $k \equiv \sqrt{\vec{k} \cdot \vec{k}}$, and Θ_l is a function assumed to be governed by statistically isotropic physics that characterizes the evolution of photons from the primordial era until today. For example, the part of Θ_l due to the Sachs-Wolfe effect is proportional to the spherical Bessel function, $j_l(kr_L)$, where r_L is the radial coordinate of the surface of last scattering. It turns out that for small l the Sachs-Wolfe effect is the dominant effect. For larger l , the important parts of Θ_l are more complicated and, for example, account for the dynamics of the photon-nucleon-electron plasma before recombination.

The covariance given this form of $\Delta T/\bar{T}$ can be seen to be

$$\begin{aligned}
C_{ll',mm'} &= \frac{(2l'+1)(2l+1)}{(4\pi)^2} \int d\vec{k}d\vec{k}' \sum_{l_1} \sum_{l_2} \frac{(2l_1+1)(2l_2+1)}{(4\pi)^2} (-i)^{l_1+l_2} \Theta_{l_1}(k) \Theta_{l_2}(k') \\
&\quad \times \langle \delta_\varepsilon(\vec{k}) \delta_\varepsilon(\vec{k}') \rangle \int d\hat{e}d\hat{e}' Y_l^{m*}(\hat{e}) Y_{l'}^{m'}(\hat{e}') P_{l_1}(\hat{k} \cdot \hat{e}) P_{l_2}(\hat{k}' \cdot \hat{e}') \\
&= \int d\vec{k}d\vec{k}' (-i)^{l+l'} \Theta_l(k) \Theta_{l'}(k') \langle \delta_\varepsilon(\vec{k}) \delta_\varepsilon(\vec{k}') \rangle Y_l^{m*}(\hat{k}) Y_{l'}^{m'}(\hat{k}'), \quad (1.9)
\end{aligned}$$

where we've used the identities,

$$P_l(\hat{e}_1 \cdot \hat{e}_2) = \frac{4\pi}{2l+1} \sum_{m=-l}^l Y_l^m(\hat{e}_1) Y_l^{m*}(\hat{e}_2), \quad (1.10)$$

and (1.3) in the last line. Again, here $\langle \dots \rangle$ denotes the cosmic mean. In concert with the ergodic theorem,¹³ inflation gives us a prediction for $\langle \delta_\varepsilon(\vec{k}) \delta_\varepsilon(\vec{k}') \rangle$. In inflation, we calculate $\langle \delta_\varepsilon(\vec{x}) \delta_\varepsilon(\vec{y}) \rangle$ interpreting $\langle \dots \rangle$ as a quantum average—an average over histories. Then the ergodic theorem says that averaging over histories should give the same result as a cosmic average—an average over vantage points.

Now if $\langle \delta_\varepsilon(\vec{x}) \delta_\varepsilon(\vec{y}) \rangle$ is translationally invariant it must depend only on $\vec{x} - \vec{y}$. In that case

$$\begin{aligned}
\langle \delta_\varepsilon(\vec{k}) \delta_\varepsilon(\vec{k}') \rangle &= \int d\vec{x} \int d\vec{y} f(\vec{x} - \vec{y}) e^{i(\vec{x} \cdot \vec{k} + \vec{y} \cdot \vec{k}')} \\
&= \int d\vec{x}_+ e^{i\vec{x}_+ \cdot (\vec{k} + \vec{k}')} \int d\vec{x}_- f(\vec{x}_-) e^{i\vec{x}_- \cdot (\vec{k} - \vec{k}')} \\
&= (2\pi)^3 \delta^{(3)}(\vec{k} + \vec{k}') \int d\vec{x}_- f(\vec{x}_-) e^{i\vec{x}_- \cdot (\vec{k} - \vec{k}')} \\
&\equiv (2\pi)^3 \delta^{(3)}(\vec{k} + \vec{k}') P(\vec{k}). \quad (1.11)
\end{aligned}$$

Here we've defined the power spectrum, $P(\vec{k})$. Plugging (1.11) back into (1.9) we find

$$C_{ll',mm'} = \int d\vec{k} (-i)^{l+l'} \Theta_l(k) \Theta_{l'}(k) (2\pi)^3 P(\vec{k}) Y_l^{m*}(\hat{k}) Y_{l'}^{m'}(\hat{k}), \quad (1.12)$$

¹³See, *e.g.*, Appendix D in [9].

where we've used the fact that $Y_l^m(-\hat{e}) = (-1)^l Y_l^m(\hat{e})$. If the power spectrum is rotationally invariant, then $P(\vec{k}) = P(k)$ and we recover (1.6):

$$\begin{aligned} C_{ll',mm'} &= \int dk (-i)^{l-l'} \Theta_l(k) \Theta_{l'}(k) (2\pi)^3 P(k) \int d\hat{k} Y_l^{m*}(\hat{k}) Y_{l'}^{m'}(\hat{k}) \\ &= \delta_{ll'} \delta_{mm'} \left(\frac{4\pi}{2l+1} \int dk (\Theta_l(k))^2 (2\pi)^3 P(k) \right). \end{aligned} \quad (1.13)$$

If the power spectrum is not rotationally invariant, then the covariance matrix does not simplify to the above diagonal form. The form of the covariance given a primordial power spectrum that slightly deviates from isotropic due to a preferred direction, \hat{n} , during the primordial era,

$$P(\vec{k}) = P_0(k) \left(1 + g(k)(\hat{n} \cdot \hat{k})^2 + \dots \right) \quad (1.14)$$

was worked out in [6]. The absence of odd powers of $\hat{n} \cdot \hat{k}$ follows from the identity $\langle \delta_\varepsilon(\vec{k}) \delta_\varepsilon(\vec{q}) \rangle = \langle \delta_\varepsilon(\vec{q}) \delta_\varepsilon(\vec{k}) \rangle$.¹⁴ It is also assumed that the effect of the preferred direction must be small (else we'd be able to see a signature by eye on the CMB), thus terms of higher order in the “small” vector \hat{n} should be negligible. In other words, they worked out the effect of a small primordial power quadrupole on the CMB covariance. They found that in addition to diagonal elements ($m = m', l = l'$) there are in general nonzero off-diagonal elements when $l = l' \pm 2$ and/or $m' \pm 2$ and/or $m' \pm 1$, depending on the direction of \hat{n} .

As mentioned earlier, the work presented in subsequent chapters of this thesis ultimately grew from thinking about models that could give rise to such a slightly statistically anisotropic spectrum. Indeed, a model of inflation that successfully reproduces a spectrum of the slightly anisotropic form in [6] is presented in chapter 4. Our main work was to calculate $g(k)$ in the model. Chapters 2 and 3 came from thinking about another class of models that could, on the face, lead to a small amount of anisotropy during inflation: æther models. I give a very brief introduction to æther models in §1.7 below.

¹⁴From the identity and the definition of the power spectrum, $P(\vec{k})$, it follows that $P(\vec{k}) = P(-\vec{k})$.

But before moving on to æther models, I'll provide evidence that it is actually rather difficult to construct a consistent model with enough¹⁵ anisotropic inflation.

1.6 The Cosmic No-Hair Theorem

Under some reasonable conditions, it can be shown that a large class of inflationary scenarios tend to wash out anisotropy. More precisely, Bob Wald proved the following theorem, known now as the *cosmic no-hair theorem* [10]:

If a space-time

- is initially expanding,
- can be foliated by homogeneous hypersurfaces,¹⁶
- evolves according to Einstein's equations with a positive cosmological constant,

$$G^\mu_\nu = -\Lambda\delta^\mu_\nu + 8\pi GT^\mu_\nu, \quad \Lambda > 0, \quad (1.15)$$

- contains matter with stress-energy, T^μ_ν , that satisfies the dominant and strong energy conditions,

$$T_{\mu\nu}t^\mu t^\nu \geq 0, \quad T_{\mu\nu}t^\nu T^{\mu\lambda}t_\lambda \leq 0, \quad \text{and} \quad T_{\mu\nu}t^\mu t^\nu \geq \frac{1}{2}T^\lambda_\lambda t^\sigma t_\sigma, \quad (1.16)$$

for all timelike t_μ (*i.e.* for all t^μ such that $t_\mu t^\mu < 0$),

then

the space-time evolves exponentially (on a timescale of $\sqrt{3/\Lambda}$) toward one with de Sitter geometry. De Sitter space can be parametrized as follows,

$$ds^2 = -dt^2 + e^{2Ht} d\vec{x} \cdot d\vec{x} \quad \text{where } H \text{ is constant,} \quad (1.17)$$

¹⁵The point will be that most models with enough inflation to solve the Horizon problem predict that any initial anisotropy will be completely wiped out early on during the inflationary era.

¹⁶All such space-times, which are homogeneous but perhaps anisotropic, fall into a Bianchi classification [11]. There's a slight caveat here: All Bianchi models *except* Bianchi type IX fall under the purview of the cosmic no-hair theorem.

and in particular is isotropic, flat, and has no distinguishing feature (no *hair*) other than the rate of expansion, H . In other words, any energy density besides that of the cosmological constant becomes totally negligible on a timescale set by $\sqrt{3/\Lambda}$.

In the course of his proof, Wald shows in particular that the shear, $\sigma_{\mu\nu}$, which characterizes the anisotropy of the space-time, satisfies the following equation,

$$\sigma_{\mu\nu}\sigma^{\mu\nu} \leq \frac{2\Lambda}{\sinh^2(t/\sqrt{3/\Lambda})}, \quad (1.18)$$

where t is proper time.

Now in order to solve the horizon problem, there must have been at least sixty e -folds of inflation.¹⁷ That is, the scale factor must have increased by a factor of e^{60} during an initial phase when the scale factor was accelerating. If the matter that drives inflation acts like a cosmological constant during inflation, then the Hubble parameter during inflation is approximately $\sqrt{\Lambda/3}$, and $t/\sqrt{3/\Lambda}$ is about equal to the number of e -foldings. Within just about 5 e -foldings of inflation, the denominator on the right-hand side of (1.18) is 1000s, and after 60 e -foldings, it's about 10^{51} ; anisotropy becomes very small (in units of $\sqrt{\Lambda} \sim H$) within just a few e -foldings of inflation, and it's minuscule after 60 e -folds.

This means that in order for anisotropy to persist even in small amounts during inflation, at least one of the premises in the cosmic no-hair theorem must *not* apply.

1.7 Æther

An obvious way to avoid Wald's theorem is to source a small anisotropy with matter that *does not* satisfy the dominant or strong energy conditions. This is how Einstein-æther theories (æther theories, for short), popularized by Jacobson and Mattingly in [12], can avoid the no-hair theorem. Usually “æther theory” refers to a theory

¹⁷See, *e.g.*, [9].

with normal Einstein gravity, plus a dynamical fixed-norm *timelike* vector field that breaks boost invariance of the vacuum and effectively leads to a universal preferred rest frame. Einstein gravity plus a cosmological constant and a dynamical fixed-norm *spacelike* vector field that breaks rotational invariance was considered as a toy model of anisotropic inflation in [6]. It was in this context that I first became interested in æther theories. But æther theories are independently interesting as effective field theories of the spontaneous breaking of Lorentz invariance. They are effective models that include preferred frame effects while leaving diffeomorphism invariance intact. For more on reasons that theorists are interested in æther theories, see, *e.g.*, [13].

The toy æther model in [6] was later shown to be classically unstable [14]. Chapter 2 revisits the stability of æther theories more generally.

1.8 Hairy Inflation

Another way to avoid the cosmic no-hair theorem is to couple matter that could source anisotropy to the matter field that sources inflation (the inflaton field). That’s the idea of the model we study in chapter 4, which was originally named “hairy inflation” by the authors of [7]. The model is built on top of standard single field inflation, but unlike in standard single field inflation, there’s a coupling between the inflaton field and a $U(1)$ gauge field that retards the dissipation of the energy density in the $U(1)$ gauge field enough to allow for a small persistent anisotropy during inflation. In chapter 4 we give a pedagogical explanation of model. The main work of chapter 4 was in calculating the spectrum of cosmological perturbations in the anisotropic background of the model. Since the model is built on top of standard single field inflation and since the results we found for cosmological perturbations in the model ought to be compared to the results from more “standard” models, below we finish this introductory chapter with a brief review of standard single-field slow-roll inflation.

1.9 Standard Slow-Roll Inflation

1.9.1 Background Equations

Assuming that over large distances (over cosmological scales) the Universe is homogeneous and isotropic,¹⁸ the space-time metric in the Universe is well parametrized by,

$$ds^2 = -dt^2 + a^2(t) \left(\frac{dr^2}{1 - Kr^2} + r^2(\sin^2 \theta d\phi^2 + d\theta^2) \right). \quad (1.19)$$

Here, K is equal to -1 , 0 , or $+1$, corresponding to whether the geometry of the Universe is open, flat, or closed (respectively). Matter that supports this geometry must also be homogeneous and isotropic. In that case its stress-energy tensor should take the form

$$T_{\nu}^{\mu} = \begin{pmatrix} -\rho(t) & & & \\ & p(t) & & \\ & & p(t) & \\ & & & p(t) \end{pmatrix}. \quad (1.20)$$

Einstein's field equations, $G_{\nu}^{\mu} = R_{\nu}^{\mu} - \frac{1}{2}R\delta_{\nu}^{\mu} = 8\pi GT_{\nu}^{\mu}$ yield the following two independent differential equations:¹⁹

$$3\frac{K}{a^2} + 3H^2 = 8\pi G\rho \quad (1.21)$$

and

$$-6\frac{\ddot{a}}{a} = -6(\dot{H} + H^2) = 8\pi G(\rho + 3p), \quad (1.22)$$

where $\dot{}$ denotes a derivative with respect to time and $H \equiv \frac{\dot{a}}{a}$ is the Hubble parameter.

¹⁸Indeed, from our vantage point the density of galaxies and other astrophysical objects on average over a variety of very large scales appears to be about the same in every direction. This observation along with the copernican principle (roughly speaking, that our neighborhood is a typical one) provides evidence that the assumption of homogeneity and isotropy of the Universe is a good one. The CMB provides even better evidence.

¹⁹The following two equations correspond to $(-G_t^t = -8\pi GT_t^t)$ and $(G_{\mu}^{\mu} - 2G_t^t = 8\pi G(T_{\mu}^{\mu} - 2T_t^t))$, respectively.

Another equation that's useful, and related to the above two equations through the identity $\nabla_\mu G^\mu_\nu = 0$ is the continuity equation:

$$\dot{\rho} = -3H(\rho + p). \quad (1.23)$$

The horizon problem can be solved if the Universe underwent accelerated expansion before recombination. From (1.22) we can see that accelerated expansion requires matter that satisfies $\rho + 3p < 0$. A homogeneous, canonical scalar field, ϕ , which has

$$\rho = \frac{1}{2}\dot{\phi}^2 + V(\phi), \quad p = \frac{1}{2}\dot{\phi}^2 - V(\phi) \quad (1.24)$$

can clearly satisfy the condition $\rho + 3p < 0$ if $\dot{\phi}^2 < V(\phi)$. The accelerated expansion is rapid if $\dot{H} \ll H^2$. Such rapid expansion occurs if $\dot{\phi}^2 \ll V(\phi)$. And expansion is nearly exponential ($a(t) \approx e^{Ht}$ where H is constant) if all derivatives of H are small. Slow-roll inflation is just the realization of this scenario—of nearly exponential expansion. The field ϕ is called an “inflaton” in this case. The slow-roll conditions relate derivatives of H to functions of the scalar field and its derivatives, thus giving the conditions that the inflaton field and its potential must satisfy in order for (rapid) inflation to occur. Let's quickly derive these relations. We'll set $K = 0$ for simplicity.

Define

$$\epsilon \equiv -\frac{\dot{H}}{H^2} \quad \text{and} \quad \delta \equiv \frac{\ddot{H}}{2H\dot{H}}, \quad (1.25)$$

and note the identity,

$$\dot{\epsilon} = 2H\epsilon(\epsilon + \delta). \quad (1.26)$$

Rearranging (1.21) and (1.22) we get

$$-\frac{\dot{H}}{H^2} = \epsilon = 4\pi G \frac{\rho + p}{H^2} = 4\pi G \left(\frac{\dot{\phi}}{H} \right)^2. \quad (1.27)$$

Differentiating this equation we get

$$4\pi G \frac{d}{dt} \dot{\phi}^2 = 2H^3 \epsilon \delta. \quad (1.28)$$

From the above two equations we can see why “slow-roll” is an appropriate name: the velocity and acceleration of the inflaton field, ϕ , must be small compared to the Hubble rate in order for inflation to occur.

We can also derive consistency relations for the form of the inflaton potential. The continuity equation (1.23) implies,

$$V'(\phi) \dot{\phi} = -3H \dot{\phi}^2 - \frac{1}{2} \frac{d}{dt} \dot{\phi}^2 = -\frac{H^3}{4\pi G} \epsilon (3 + \delta), \quad (1.29)$$

and plugging (1.27) into (1.21) we get

$$V(\phi) = \frac{H^2}{8\pi G} (3 - \epsilon). \quad (1.30)$$

Combining these two equations and (1.27) we see

$$\left(\frac{V'(\phi)}{V(\phi)} \right)^2 = 4\epsilon^2 \frac{H^2}{\dot{\phi}^2} \left(\frac{3 + \delta}{3 - \epsilon} \right)^2 = 16\pi G \epsilon \left(\frac{3 + \delta}{3 - \epsilon} \right)^2 \approx 16\pi G \epsilon. \quad (1.31)$$

Differentiating this equation we get

$$2 \frac{V'(\phi)}{V(\phi)} \dot{\phi} \left(\frac{V''(\phi)}{V(\phi)} - \left(\frac{V'(\phi)}{V(\phi)} \right)^2 \right) \approx 16\pi G \dot{\epsilon}, \quad (1.32)$$

and using (1.29) and (1.30) to sub in for $\frac{V'(\phi)}{V(\phi)} \dot{\phi}$ this leads to

$$\left(\frac{V''(\phi)}{V(\phi)} \right) \approx -8\pi G \frac{\dot{\epsilon}}{2H\epsilon} + \left(\frac{V'(\phi)}{V(\phi)} \right)^2 \approx 8\pi G (\epsilon - \delta). \quad (1.33)$$

Insisting that the magnitudes of ϵ and δ are much much less than one, equations

(1.31) and (1.33) lead to flatness conditions on the inflaton potential.

Inflation ends when the inflaton reaches the minimum of its potential. Once the inflaton nears the minimum of its potential, it begins oscillating about its minimum and decaying into other matter fields. This is called “reheating”.

1.9.2 Perturbations from Single-Field Slow-Roll Inflation

So how does slow-roll inflation give rise to primordial density perturbations? Let’s consider the evolution of the quantum-mechanical degrees of freedom in a slow-roll inflation model, with the dynamical inflaton field, ϕ , and the gravitational field, $g_{\mu\nu}$. The quantum-mechanical degrees of freedom are the small space-time dependent fluctuations of these fields about the homogeneous background values in a slow-roll inflation scenario as described above. So

$$\phi = \bar{\phi}(t) + \delta\phi(t, \vec{x}) \quad \text{and} \quad g_{\mu\nu} = \bar{g}_{\mu\nu}(t) + \delta g_{\mu\nu}(t, \vec{x}), \quad (1.34)$$

where the background fields are barred. Given a homogeneous background, it’s standard to Fourier transpose the perturbations:

$$\delta f(t, \vec{x}) \equiv \int \frac{d\vec{k}}{(2\pi)^3} \delta f(t, \vec{k}) e^{i\vec{k} \cdot \vec{x}}. \quad (1.35)$$

The perturbation δf is promoted to a quantum-mechanical operator, so

$$\begin{aligned} \delta f(t, \vec{k}) &= \chi(k, t) \hat{a}_{\vec{k}} + \chi^*(k, t) \hat{a}_{-\vec{k}}^\dagger, \\ \text{where} \quad [\hat{a}_{\vec{k}}, \hat{a}_{\vec{k}'}^\dagger] &= (2\pi)^3 \delta^{(3)}(\vec{k} - \vec{k}'), \quad [\hat{a}_{\vec{k}}, \hat{a}_{\vec{k}'}] = 0 = [\hat{a}_{\vec{k}}^\dagger, \hat{a}_{\vec{k}'}^\dagger] \end{aligned} \quad (1.36)$$

where here $\hat{}$ denotes a quantum operator, χ is an appropriately normalized mode function, $k = |\vec{k}|$ is the wavelength of the mode, and $k_{phys} = |\vec{k}|/a$ is the physical wavelength of the mode.

Energy density perturbations during inflation are thought to arise in the following way. The Universe is inflating due to an inflaton rolling down its (flat) potential and is in its quantum-mechanical ground state, so, *e.g.*, $\langle \delta\phi \rangle = 0$. But there are necessarily vacuum fluctuations with nonzero dispersion, $\langle \delta\phi \delta\phi \rangle \neq 0$. By the equivalence principle, when curvature is unimportant (for modes with physical wavelength much less than the Hubble radius), the normalization of quantum-mechanical modes is canonical.²⁰ As curvature becomes important for a given mode (*i.e.*, as the physical wavelength of a given mode becomes greater than the Hubble radius) the quantum-mechanical correlations are frozen into classical density perturbations that form the seeds of structure formation and lead to statistical temperature correlations on the CMB sky.

Canonically normalizing the modes takes a bit of work. It's done by expanding the action

$$S = \int \sqrt{-g} d^4x \left(\frac{R}{16\pi G} - \frac{1}{2} \nabla_\mu \phi \nabla^\mu \phi - V(\phi) \right) \quad (1.37)$$

to quadratic order in the perturbations $\delta\phi$ and $\delta g_{\mu\nu}$, eliminating non-dynamical degrees of freedom, and combining the dynamical fields into combinations so that the kinetic term in the action is canonically normalized. It's the field variables with canonically normalized kinetic terms that get canonically quantized.

It is convenient to use conformal time,

$$d\eta = a(t) dt. \quad (1.38)$$

In Newtonian gauge, the metric fluctuation may be decomposed as follows,

$$ds^2 = a(\eta)^2 \left[-(1 + 2\Phi) d\eta^2 + (\delta_{ij}(\eta)(1 - 2\Psi) + \partial_i E_j + \partial_j E_i + 2E_{ij}) dx^i dx^j \right], \quad (1.39)$$

²⁰There are ambiguities having to do with renormalization that I'm glossing over here.

where E_j is transverse ($\delta^{ij}\partial_i E_j = 0$) and E_{ij} is symmetric, transverse and traceless.

After solving several constraint equations derived from the quadratic action and substituting those solutions back into the action, using the background equations of motion, and integrating by parts several times, the quadratic action can be expressed

$$S^{(2)} = \int d\eta \int \frac{d\vec{k}}{(2\pi)^3} \left(\frac{1}{2} r'(\eta, -\vec{k}) r'(\eta, \vec{k}) - \frac{1}{2} \left(\vec{k} \cdot \vec{k} - \frac{z''}{z} \right) r(\eta, -\vec{k}) r(\eta, \vec{k}) \right. \\ \left. + \frac{1}{2} \sum_{s=+, \times} \left[\tilde{h}'_s(\eta, -\vec{k}) \tilde{h}'_s(\eta, \vec{k}) - \left(\vec{k} \cdot \vec{k} - \frac{a''}{a} \right) \tilde{h}_s(\eta, -\vec{k}) \tilde{h}_s(\eta, \vec{k}) \right] \right), \quad (1.40)$$

where ' denotes derivatives with respect to conformal time,

$$z \equiv a \frac{\dot{\phi}}{H}, \quad (1.41)$$

and where

$$r(\eta, \vec{k}) \equiv a \left(\delta\phi(\eta, \vec{k}) + \frac{\dot{\phi}}{H} \Psi(\eta, \vec{k}) \right), \quad (1.42)$$

and

$$\tilde{h}_+(\eta, \vec{k}) = \frac{a}{\sqrt{8\pi G}} \left(\frac{(e_1^i e_1^j - e_2^i e_2^j)}{\sqrt{2}} E_{ij}(\eta, \vec{k}) \right), \quad (1.43)$$

$$\tilde{h}_\times(\eta, \vec{k}) = \frac{a}{\sqrt{8\pi G}} \left(\frac{(e_1^i e_2^j + e_2^i e_1^j)}{\sqrt{2}} E_{ij}(\eta, \vec{k}) \right), \quad (1.44)$$

where \vec{e}_1 and \vec{e}_2 are two unit 3-vectors satisfying $\vec{e}_a \cdot \vec{e}_b = \delta_{ab}$ and $\vec{e}_a \cdot \vec{k} = 0$. The fields $2\sqrt{8\pi G}\tilde{h}_{+, \times}/a(\eta)$ are the two gravitational wave amplitudes. When $|\vec{k}| \ll aH$, the quantity $-r(\eta, \vec{k})H/a\dot{\phi}$ is equal to the so-called curvature perturbation, $\zeta(\vec{k}, \eta)$.²¹

²¹There is a gauge where the spatial part of the metric perturbation takes the form $\delta g_{ij} = a^2 e^{2\zeta} [\exp \gamma]_{ij}$, $\gamma_{ii} = 0$, $\partial_i \gamma_{ij} = 0$. See *e.g.*, [15] pg. 4.

The equations of motion for r and \tilde{h}_s are

$$r'' = - \left(\vec{k} \cdot \vec{k} - \frac{z''}{z} \right) r \quad \text{and} \quad \tilde{h}_s'' = - \left(\vec{k} \cdot \vec{k} - \frac{a''}{a} \right) \tilde{h}_s. \quad (1.45)$$

To quantize, we promote r and \tilde{h}_s to operators as in (1.36). The mode functions χ_r and $\chi_{\tilde{h}_s}$ must solve the above equations of motion. First notice that

$$\frac{a''}{a} = \frac{d}{dt} a^2 H = a^2 H^2 (2 - \epsilon) \quad (1.46)$$

and

$$\begin{aligned} \frac{z''}{z} &= \frac{1}{\sqrt{\epsilon}} \frac{d}{dt} a^2 \sqrt{\epsilon} H \left(1 + \frac{\dot{\epsilon}}{2H\epsilon} \right) = \frac{1}{\sqrt{\epsilon}} \frac{d}{dt} a^2 \sqrt{\epsilon} H (1 + \epsilon + \delta) \\ &= a^2 H^2 \left((2 + \delta)(1 + \epsilon + \delta) + (\dot{\epsilon}/H + \dot{\delta}/H) \right). \end{aligned} \quad (1.47)$$

During slow-roll inflation, $|\dot{\epsilon}/H|, |\dot{\delta}/H| \ll |\epsilon|, |\delta| \ll 1$ and so $H \approx \text{constant}$. That means $a \approx -\frac{1}{H\eta}$ where $\eta \rightarrow -\infty$ in the past and so

$$\frac{a''}{a} \approx (2 - \epsilon)/\eta^2, \quad \frac{z''}{z} \approx (2 + 2\epsilon + 3\delta)/\eta^2. \quad (1.48)$$

Using these expressions for a''/a and z''/z and treating ϵ and δ as constants, the solutions to (1.45) are Hermite polynomials. Setting ϵ and δ to zero, the solutions become even simpler. The solution to

$$f'' = -(k^2 - 2/\eta^2)f \quad (1.49)$$

is

$$f = c_1(k) \left(1 - \frac{i}{k\eta} \right) e^{-ik\eta} + c_2(k) \left(1 + \frac{i}{k\eta} \right) e^{ik\eta}. \quad (1.50)$$

Notice that in the long wavelength limit, when $k\eta \gg 1$,²² the equations of motion for r and \tilde{h}_s are just harmonic oscillator equations. Invoking the equivalence principle, we use this fact to normalize the mode functions. The mode function should satisfy,

$$\chi_k \partial_\eta \chi_k^* - \chi_k^* \partial_\eta \chi_k = i \quad (\text{long wavelength limit}). \quad (1.51)$$

In the approximation where $\epsilon = \delta = 0$, it's clear that the correctly normalized mode functions are

$$\chi_{rk} = \chi_{\tilde{h}_s k} = \frac{1}{\sqrt{2k}} \left(1 - \frac{i}{k\eta} \right) e^{-ik\eta}. \quad (1.52)$$

We can now calculate the two-point function for r and for \tilde{h} . In general for a field f with mode expansion $f(\eta, \vec{x}) = \int \frac{d\vec{k}}{(2\pi)^3} \left(\chi_k(\eta) e^{i\vec{k} \cdot \vec{x}} \hat{a}_{\vec{k}} + \chi_k^*(\eta) e^{-i\vec{k} \cdot \vec{x}} \hat{a}_{\vec{k}}^\dagger \right)$, it's not hard to show that

$$\begin{aligned} \langle f(\eta, \vec{x}) f(\eta, \vec{y}) \rangle &= \int \frac{d\vec{k}}{(2\pi)^3} \int \frac{d\vec{q}}{(2\pi)^3} \chi_k(\eta) \chi_q^*(\eta) e^{i(\vec{k} \cdot \vec{x} - \vec{q} \cdot \vec{y})} [a_{\vec{k}}, a_{\vec{q}}^\dagger] \\ &= \int \frac{d\vec{k}}{(2\pi)^3} \chi_k(\eta) \chi_k^*(\eta) e^{i\vec{k} \cdot (\vec{x} - \vec{y})} \end{aligned} \quad (1.53)$$

$$\equiv \int \frac{d\vec{k}}{(2\pi)^3} P_f(k; \eta) e^{i\vec{k} \cdot (\vec{x} - \vec{y})}, \quad (1.54)$$

where $P_f(k; \eta)$ is the power spectrum at time η . It's also not hard to show for the Fourier-transformed functions that

$$\begin{aligned} \langle f(\eta, \vec{k}) f(\eta, \vec{q}) \rangle &= \chi_k(\eta) \chi_q^*(\eta) [a_{\vec{k}}, a_{-\vec{q}}^\dagger] \\ &= \chi_k(\eta) \chi_k^*(\eta) (2\pi)^3 \delta^{(3)}(\vec{k} + \vec{q}) \end{aligned} \quad (1.55)$$

$$= P_f(k; \eta) (2\pi)^3 \delta^{(3)}(\vec{k} + \vec{q}). \quad (1.56)$$

As mentioned above, the $\delta^{(3)}(\vec{k} + \vec{q})$ dependence can be independently derived from

²²Note that $\frac{\ddot{z}}{z} \approx \frac{\ddot{a}}{a} \approx (aH)^2$ during slow-roll.

the fact that the position space two-point function is invariant under translations.

Let's think for a moment about the short wavelength limit (when $k \ll aH$). The equations then take the form

$$f'' = \frac{\gamma''}{\gamma} f, \quad (1.57)$$

the solution to which is

$$f = c_1 \gamma + c_2 \gamma \int \frac{d\eta}{\gamma^2}. \quad (1.58)$$

For $\gamma = z$ or a during slow-roll inflation, $\int \frac{d\eta}{\gamma^2} \sim a^{-3}$. Thus the exact solution for χ_{rk}/z and for $\chi_{\tilde{h}_s k}/a$ when $k \ll aH$ is a constant plus a decaying part. In other words $r(\eta, \vec{k})/z$ and $\tilde{h}_s(\eta, \vec{k})/a$ are conserved outside the Hubble horizon. In particular, for modes that cross the Hubble horizon well before the end of inflation (when ϵ and δ are much much less than one), the solution (1.52) should be a very good approximation just after Horizon crossing ($-\frac{1}{\eta} \approx aH > k$). Then we know that much after horizon crossing the amplitudes of r/z and \tilde{h}/a should be conserved. That means

$$P_{r/z}(k; \eta > \eta_{\times, k}) \approx \frac{1}{z^2} \frac{1}{2k} \left(1 - \frac{i}{k\eta}\right) \left(1 + \frac{i}{k\eta}\right) \approx \frac{1}{z^2} \frac{1}{2k} \left(\frac{1}{k\eta}\right)^2 \approx \text{constant}, \quad (1.59)$$

where $\eta_{\times, k}$ is η at horizon crossing for wavelength k . Recalling that $z = a\dot{\phi}/H$ we can see that

$$P_{r/z}(k; \eta \gg \eta_{\times, k}) \approx \frac{H^2}{2k^3} \left(\frac{H}{\dot{\phi}}\right)^2 \Big|_{\text{Horizon crossing}} = \frac{H^2}{2k^3} \left(\frac{\epsilon}{4\pi G}\right)^{-1} \Big|_{\text{Horizon crossing}}. \quad (1.60)$$

Similarly,

$$P_{\tilde{h}/a}(k; \eta \gg \eta_{\times, k}) \approx \frac{H^2}{2k^3} \Big|_{\text{Horizon crossing}}. \quad (1.61)$$

We see that $P(k) \propto k^{-3}$ for both r and \tilde{h} . This means that the position space

two-point correlation function,

$$P(\vec{x} - \vec{y}) = \int \frac{d\vec{k}}{(2\pi)^3} P(k) e^{i\vec{k} \cdot (\vec{x} - \vec{y})}, \quad (1.62)$$

is invariant under scale transformations, $\vec{k} \rightarrow \lambda^{-1}\vec{k}$, $\vec{x} \rightarrow \lambda\vec{x}$. For this reason, a power spectrum proportional to k^{-3} is called *scale invariant*. Actually, if we'd used the more precise expressions (1.48) for a''/a and z''/z and used the corresponding more precise Hermite polynomials as our mode functions, we would have found a very slightly scale-noninvariant power spectrum (with the deviation from scale invariance controlled by ϵ and δ). Measurements of the CMB (and the distribution of structures in the Universe) do indeed indicate that the primordial power spectrum is nearly scale invariant. And measurements are now getting sensitive enough to probe very slight deviations from scale invariance. So, given that the slow-roll parameters are related to the shape of the inflaton potential, in a sense we're on the brink of being able to probe the form of the inflaton potential.

I mentioned earlier that the two gravitational wave amplitudes are

$$h_s = 2\sqrt{8\pi G} \tilde{h}_s / a(\eta), \quad \text{where} \quad s = + \text{ or } \times, \quad (1.63)$$

and that the curvature perturbation ζ is equal to $-r(\eta, \vec{k})H/a\dot{\phi}$ outside the horizon. Thus for modes outside the horizon the ratio of power in gravitational waves and the curvature power is

$$\frac{P_{h_+} + P_{h_\times}}{P_\zeta} \approx 2(2\sqrt{8\pi G})^2 \left(\frac{\epsilon}{4\pi G} \right) = 16\epsilon, \quad (1.64)$$

where ϵ is evaluated near horizon crossing. This is known as the tensor-to-scalar ratio. It turns out that the gravitational wave power spectrum and the curvature perturbation power spectrum are expected to be conserved outside the horizon in very

generic circumstances, even after inflation ends and the evolution of the background space-time changes substantially [16],[17]. I mentioned above that deviations of the power spectrum from scale invariance are controlled by the slow-roll parameters. Comparing these deviations to the size of the tensor-to-scalar ratio is an important cross-check of slow-roll models. There are other such cross-checks that can be made, such as comparing the sizes of non-Gaussianities to the tensor-to-scalar ratio and to deviations from scale invariance. The theoretical predictions for ratios of such observable quantities (which should be *numbers*, independent of slow-roll parameters) are known as consistency conditions. We will derive a consistency condition for hairy inflation models in chapter 4.

Chapter 2

Instabilities in the \mathcal{A} ether

We investigate the stability of theories in which Lorentz invariance is spontaneously broken by fixed-norm vector “æther” fields. Models with generic kinetic terms are plagued either by ghosts or by tachyons, and are therefore physically unacceptable. There are precisely three kinetic terms that are not manifestly unstable: a sigma model $(\partial_\mu A_\nu)^2$, the Maxwell Lagrangian $F_{\mu\nu}F^{\mu\nu}$, and a scalar Lagrangian $(\partial_\mu A^\mu)^2$. The timelike sigma-model case is well defined and stable when the vector norm is fixed by a constraint; however, when it is determined by minimizing a potential there is necessarily a tachyonic ghost, and therefore an instability. In the Maxwell and scalar cases, the Hamiltonian is unbounded below, but at the level of perturbation theory there are fewer degrees of freedom and the models are stable. However, in these two theories there are obstacles to smooth evolution for certain choices of initial data.

The contents of this chapter were written in collaboration with Sean Carroll, Tim Dulaney, and Heywood Tam and have been published in [1].

2.1 Introduction

The idea of spontaneous violation of Lorentz invariance through tensor fields with non-vanishing expectation values has garnered substantial attention in recent years [18, 19, 20, 21, 12, 22, 23, 24, 25, 26, 27, 28]. Hypothetical interactions between

Standard Model fields and Lorentz-violating (LV) tensor fields are tightly constrained by a wide variety of experimental probes, in some cases leading to limits at or above the Planck scale [21, 29, 23, 30, 31, 32, 13].

If these constraints are to be taken seriously, it is necessary to have a sensible theory of the dynamics of the LV tensor fields themselves, at least at the level of low-energy effective field theory. The most straightforward way to construct such a theory is to follow the successful paradigm of scalar field theories with spontaneous symmetry breaking, by introducing a tensor potential that is minimized at some non-zero expectation value, in addition to a kinetic term for the fields. (Alternatively, it can be a derivative of the field that obtains an expectation value, as in ghost condensation models [33, 34, 35].) As an additional simplification, we may consider models in which the nonzero expectation value is enforced by a Lagrange multiplier constraint, rather than by dynamically minimizing a potential; this removes the “longitudinal” mode of the tensor from consideration, and may be thought of as a limit of the potential as the mass near the minimum is taken to infinity. In that case, there will be a vacuum manifold of zero-energy tensor configurations, specified by the constraint.

All such models must confront the tricky question of stability. Ultimately, stability problems stem from the basic fact that the metric has an indefinite signature in a Lorentzian spacetime. Unlike in the case of scalar fields, for tensors it is necessary to use the spacetime metric to define both the kinetic and potential terms for the fields. A generic choice of potential would have field directions in which the energy is unbounded from below, leading to tachyons, while a generic choice of kinetic term would have modes with negative kinetic energies, leading to ghosts. Both phenomena represent instabilities; if the theory has tachyons, small perturbations grow exponentially in time at the linearized level, while if the theory has ghosts, nonlinear interactions create an unlimited number of positive- and negative-energy excitations [36]. There is no simple argument that these unwanted features are necessarily present in any

model of LV tensor fields, but the question clearly warrants careful study.

In this chapter we revisit the question of the stability of theories of dynamical Lorentz violation, and argue that most such theories are unstable. In particular, we examine in detail the case of a vector field A_μ with a nonvanishing expectation value, known as the “æther” model or a “bumblebee” model. For generic choices of kinetic term, it is straightforward to show that the Hamiltonian of such a model is unbounded from below, and there exist solutions with bounded initial data that grow exponentially in time.

There are three specific choices of kinetic term for which the analysis is more subtle. These are the sigma-model kinetic term,

$$\mathcal{L}_K = -\frac{1}{2}\partial_\mu A_\nu \partial^\mu A^\nu, \quad (2.1)$$

which amounts to a set of four scalar fields defined on a target space with a Minkowski metric; the Maxwell kinetic term,

$$\mathcal{L}_K = -\frac{1}{4}F_{\mu\nu}F^{\mu\nu}, \quad (2.2)$$

where $F_{\mu\nu} = \partial_\mu A_\nu - \partial_\nu A_\mu$ is familiar from electromagnetism; and what we call the “scalar” kinetic term,

$$\mathcal{L}_K = \frac{1}{2}(\partial_\mu A^\mu)^2, \quad (2.3)$$

featuring a single scalar degree of freedom. Our findings may be summarized as follows:

- The sigma-model Lagrangian with the vector field constrained by a Lagrange multiplier to take on a timelike expectation value is the only æther theory for which the Hamiltonian is bounded from below in every frame, ensuring stability. In the next chapter, we examine the cosmological behavior and observational

constraints on this model [2]. If the vector field is spacelike, the Hamiltonian is unbounded and the model is unstable. However, if the constraint in the sigma-model theory is replaced by a smooth potential, allowing the length-changing mode to become a propagating degree of freedom, that mode is necessarily ghostlike (negative kinetic energy) and tachyonic (correct sign mass term), and the Hamiltonian is unbounded below, even in the timelike case. It is therefore unclear whether models of this form can arise in any full theory.

- In the Maxwell case, the Hamiltonian is unbounded below; however, a perturbative analysis does not reveal any explicit instabilities in the form of tachyons or ghosts. The timelike mode of the vector acts as a Lagrange multiplier, and there are fewer propagating degrees of freedom at the linear level (a “spin-1” mode propagates, but not a “spin-0” mode). Nevertheless, singularities can arise in evolution from generic initial data: for a spacelike vector, for example, the field evolves to a configuration in which the fixed-norm constraint cannot be satisfied (or perhaps just to a point where the effective field theory breaks down). In the timelike case, a certain subset of initial data is well behaved, but, provided the vector field couples only to conserved currents, the theory reduces precisely to conventional electromagnetism, with no observable violations of Lorentz invariance. It is unclear whether there exists a subset of initial data that leads to observable violations of Lorentz invariance while avoiding problems in smooth time evolution.
- The scalar case is superficially similar to the Maxwell case, in that the Hamiltonian is unbounded below, but a perturbative analysis does not reveal any instabilities. Again, there are fewer degrees of freedom at the linear level; in this case, the spin-1 mode does not propagate. There is a scalar degree of freedom, but it does not correspond to a propagating mode at the level of pertur-

bation theory (the dispersion relation is conventional, but the energy vanishes to quadratic order in the perturbations). For the timelike æther field, obstacles arise in the time evolution that are similar to those of a spacelike vector in the Maxwell case; for a spacelike æther field with a scalar action, the behavior is less clear.

- For any other choice of kinetic term, æther theories are always unstable.

Interestingly, these three choices of æther dynamics are precisely those for which there is a unique propagation speed for all dynamical modes; this is the same condition required to ensure that the Generalized Second Law is respected by a Lorentz-violating theory [37, 38].

One reason why our findings concerning stability seem more restrictive than those of some previous analyses is that we insist on perturbative stability in all Lorentz frames, which is necessary in theories where the form of the Hamiltonian is frame dependent. In a Lorentz-invariant field theory, it suffices to pick a Lorentz frame and examine the behavior of small fluctuations; if they grow exponentially, the model is unstable, while if they oscillate, the model is stable. In Lorentz-violating theories, in contrast, such an analysis might miss an instability in one frame that is manifest at the linear level in some other frame [39, 31, 40]. This can be traced to the fact that a perturbation that is “small” in one frame (the value of the perturbation is bounded everywhere along some initial spacelike slice), but grows exponentially with time as measured in that frame, will appear “large” (unbounded on every spacelike slice) in some other frame.

As an explicit example, consider a model of a timelike vector with a background configuration $\bar{A}_\mu = (m, 0, 0, 0)$, and perturbations $\delta a^\mu = \epsilon^\mu e^{-i\omega t} e^{i\vec{k} \cdot \vec{x}}$, where ϵ^μ is some constant polarization vector. In this frame, we will see that the dispersion relation

takes the form

$$\omega^2 = v^2 \vec{k}^2. \quad (2.4)$$

Clearly, the frequency ω will be real for every real wave vector \vec{k} , and such modes simply oscillate rather than growing in time. It is tempting to conclude that models of this form are perturbatively stable for any value of v . However, we will see below that when $v > 1$, there exist other frames (boosted with respect to the original) in which \vec{k} can be real but ω is necessarily complex, indicating an instability. These correspond to wave vectors for which, evaluated in the original frame, both ω and \vec{k} are complex. Modes with complex spatial wave vectors are not considered to be “perturbations,” since the fields blow up at spatial infinity. However, in the presence of Lorentz violation, a complex spatial wave vector in one frame may correspond to a real spatial wave vector in a boosted frame. We will show that instabilities can arise from initial data defined on a constant-time hypersurface (in a boosted frame) constructed solely from modes with real spatial wave vectors. Such modes are bounded at spatial infinity (in that frame), and could be superimposed to form wave packets with compact support. Since the notion of stability is not frame dependent, the existence of at least one such frame indicates that the theory is unstable, even if there is no linear instability in the æther rest frame.

Several prior investigations have considered the question of stability in theories with LV vector fields. Lim [25] calculated the Hamiltonian for small perturbations around a constant timelike vector field in the rest frame, and derived restrictions on the coefficients of the kinetic terms. Bluhm et al. [41] also examined the timelike case with a Lagrange multiplier constraint, and showed that the Maxwell kinetic term led to stable dynamics on a certain branch of the solution space if the vector was coupled to a conserved current. It was also found, in [41], that most LV vector field theories have Hamiltonians that are unbounded below. Boundedness of the Hamiltonian was also considered in [42]. In the context of effective field theory, Gripiaios [43] analyzed

small fluctuations of LV vector fields about a flat background. Dulaney, Gresham and Wise [27] showed that only the Maxwell choice was stable to small perturbations in the spacelike case assuming the energy of the linearized modes was non-zero.¹ Elliot, Moore, and Stoica [30] showed that the sigma-model kinetic term is stable in the presence of a constraint, but not with a potential.

In the next section, we define notation and fully specify the models we are considering. We then turn to an analysis of the Hamiltonians for such models, and show that they are always unbounded below unless the kinetic term takes on the sigma-model form and the vector field is timelike. This result does not by itself indicate an instability, as there may not be any dynamical degree of freedom that actually evolves along the unstable direction. Therefore, in the following section we look carefully at linear stability around constant configurations, and isolate modes that grow exponentially with time. In the section after that we show that the models that are not already unstable at the linear level end up having ghosts, with the exception of the Maxwell and scalar cases. We then examine some features of those two theories in particular.

2.2 Models

We will consider a dynamical vector field A_μ propagating in Minkowski spacetime with signature $(-+++)$. The action takes the form

$$S_A = \int d^4x (\mathcal{L}_K + \mathcal{L}_V) , \tag{2.5}$$

¹This effectively eliminates the scalar case.

where \mathcal{L}_K is the kinetic Lagrange density and \mathcal{L}_V is (minus) the potential. A general kinetic term that is quadratic in derivatives of the field can be written²

$$\mathcal{L}_K = -\beta_1(\partial_\mu A_\nu)(\partial^\mu A^\nu) - \beta_2(\partial_\mu A^\mu)^2 - \beta_3(\partial_\mu A_\nu)(\partial^\nu A^\mu) - \beta_4 \frac{A^\mu A^\nu}{m^2}(\partial_\mu A_\rho)(\partial_\nu A^\rho). \quad (2.7)$$

In flat space-time, setting the fields to constant values at infinity, we can integrate by parts to write an equivalent Lagrange density as

$$\mathcal{L}_K = -\frac{1}{2}\beta_1 F_{\mu\nu} F^{\mu\nu} - \beta_*(\partial_\mu A^\mu)^2 - \beta_4 \frac{A^\mu A^\nu}{m^2}(\partial_\mu A_\rho)(\partial_\nu A^\rho), \quad (2.8)$$

where $F_{\mu\nu} = \partial_\mu A_\nu - \partial_\nu A_\mu$ and we have defined

$$\beta_* = \beta_1 + \beta_2 + \beta_3. \quad (2.9)$$

In terms of these variables, the models specified above with no linear instabilities or negative-energy ghosts are

- Sigma model: $\beta_1 = \beta_*$,
- Maxwell: $\beta_* = 0$, and
- Scalar: $\beta_1 = 0$,

in all cases with $\beta_4 = 0$.

The vector field will obtain a nonvanishing vacuum expectation value from the potential. For most of the chapter we will take the potential to be a Lagrange multiplier

²In terms of the coefficients, c_i , defined in [24] and used in many other publications on æther theories,

$$\beta_i = \frac{c_i}{16\pi G m^2} \quad (2.6)$$

where G is the gravitational constant.

constraint that strictly fixes the norm of the vector:

$$\mathcal{L}_V = \lambda(A^\mu A_\mu \pm m^2), \quad (2.10)$$

where λ is a Lagrange multiplier whose variation enforces the constraint

$$A^\mu A_\mu = \mp m^2. \quad (2.11)$$

If the upper sign is chosen, the vector will be timelike, and it will be spacelike for the lower sign. Later we will examine how things change when the constraint is replaced by a smooth potential of the form $\mathcal{L}_V = -V(A_\mu) \propto \xi(A_\mu A^\mu \pm m^2)^2$. It will turn out that the theory defined with a smooth potential is only stable in the limit as $\xi \rightarrow \infty$. In any case, unless we specify otherwise, we assume that the norm of the vector is determined by the constraint (2.11).

We are left with an action

$$S_A = \int d^4x \left[-\frac{1}{2}\beta_1 F_{\mu\nu} F^{\mu\nu} - \beta_2 (\partial_\mu A^\mu)^2 - \beta_4 \frac{A^\mu A^\nu}{m^2} (\partial_\mu A_\rho)(\partial_\nu A^\rho) + \lambda(A^\mu A_\mu \pm m^2) \right]. \quad (2.12)$$

The Euler-Lagrange equation obtained by varying with respect to A_μ is

$$\beta_1 \partial_\mu F^{\mu\nu} + \beta_2 \partial^\nu \partial_\mu A^\mu + \beta_4 G^\nu = -\lambda A^\nu, \quad (2.13)$$

where we have defined

$$G^\nu = \frac{1}{m^2} [A^\lambda (\partial_\lambda A^\sigma) F_\sigma{}^\nu + A^\sigma (\partial_\lambda A^\lambda \partial_\sigma A^\nu + A^\lambda \partial_\lambda \partial_\sigma A^\nu)]. \quad (2.14)$$

Since the fixed-norm condition (2.11) is a constraint, we can consistently plug it back into the equations of motion. Multiplying (2.13) by A_ν and using the constraint, we

can solve for the Lagrange multiplier,

$$\lambda = \pm \frac{1}{m^2} (\beta_1 \partial_\mu F^{\mu\nu} + \beta_* \partial^\nu \partial_\mu A^\mu + \beta_4 G^\nu) A_\nu. \quad (2.15)$$

Inserting this back into (2.13), we can write the equation of motion as a system of three independent equations:

$$Q_\rho \equiv \left(\eta_{\rho\nu} \pm \frac{A_\rho A_\nu}{m^2} \right) (\beta_1 \partial_\mu F^{\mu\nu} + \beta_* \partial^\nu \partial_\mu A^\mu + \beta_4 G^\nu) = 0. \quad (2.16)$$

The tensor $\eta_{\rho\nu} \pm m^{-2} A_\rho A_\nu$ acts to take what would be the equation of motion in the absence of the constraint, and project it into the hyperplane orthogonal to A_μ . There are only three independent equations because $A^\rho Q_\rho$ vanishes identically, given the fixed norm constraint.

2.2.1 Validity of Effective Field Theory

As in this chapter we will restrict our attention to classical field theory, it is important to check that any purported instabilities are found in a regime where a low-energy effective field theory should be valid. The low-energy degrees of freedom in our models are Goldstone bosons resulting from the breaking of Lorentz invariance. The effective Lagrangian will consist of an infinite series of terms of progressively higher order in derivatives of the fields, suppressed by appropriate powers of some ultraviolet mass scale M . If we were dealing with the theory of a scalar field Φ , the low-energy effective theory would be valid when the canonical kinetic term $(\partial\Phi)^2$ was large compared to a higher-derivative term such as

$$\frac{1}{M^2} (\partial^2 \Phi)^2. \quad (2.17)$$

For fluctuations with wavevector $k^\mu = (\omega, \vec{k})$, we have $\partial\Phi \sim k\Phi$, and the lowest-order terms accurately describe the dynamics whenever $|\vec{k}| < M$. A fluctuation that has a low momentum in one frame can, of course, have a high momentum in some other frame, but the converse is also true; the set of perturbations that can be safely considered “low-energy” looks the same in any frame.

With a Lorentz-violating vector field, the situation is altered. In addition to higher-derivative terms of the form $M^{-2}(\partial^2 A)^2$, the possibility of extra factors of the vector expectation value leads us to consider terms such as

$$\mathcal{L}_4 = \frac{1}{M^8} A^6 (\partial^2 A)^2. \quad (2.18)$$

The number of such higher dimension operators in the effective field theory is greatly reduced because $A_\mu A^\mu = -m^2$ and, therefore, $A_\mu \partial_\nu A^\mu = 0$. It can be shown that an independent operator with n derivatives includes at most $2n$ vector fields, so that the term highlighted here has the largest number of A ’s with four derivatives. We expect that the ultraviolet cutoff M is of order the vector norm, $M \approx m$. Hence, when we consider a background timelike vector field in its rest frame,

$$\bar{A}_\mu = (m, 0, 0, 0), \quad (2.19)$$

the \mathcal{L}_4 term reduces to $m^{-2}(\partial^2 A)^2$, and the effective field theory is valid for modes with $k < m$, just as in the scalar case.

But now consider a highly boosted frame, with

$$\bar{A}_\mu = (m \cosh \eta, m \sinh \eta, 0, 0). \quad (2.20)$$

At large η , individual components of A will scale as $e^{|\eta|}$, and the higher-derivative

term schematically becomes

$$\mathcal{L}_4 \sim \frac{1}{m^2} e^{6|\eta|} (\partial^2 A)^2. \quad (2.21)$$

For modes with spatial wave vector $k = |\vec{k}|$ (as measured in this boosted frame), we are therefore comparing $m^{-2} e^{6|\eta|} k^4$ with the canonical term k^2 . The lowest-order terms therefore only dominate for wave vectors with

$$k < e^{-3|\eta|} m. \quad (2.22)$$

In the presence of Lorentz violation, therefore, the realm of validity of the effective field theory may be considerably diminished in highly boosted frames. We will be careful in what follows to restrict our conclusions to those that can be reached by only considering perturbations that are accurately described by the two-derivative terms. The instabilities we uncover are infrared phenomena, which cannot be cured by changing the behavior of the theory in the ultraviolet. We have been careful to include all of the lowest-order terms in the effective field theory expansion—the terms in (2.8).

2.3 Boundedness of the Hamiltonian

We would like to establish whether there are any values of the parameters β_1 , β_* and β_4 for which the æther model described above is physically reasonable. In practice, we take this to mean that there exist background configurations that are stable under small perturbations. It seems hard to justify taking an unstable background as a starting point for phenomenological investigations of experimental constraints, as we would expect the field to evolve on microscopic timescales away from its starting point.

“Stability” of a background solution X_0 to a set of classical equations of motion means that, for any small neighborhood U_0 of X_0 in the phase space, there is another neighborhood U_1 of X_0 such that the time evolution of any point in U_0 remains in U_1 for all times. More informally, small perturbations oscillate around the original background, rather than growing with time. A standard way of demonstrating stability is to show that the Hamiltonian is a local minimum at the background under consideration. Since the Hamiltonian is conserved under time evolution, the allowed evolution of a small perturbation will be bounded to a small neighborhood of that minimum, ensuring stability. Note that the converse does not necessarily hold; the presence of other conserved quantities can be enough to ensure stability even if the Hamiltonian is not bounded from below.

One might worry about invoking the Hamiltonian in a theory where Lorentz invariance has been spontaneously violated. Indeed, as we shall see, the form of the Hamiltonian for small perturbations will depend on the Lorentz frame in which they are expressed. To search for possible linear instabilities, it is necessary to consider the behavior of small perturbations in every Lorentz frame.

The Hamiltonian density, derived from the action (2.12) via a Legendre transformation, is

$$\mathcal{H} = \frac{\partial \mathcal{L}_A}{\partial(\partial_0 A_\mu)} \partial_0 A_\mu - \mathcal{L}_A \quad (2.23)$$

$$\begin{aligned} &= \frac{\beta_1}{2} F_{ij}^2 + \beta_1 (\partial_0 A_i)^2 - \beta_1 (\partial_i A_0)^2 + \beta_* (\partial_i A_i)^2 - \beta_* (\partial_0 A_0)^2 \\ &\quad + \beta_4 \frac{A^j A^k}{m^2} (\partial_j A_\rho) (\partial_k A^\rho) - \beta_4 \frac{A^0 A^0}{m^2} (\partial_0 A_\rho) (\partial_0 A^\rho), \end{aligned} \quad (2.24)$$

where Latin indices i, j run over $\{1, 2, 3\}$. The total Hamiltonian corresponding to

this density is

$$\begin{aligned}
H &= \int d^3x \mathcal{H} \\
&= \int d^3x \left(\beta_1 (\partial_\mu A_i \partial_\mu A_i - \partial_\mu A_0 \partial_\mu A_0) + (\beta_1 - \beta_*) [(\partial_0 A_0)^2 - (\partial_i A_i)^2] \right. \\
&\quad \left. + \beta_4 \frac{A_j A_k}{m^2} (\partial_j A_\rho) (\partial_k A^\rho) - \beta_4 \frac{A_0 A_0}{m^2} (\partial_0 A_\rho) (\partial_0 A^\rho) \right). \tag{2.25}
\end{aligned}$$

We have integrated by parts and assumed that $\partial_i A_j$ vanishes at spatial infinity; repeated lowered indices are summed (without any factors of the metric). Note that this Hamiltonian is identical to that of a theory with a smooth (positive semidefinite) potential instead of a Lagrange multiplier term, evaluated at field configurations for which the potential is minimized. Therefore, if the Hamiltonian is unbounded when the fixed-norm constraint is enforced by a Lagrange multiplier, it will also be unbounded in the case of a smooth potential.

There are only three dynamical degrees of freedom, so we may reparameterize A_μ such that the fixed-norm constraint is automatically enforced and the allowed 3-dimensional subspace is manifest. We define a boost variable ϕ and angular variables θ and ψ , so that we can write

$$A_0 \equiv m \cosh \phi \tag{2.26}$$

$$A_i \equiv m \sinh \phi f_i(\theta, \psi) \tag{2.27}$$

in the timelike case with $A_\mu A^\mu = -m^2$, and

$$A_0 \equiv m \sinh \phi \tag{2.28}$$

$$A_i \equiv m \cosh \phi f_i(\theta, \psi) \tag{2.29}$$

in the spacelike case with $A_\mu A^\mu = +m^2$. In these expressions,

$$f_1 \equiv \cos \theta \cos \psi \quad (2.30)$$

$$f_2 \equiv \cos \theta \sin \psi \quad (2.31)$$

$$f_3 \equiv \sin \theta, \quad (2.32)$$

so that $f_i f_i = 1$. In terms of this parameterization, the Hamiltonian density for a timelike æther field becomes

$$\begin{aligned} \frac{\mathcal{H}^{(t)}}{m^2} = & \beta_1 \sinh^2 \phi \partial_\mu f_i \partial_\mu f_i + \beta_1 \partial_\mu \phi \partial_\mu \phi \\ & + (\beta_1 - \beta_*) [(\partial_0 \phi)^2 \sinh^2 \phi - (\cosh \phi f_i \partial_i \phi + \sinh \phi \partial_i f_i)^2] \\ & + \beta_4 \sinh^2 \phi [(f_i \partial_i \phi)^2 + \sinh^2 \phi (f_i \partial_i f_l)(f_j \partial_j f_l)] - \beta_4 \cosh^2 \phi [(\partial_0 \phi)^2 + \sinh^2 \phi (\partial_0 f_i)^2], \end{aligned} \quad (2.33)$$

while for the spacelike case we have

$$\begin{aligned} \frac{\mathcal{H}^{(s)}}{m^2} = & \beta_1 \cosh^2 \phi \partial_\mu f_i \partial_\mu f_i - \beta_1 \partial_\mu \phi \partial_\mu \phi \\ & + (\beta_1 - \beta_*) [(\partial_0 \phi)^2 \cosh^2 \phi - (\sinh \phi f_i \partial_i \phi + \cosh \phi \partial_i f_i)^2] \\ & - \beta_4 \cosh^2 \phi [(f_i \partial_i \phi)^2 - \cosh^2 \phi (f_i \partial_i f_l)(f_j \partial_j f_l)] + \beta_4 \sinh^2 \phi [(\partial_0 \phi)^2 - \cosh^2 \phi (\partial_0 f_i)^2]. \end{aligned} \quad (2.34)$$

Expressed in terms of the variables ϕ, θ, ψ , the Hamiltonian is a function of initial data that automatically respects the fixed-norm constraint. We assume that the derivatives $\partial_\mu A_\nu(t_0, \vec{x})$ vanish at spatial infinity.

2.3.1 Timelike Vector Field

We can now determine which values of the parameters $\{\beta_1, \beta_*, \beta_4\}$ lead to Hamiltonians that are bounded below, starting with the case of a timelike æther field. We can examine the various possible cases in turn.

- **Case One:** $\beta_1 = \beta_*$ and $\beta_4 = 0$.

This is the sigma-model kinetic term (2.1). In this case the Hamiltonian density simplifies to

$$\mathcal{H}^{(t)} = m^2 \beta_1 (\sinh^2 \phi \partial_\mu f_i \partial_\mu f_i + \partial_\mu \phi \partial_\mu \phi). \quad (2.35)$$

It is manifestly non-negative when $\beta_1 > 0$, and non-positive when $\beta_1 < 0$. The sigma-model choice $\beta_1 = \beta_* > 0$ therefore results in a theory that is stable. (See also §6.2 of [26].)

- **Case Two:** $\beta_1 < 0$ and $\beta_4 = 0$.

In this case, consider configurations with $(\partial_0 f_i) \neq 0$, $(\partial_i f_j) = 0$, $\partial_\mu \phi = 0$, $\sinh^2 \phi \gg 1$. Then we have

$$\mathcal{H}^{(t)} \sim m^2 \beta_1 \sinh^2 \phi (\partial_0 f_i)^2. \quad (2.36)$$

For $\beta_1 < 0$, the Hamiltonian can be arbitrarily negative for any value of β_* .

- **Case Three:** $\beta_1 \geq 0$, $\beta_* < \beta_1$, and $\beta_4 = 0$.

We consider configurations with $\partial_\mu f_i = 0$, $f_i \partial_i \phi \neq 0$, $\partial_0 \phi = 0$, $\cosh^2 \phi \gg 1$, which gives

$$\mathcal{H}^{(t)} \sim m^2 (\beta_* - \beta_1) \cosh^2 \phi (f_i \partial_i \phi)^2. \quad (2.37)$$

Again, this can be arbitrarily negative.

- **Case Four:** $\beta_1 \geq 0$, $\beta_* > \beta_1$, and $\beta_4 = 0$.

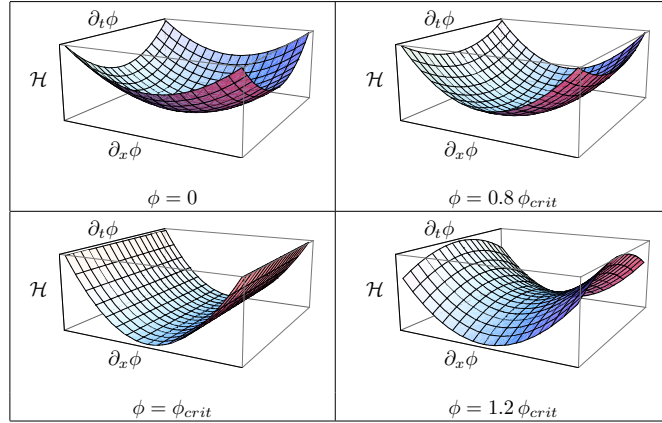


Figure 2.1: Hamiltonian density (vertical axis) when $\beta_1 = 1$, $\beta_* = 1.1$, and $\theta = \psi = \partial_y \phi = \partial_z \phi = 0$ as a function of $\partial_t \phi$ (axis pointing into page) and $\partial_x \phi$ (axis pointing out of page) for various ϕ ranging from zero to $\phi_{crit} = \tanh^{-1} \sqrt{\beta_1/\beta_*}$, the value of ϕ for which the Hamiltonian is flat at $\partial_x \phi = 0$, and beyond. Notice that the Hamiltonian density turns over and becomes negative in the $\partial_t \phi$ direction when $\phi > \phi_{crit}$.

Now we consider configurations with $\partial_\mu f_i = 0$, $f_i \partial_i \phi = 0$, $\partial_0 \phi \neq 0$, $\sinh^2 \phi \gg 1$.

Then,

$$\mathcal{H}^{(t)} \sim m^2 (\beta_1 - \beta_*) \sinh^2 \phi (\partial_0 \phi)^2, \quad (2.38)$$

which can be arbitrarily negative.

• **Case Five:** $\beta_4 \neq 0$.

Now we consider configurations with $\partial_\mu f_i \neq 0$, $\partial_\mu \phi = 0$ and $\sinh^2 \phi \gg 1$. Then,

$$\mathcal{H}^{(t)} \sim m^2 \beta_4 \left[\sinh^4 \phi (f_i \partial_i f_l) (f_k \partial_k f_l) - \sinh^2 \phi \cosh^2 \phi (\partial_0 f_i)^2 \right], \quad (2.39)$$

which can be arbitrarily negative for any non-zero β_4 and for any values of β_1 and β_* .

For any case other than the sigma-model choice $\beta_1 = \beta_*$, it is therefore straightforward to find configurations with arbitrarily negative values of the Hamiltonian.

Nevertheless, a perturbative analysis of the Hamiltonian would not necessarily discover that it was unbounded. The reason for this is shown in Fig. 2.1, which shows the Hamiltonian density for the theory with $\beta_1 = 1$, $\beta_* = 1.1$, in a restricted subspace where $\partial_y\phi = \partial_z\phi = 0$ and $\theta = \phi = 0$, leaving only ϕ , $\partial_t\phi$, and $\partial_x\phi$ as independent variables. We have plotted \mathcal{H} as a function of $\partial_t\phi$ and $\partial_x\phi$ for four different values of ϕ . When ϕ is sufficiently small, so that the vector is close to being purely timelike, the point $\partial_t\phi = \partial_x\phi = 0$ is a local minimum. Consequently, perturbations about constant configurations with small ϕ would appear stable. But for large values of ϕ , the unboundedness of the Hamiltonian becomes apparent. This phenomenon will arise again when we consider the evolution of small perturbations in the next section. At the end of this section, we will explain why such regions of large ϕ are still in the regime of validity of the effective field theory expansion.

2.3.2 Spacelike Vector Field

We now perform an equivalent analysis for an æther field with a spacelike expectation value. In this case all of the possibilities lead to Hamiltonians (2.34) that are unbounded below, and the case $\beta_1 = \beta_* > 0$ is not picked out.

- **Case One:** $\beta_1 < 0$ and $\beta_4 = 0$.

Taking $(\partial_\mu\phi) = 0$, $\partial_j f_i = 0$, $\partial_0 f_i \neq 0$, we find

$$\mathcal{H}^{(s)} \sim m^2 \beta_1 \cosh^2 \phi (\partial_0 f_i)^2. \quad (2.40)$$

- **Case Two:** $\beta_1 > 0$, $\beta_* \leq \beta_1$, and $\beta_4 = 0$.

Now we consider $\partial_\mu f_i = 0$, $\partial_i \phi \neq 0$, $\partial_0 \phi = 0$, giving

$$\mathcal{H}^{(s)} \sim m^2 \left[-\beta_1 \partial_i \phi \partial_i \phi + (\beta_* - \beta_1) \sinh^2 \phi (f_i \partial_i \phi)^2 \right]. \quad (2.41)$$

- **Case Three:** $\beta_1 \geq 0$, $\beta_* > \beta_1$, and $\beta_4 = 0$.

In this case we examine $(\partial_0 \phi) \neq 0$, $\partial_\mu f_i = 0$, $\partial_i \phi = 0$, which leads to

$$\mathcal{H}^{(s)} \sim m^2(\beta_1 - \beta_*) \cosh^2 \phi (\partial_0 \phi)^2. \quad (2.42)$$

- **Case Four:** $\beta_4 \neq 0$.

Now we consider configurations with $\partial_\mu f_i \neq 0$, $\partial_\mu \phi = 0$ and $\sinh^2 \phi \gg 1$. Then,

$$\mathcal{H}^{(s)} \sim m^2 \beta_4 \left(\cosh^4 \phi (f_i \partial_i f_l) (f_k \partial_k f_l) - \cosh^2 \phi \sinh^2 \phi (\partial_0 f_i)^2 \right). \quad (2.43)$$

In every case, it is clear that we can find initial data for a spacelike vector field that makes the Hamiltonian as negative as we please, for all possible β_1 , β_4 and β_* .

2.3.3 Smooth Potential

The usual interpretation of a Lagrange multiplier constraint is that it is the low-energy limit of smooth potentials when the massive degrees of freedom associated with excitations away from the minimum cannot be excited. We now investigate whether these degrees of freedom can destabilize the theory. Consider the most general, dimension four, positive semi-definite smooth potential that has a minimum when the vector field takes a timelike vacuum expectation value,

$$V = \frac{\xi}{4} (A_\mu A^\mu + m^2)^2, \quad (2.44)$$

where ξ is a positive dimensionless parameter. The precise form of the potential should not affect the results as long as the potential is non-negative and has the global minimum at $A_\mu A^\mu = -m^2$.

We have seen that the Hamiltonian is unbounded from below unless the kinetic

term takes the sigma-model form, $(\partial_\mu A_\nu)(\partial^\mu A^\nu)$. Thus we take the Lagrangian to be

$$\mathcal{L} = -\frac{1}{2}(\partial_\mu A_\nu)(\partial^\mu A^\nu) - \frac{\xi}{4}(A_\mu A^\mu + m^2)^2. \quad (2.45)$$

Consider some fixed timelike vacuum \bar{A}_μ satisfying $\bar{A}_\mu \bar{A}^\mu = -m^2$. We may decompose the æther field into a scaling of the norm, represented by a scalar Φ , and an orthogonal displacement, represented by vector B_μ satisfying $\bar{A}_\mu B^\mu = 0$. We thus have

$$A_\mu = \bar{A}_\mu - \frac{\bar{A}_\mu \Phi}{m} + B_\mu, \quad (2.46)$$

where

$$B_\mu = \left(\eta_{\mu\nu} + \frac{\bar{A}_\mu \bar{A}_\nu}{m^2} \right) A^\nu \quad \text{and} \quad \Phi = \frac{\bar{A}_\mu A^\mu}{m} + m. \quad (2.47)$$

With this parameterization, the Lagrangian is

$$\mathcal{L} = \frac{1}{2}(\partial_\mu \Phi)(\partial^\mu \Phi) - \frac{1}{2}(\partial_\mu B_\nu)(\partial^\mu B^\nu) - \frac{\xi}{4}(2m\Phi + B_\mu B^\mu - \Phi^2)^2. \quad (2.48)$$

The field Φ automatically has a wrong-sign kinetic term, and, at the linear level, propagates with a dispersion relation of the form

$$\omega_\Phi^2 = \vec{k}^2 - 2\xi m^2. \quad (2.49)$$

We see that in the case of a smooth potential, there exists a ghostlike mode (wrong-sign kinetic term) that is also tachyonic with spacelike wave vector and a group velocity that generically exceeds the speed of light. It is easy to see that sufficiently long-wavelength perturbations will exhibit exponential growth. The existence of a ghost when the norm of the vector field is not strictly fixed was shown in [30].

In the limit as ξ goes to infinity, the equations of motion enforce a fixed-norm constraint and the ghostlike and tachyonic degree of freedom freezes. The theory is

equivalent to one of a Lagrange multiplier if the limit is taken appropriately.

2.3.4 Discussion

To summarize, we have found that the action in (2.12) leads to a Hamiltonian that is globally bounded from below only in the case of a timelike sigma-model Lagrangian, corresponding to $\beta_1 = \beta_* > 0$ and $\beta_4 = 0$. Furthermore, we have verified (as was shown in [30]) that if the Lagrange multiplier term is replaced by a smooth, positive semi-definite potential, then a tachyonic ghost propagates and the theory is destabilized.

If the Hamiltonian is bounded below, the theory is stable, but the converse is not necessarily true. The sigma-model theory is the only one for which this criterion suffices to guarantee stability. In the next section, we will examine the linear stability of these models by considering the growth of perturbations. Although some models are stable at the linear level, we will see in the following section that most of these have negative-energy ghosts, and are therefore unstable once interactions are included. The only exceptions, both ghost-free and linearly stable, are the Maxwell (2.2) and scalar (2.3) models.

We showed in the previous section that, unless $\beta_* - \beta_1$ and β_4 are exactly zero, the Hamiltonian is unbounded from below. However, the effective field theory breaks down before arbitrarily negative values of the Hamiltonian can be reached; when $\beta_* \neq \beta_1$ and/or $\beta_4 \neq 0$, in regions of phase space in which $\mathcal{H} < 0$ (schematically),

$$\mathcal{H} \sim -m^2 e^{4|\phi|} (\partial\Theta)^2 \quad \text{where} \quad \Theta \in \{\phi, \theta, \psi\}. \quad (2.50)$$

The effective field theory breaks down when kinetic terms with four derivatives (the terms of next highest order in the effective field theory expansion) are on the order

of terms with two derivatives, or, in the angle parameterization, when

$$m^2 e^{4|\phi|} (\partial\Theta)^2 \sim e^{8|\phi|} (\partial\Theta)^4. \quad (2.51)$$

In other words, the effective field theory is only valid when

$$e^{2|\phi|} |\partial\Theta| < m. \quad (2.52)$$

In principle, terms in the effective action with four or more derivatives could add positive contributions to the Hamiltonian to make it bounded from below. However, our analysis shows that the Hamiltonian (in models other than the timelike sigma model with fixed norm) is necessarily concave down around the set of configurations with constant æther fields. If higher-derivative terms intervene to stabilize the Hamiltonian, the true vacuum would not have $H = 0$. Theories could also be deemed stable if there are additional symmetries that lead to conserved currents (other than energy-momentum density) or to a reduced number of physical degrees of freedom.

Regardless of the presence of terms beyond leading order in the effective field theory expansion, due to the presence of the ghostlike and tachyonic mode (found in the previous section), there is an unavoidable problem with perturbations when the field moves in a smooth, positive semi-definite potential. This exponential instability will be present regardless of higher order terms in the effective field theory expansion because it occurs for very long-wavelength modes (at least around constant-field backgrounds).

2.4 Linear Instabilities

We have found that the Hamiltonian of a generic æther model is unbounded below. In this section, we investigate whether there exist actual physical instabilities at the

linear level—*i.e.*, whether small perturbations grow exponentially with time. It will be necessary to consider the behavior of small fluctuations in every Lorentz frame,³ not only in the æther rest frame [39, 31, 40]. We find a range of parameters β_i for which the theories are tachyon free; these correspond (unsurprisingly) to dispersion relations for which the phase velocity satisfies $0 \leq v^2 \leq 1$. In §2.5 we consider the existence of ghosts.

2.4.1 Timelike Vector Field

Suppose Lorentz invariance is spontaneously broken so that there is a preferred rest frame, and imagine that perturbations of some field in that frame have the following dispersion relation:

$$v^{-2}\omega^2 = \vec{k} \cdot \vec{k}. \quad (2.53)$$

This can be written in frame-invariant notation as

$$(v^{-2} - 1)(t^\mu k_\mu)^2 = k_\mu k^\mu, \quad (2.54)$$

where t^μ is a timelike Lorentz vector that characterizes the 4-velocity of the preferred rest frame. So, in the rest frame, $t^\mu = \{1, 0, 0, 0\}$. Indeed, in the appendix, we find dispersion relations for the æther modes of exactly the form in (3.12) with $t^\mu = \bar{A}^\mu/m$ and (2.140)

$$v^2 = \frac{\beta_1}{\beta_1 - \beta_4} \quad (2.55)$$

and (2.141)

$$v^2 = \frac{\beta_*}{\beta_1 - \beta_4}. \quad (2.56)$$

Now consider the dispersion relation for perturbations of the field in another

³The theory of perturbations about a constant background is equivalent to a theory with explicit Lorentz violation because the first order Lagrange density includes the term, $\lambda \bar{A}^\mu \delta A_\mu$, where \bar{A}^μ is effectively some constant coefficient.

(“primed”) frame. Let’s solve for $k'_0 = \omega'$, the frequency of perturbations in the new frame. Expanded out, the dispersion relation reads

$$\omega'^2(1 + (v^{-2} - 1)(t'^0)^2) + 2\omega'(v^{-2} - 1)t'^0 t'^i k'_i - \vec{k}' \cdot \vec{k}' + (v^{-2} - 1)(t'^i k'_i)^2 = 0, \quad (2.57)$$

where $i \in \{1, 2, 3\}$. The solution for ω' is

$$\omega' = \frac{-(v^{-2} - 1)t'^0 t'^i k'_i \pm \sqrt{D_{(t)}}}{1 + (v^{-2} - 1)(t'^0)^2}, \quad (2.58)$$

where

$$D_{(t)} = \vec{k}' \cdot \vec{k}' + (v^{-2} - 1) \left((t'^0)^2 \vec{k}' \cdot \vec{k}' - (t'^i k'_i)^2 \right). \quad (2.59)$$

In general, $t'^0 = \cosh \eta$ and $t'^i = \sinh \eta \hat{n}^i$, where $\hat{n}_i \hat{n}^i = 1$ and $\eta = \cosh^{-1} \gamma$ is a boost parameter. We therefore have

$$D_{(t)} = \vec{k}' \cdot \vec{k}' \left\{ 1 + (v^{-2} - 1) \left[\cosh^2 \eta - \sinh^2 \eta (\hat{n} \cdot \hat{k}')^2 \right] \right\}, \quad (2.60)$$

where $\hat{k}' = \vec{k}'/|\vec{k}'|$. Thus $D_{(t)}$ is clearly greater than zero if $v \leq 1$. However, if $v > 1$ then $D_{(t)}$ can be negative for very large boosts if \vec{k}' is not parallel to the boost direction.

The sign of the discriminant $D_{(t)}$ determines whether the frequency ω' is real or complex valued. We have shown that when the phase velocity v of some field excitation is greater than the speed of light in a preferred rest frame, then there is a (highly boosted) frame in which the excitation looks unstable—that is, the frequency of the field excitation can be imaginary. More specifically, plane waves traveling along the boost direction with boost parameter $\gamma = \cosh \eta$ have a growing amplitude if $\gamma^2 > 1/(1 - v^{-2}) > 0$.

In appendix 2.A, we find dispersion relations of the form in (3.12) for the various massless excitations about a constant timelike background ($t^\mu = \bar{A}^\mu/m$). Requiring

stability and thus $0 \leq v^2 \leq 1$ leads to the inequalities,

$$0 \leq \frac{\beta_1}{\beta_1 - \beta_4} \leq 1 \quad (2.61)$$

and

$$0 \leq \frac{\beta_*}{\beta_1 - \beta_4} \leq 1. \quad (2.62)$$

Models satisfying these relations are stable with respect to linear perturbations in any Lorentz frame.

2.4.2 Spacelike Vector Field

We show in appendix 2.A that fluctuations about a spacelike, fixed-norm, vector field background have dispersion relations of the form

$$(v^2 - 1)(s^\mu k_\mu)^2 = -k_\mu k^\mu, \quad (2.63)$$

with $s^\mu = \bar{A}^\mu/m$ and (2.140)

$$v^2 = \frac{\beta_1 + \beta_4}{\beta_1} \quad (2.64)$$

and (2.141)

$$v^2 = \frac{\beta_1 + \beta_4}{\beta_*}. \quad (2.65)$$

In frames where $s^\mu = \{0, \hat{s}\}$, v is the phase velocity in the \hat{s} direction.

Consider solving for $k'_0 = \omega'$ in an arbitrary (“primed”) frame. The solution is as in (2.58), but with $v^{-2} \rightarrow 2 - v^2$ and $t'^\mu \rightarrow s'^\mu$. Thus,

$$\omega' = \frac{(v^2 - 1)s'^0 s'^i k'_i \pm \sqrt{D_{(s)}}}{1 + (1 - v^2)(s'^0)^2}, \quad (2.66)$$

where

$$D_{(s)} = \vec{k}' \cdot \vec{k}' - (v^2 - 1) \left[(s'^0)^2 \vec{k}' \cdot \vec{k}' - (s'^i k'_i)^2 \right]. \quad (2.67)$$

In general, $s'^0 = \sinh \eta$ and $s'^i = \cosh \eta \hat{n}^i$ where $\hat{n}_i \hat{n}^i = 1$ and $\eta = \cosh^{-1} \gamma$ is a boost parameter. So,

$$D_{(s)} = \vec{k}' \cdot \vec{k}' \left\{ 1 - (v^2 - 1) \left[\sinh^2 \eta - \cosh^2 \eta (\hat{n} \cdot \hat{k}')^2 \right] \right\}. \quad (2.68)$$

which can be rewritten,

$$D_{(s)} = \vec{k}' \cdot \vec{k}' \left\{ v^2 + (1 - v^2) \cosh^2 \eta \left[1 - (\hat{n} \cdot \hat{k}')^2 \right] \right\}. \quad (2.69)$$

It is clear that $D_{(s)}$ is non-negative for all values of η if and only if $0 \leq v^2 \leq 1$. The theory will be unstable unless $0 \leq v^2 \leq 1$.

The dispersion relations of the form (2.63) for the massless excitations about the spacelike background are given in appendix 2.A. The requirement that $0 \leq v^2 \leq 1$ implies

$$0 \leq \frac{\beta_1 + \beta_4}{\beta_1} \leq 1 \quad (2.70)$$

and

$$0 \leq \frac{\beta_1 + \beta_4}{\beta_*} \leq 1. \quad (2.71)$$

Models of spacelike æther fields will only be stable with respect to linear perturbations if these relations are satisfied.

The requirements (2.62) or (2.71) do not apply in the Maxwell case (when $\beta_* = 0 = \beta_4$), and those of (2.61) or (2.70) do not apply in the scalar case (when $\beta_1 = 0 = \beta_4$), since the corresponding degrees of freedom in each case do not propagate.

2.4.3 Stability is Not Frame Dependent

The excitations about a constant background are massless (*i.e.*, the frequency is proportional to the magnitude of the spatial wave vector), but they generally do not propagate along the light cone. In fact, when $v > 1$, the wave vector is timelike even though the cone along which excitations propagate is strictly outside the light cone. We have shown that such excitations blow up in some frame. The exponential instability occurs for observers in boosted frames. In these frames, portions of constant-time hypersurfaces are actually inside the cone along which excitations propagate.

Why do we see the instability in only *some* frames when performing a linear stability analysis? Consider boosting the wave 4-vectors of such excitations with complex-valued frequencies and real-valued spatial wave vectors back to the rest frame. Then, in the rest frame, both the frequency and the spatial wave vector will have non-zero imaginary parts. Such solutions with complex-valued \vec{k} require initial data that grow at spatial infinity and are therefore not really “perturbations” of the background. But even though the æther field defines a rest frame, there is no restriction against considering small perturbations defined on a constant-time hypersurface in any frame. Well-behaved initial data can be decomposed into modes with real spatial wave vectors; if any such modes lead to runaway growth, the theory is unstable.

2.5 Negative Energy Modes

We found above that manifest perturbative stability in all frames requires $0 \leq v^2 \leq 1$. In the appendix, we show that there are two kinds of propagating modes, except when $\beta_* = \beta_4 = 0$ or when $\beta_1 = \beta_4 = 0$. Based on the dispersion relations for these modes, the $0 \leq v^2 \leq 1$ stability requirements translated into the inequalities for β_*, β_1 , and β_4 in (2.61)-(2.62) for timelike æther and (2.70)-(2.71) for spacelike æther. We shall henceforth assume that these inequalities hold and, therefore, that ω and \vec{k} for each

mode are real in every frame. We will now show that, even when these requirements are satisfied and the theories are linearly stable, there will be negative-energy ghosts that imply instabilities at the nonlinear level (except for the sigma model, Maxwell, and scalar cases).

For timelike vector fields, with respect to the æther rest frame, the various modes correspond to two spin-1 degrees of freedom and one spin-0 degree of freedom. Based on their similarity in form to the timelike æther rest frame modes, we will label these modes once and for all as “spin-1” or “spin-0,” even though these classifications are only technically correct for timelike fields in the æther rest frame.

The solutions to the first order equations of motion for perturbations δA_μ about an arbitrary, constant, background \bar{A}_μ satisfying $\bar{A}^\mu \bar{A}_\mu \pm m^2 = 0$ are (see appendix 2.A)

$$\delta A_\mu = \int d^4k q_\mu(k) e^{ik_\mu x^\mu}, \quad q_\mu(k) = q_\mu^*(-k), \quad (2.72)$$

where either

$$q_\mu(k) = i\alpha^\nu k^\rho \frac{\bar{A}^\sigma}{m} \epsilon_{\mu\nu\rho\sigma} \quad \text{and} \quad \beta_1 k_\mu k^\mu + \beta_4 \frac{(\bar{A}_\mu k^\mu)^2}{m^2} = 0 \quad \text{and} \quad \alpha^\nu \bar{A}_\nu = 0 \quad (\text{spin-1}) \quad (2.73)$$

where α^ν are real-valued constants, or

$$q_\mu = i\alpha \left(\eta_{\mu\nu} \pm \frac{\bar{A}_\mu \bar{A}_\nu}{m^2} \right) k^\nu \quad \text{and} \quad \left(\beta_* \eta_{\mu\nu} + (\beta_4 \pm (\beta_* - \beta_1)) \frac{\bar{A}_\mu \bar{A}_\nu}{m^2} \right) k^\mu k^\nu = 0 \quad (\text{spin-0}) \quad (2.74)$$

where α is a real-valued constant.

Note that when $\beta_1 = \beta_4 = 0$, corresponding to the scalar form of (2.3), the spin-1 dispersion relation is satisfied trivially, because the spin-1 mode does not propagate in this case. Similarly, when $\beta_* = \beta_4 = 0$, the kinetic term takes on the Maxwell form

in (2.2) and the spin-0 dispersion relation becomes $\bar{A}_\mu k^\mu = 0$; the spin-0 mode does not propagate in that case.

The Hamiltonian (2.25) for either of these modes is

$$H = \int d^3k \left\{ \left[\beta_1(\omega^2 + \vec{k} \cdot \vec{k}) + \beta_4(-(\bar{a}^0 \omega)^2 + (\bar{a}^i k_i)^2) \right] q^\mu q_\mu^* + (\beta_1 - \beta_*) (\omega^2 q_0^* q_0 + k_i q_i^* k_j q_j) \right\}, \quad (2.75)$$

where $k_0 = \omega = \omega(\vec{k})$ is given by the solution to a dispersion relation and where $\bar{a}^\mu \equiv \bar{A}^\mu/m$. One can show that, as long as β_1 and β_4 satisfy the conditions (2.61) or (2.70) that guarantee real frequencies ω in all frames, we will have

$$q_\mu^* q^\mu \geq 0 \quad (2.76)$$

for all timelike and spacelike vector perturbations. We will now proceed to evaluate the Hamiltonian for each mode in different theories.

2.5.1 Spin-1 Energies

In this section we consider nonvanishing β_4 , and show that the spin-1 mode can carry negative energy even when the conditions for linear stability are satisfied.

Timelike vector field. Without loss of generality, set

$$\bar{A}_\mu = m(\cosh \eta, \sinh \eta \hat{n}), \quad (2.77)$$

where $\hat{n} \cdot \hat{n} = 1$. The energy of the spin-1 mode in the timelike case is given by

$$H = \int d^3k (\vec{k} \cdot \vec{k}) q_\mu^* q^\mu \left[\frac{2X \mp \beta_4 \sinh(2\eta)(\hat{n} \cdot \hat{k})\sqrt{X}}{\beta_1 - \beta_4 \cosh^2 \eta} \right], \quad (2.78)$$

where

$$X = \beta_1 \left\{ \beta_1 + \beta_4 \left[(\hat{n} \cdot \hat{k})^2 \sinh^2 \eta - \cosh^2 \eta \right] \right\}. \quad (2.79)$$

Looking specifically at modes for which $\hat{n} \cdot \hat{k} = +1$, we find

$$H = \int d^3k (\vec{k} \cdot \vec{k}) q_\mu^* q^\mu \left[\frac{2\beta_1(\beta_1 - \beta_4) \mp \beta_4 \sinh(2\eta) \sqrt{\beta_1(\beta_1 - \beta_4)}}{\beta_1 - \beta_4 \cosh^2 \eta} \right]. \quad (2.80)$$

The energy of such a spin-1 perturbation can be negative when $|\beta_4 \sinh(2\eta)| > 2\sqrt{\beta_1(\beta_1 - \beta_4)}$. Thus it is possible to have negative energy perturbations whenever $\beta_4 \neq 0$. Perturbations with wave numbers perpendicular to the boost direction have positive semi-definite energies.

Spacelike vector field. Without loss of generality, for the spacelike case we set

$$\bar{A}_\mu = m(\sinh \eta, \cosh \eta \hat{n}), \quad (2.81)$$

where $\hat{n} \cdot \hat{n} = 1$. The energy of the spin-1 mode in this case is given by

$$H = \int d^3k (\vec{k} \cdot \vec{k}) q_\mu^* q^\mu \left[\frac{2X \mp \beta_4 \sinh(2\eta) (\hat{n} \cdot \hat{k}) \sqrt{X}}{\beta_1 - \beta_4 \sinh^2 \eta} \right], \quad (2.82)$$

where

$$X = \beta_1 \left\{ \beta_1 + \beta_4 \left[(\hat{n} \cdot \hat{k})^2 \cosh^2 \eta - \sinh^2 \eta \right] \right\}. \quad (2.83)$$

Looking at modes for which $\hat{n} \cdot \hat{k} = +1$, we find

$$H = \int d^3k (\vec{k} \cdot \vec{k}) q_\mu^* q^\mu \left[\frac{2\beta_1(\beta_1 + \beta_4) \mp \beta_4 \sinh(2\eta) \sqrt{\beta_1(\beta_1 + \beta_4)}}{\beta_1 - \beta_4 \sinh^2 \eta} \right]. \quad (2.84)$$

Thus, the energy of perturbations can be negative when $|\beta_4 \sinh(2\eta)| > 2\sqrt{\beta_1(\beta_1 + \beta_4)}$.

Thus it is possible to have negative energy perturbations whenever $\beta_4 \neq 0$. Perturbations with wave numbers perpendicular to the boost direction have positive semi-

definite energies. In either the timelike or spacelike case, models with $\beta_4 \neq 0$ feature spin-1 modes that can be ghostlike.

We note that the effective field theory is valid when $k < e^{-3|\eta|}m$, as detailed in §2.2.1. But even if η is very large, the effective field theory is still valid for very long wavelength perturbations, and therefore such long wavelength modes with negative energies lead to genuine instabilities.

2.5.2 Spin-0 Energies

We now assume the inequalities required for linear stability, (2.62) or (2.71), and also that $\beta_4 = 0$. We showed above that, otherwise, there are growing modes in some frame or there are propagating spin-1 modes that have negative energy in some frame. When $\beta_* \neq 0$, the energy of the spin-0 mode in (2.74) is given by

$$H = 2\beta_1\alpha^2 \int d^3k (\bar{a}_\rho k^\rho)^2 \left(\omega^2(\vec{k}) [\pm 1 - (1 - \beta_1/\beta_*)\bar{a}_0^2] + \omega(\vec{k}) \bar{a}_0(1 - \beta_1/\beta_*)\bar{a}_i k_i \right) \quad (2.85)$$

for $\bar{A}_\mu \bar{A}^\mu \pm m^2 = 0$ and $\bar{a}_\mu \equiv \bar{A}_\mu/m$.

Timelike vector field. We will now show that the quadratic order Hamiltonian can be negative when the background is timelike and the kinetic term does not take one of the special forms (sigma model, Maxwell, or scalar). Without loss of generality we set $\bar{a}_0 = \cosh \eta$ and $\bar{a}_i = \sinh \eta \hat{n}_i$, where $\hat{n} \cdot \hat{n} = 1$. Then plugging the frequency $\omega(\vec{k})$, as defined by the spin-0 dispersion relation, into the Hamiltonian (2.85) gives

$$H = \beta_1\alpha^2 \int d^3k (\bar{a}_\rho k^\rho)^2 \left[\frac{2X \pm (1 - \beta_1/\beta_*) \sinh 2\eta (\hat{n} \cdot \hat{k}) \sqrt{X}}{1 + (\beta_1/\beta_* - 1) \cosh^2 \eta} \right], \quad (2.86)$$

where

$$X = 1 + (\beta_1/\beta_* - 1)[\cosh^2 \eta - (\hat{n} \cdot \hat{k})^2 \sinh^2 \eta]. \quad (2.87)$$

If $\hat{n} \cdot \hat{k} \neq 0$, the energy can be negative. In particular, if $\hat{n} \cdot \hat{k} = 1$ we have

$$H = \beta_1 \alpha^2 \int d^3k (\bar{a}_\rho k^\rho)^2 \left[\frac{2\beta_1/\beta_* \pm (1 - \beta_1/\beta_*) \sinh 2\eta \sqrt{\beta_1/\beta_*}}{1 + (\beta_1/\beta_* - 1) \cosh^2 \eta} \right]. \quad (2.88)$$

Given that $\beta_1/\beta_* - 1 \geq 0$, H can be negative when $|\sinh 2\eta| > 2\sqrt{\beta_1/\beta_*}/(\beta_1/\beta_* - 1)$.

We have thus shown that, for timelike backgrounds, there are modes that in some frame have negative energies and/or growing amplitudes as long as $\beta_1 \neq \beta_*$, $\beta_1 \neq 0$, and $\beta_* \neq 0$. Therefore, the only possibly stable theories of timelike æther fields are the special cases mentioned earlier: the sigma-model ($\beta_1 = \beta_*$), Maxwell ($\beta_* = 0$), and scalar ($\beta_1 = 0$) kinetic terms.

Spacelike vector field. For the spacelike case, without loss of generality we set $\bar{a}_0 = \sinh \eta$ and $\bar{a}_i = \cosh \eta \hat{n}_i$, where $\hat{n} \cdot \hat{n} = 1$. Once again, plugging the frequency $\omega(k)$ into the Hamiltonian (2.85) gives

$$H = \beta_1 \alpha^2 \int d^3k (\bar{a}_\rho k^\rho)^2 \left[\frac{-2X \pm (1 - \beta_1/\beta_*) \sinh 2\eta (\hat{n} \cdot \hat{k}) \sqrt{X}}{1 + (1 - \beta_1/\beta_*) \sinh^2 \eta} \right], \quad (2.89)$$

where

$$X = 1 + (1 - \beta_1/\beta_*) \left[\sinh^2 \eta - (\hat{n} \cdot \hat{k})^2 \cosh^2 \eta \right]. \quad (2.90)$$

Upon inspection, one can see that there are values of $\hat{n} \cdot \hat{k}$ and η that make H negative, except when $\beta_* = 0$ (Maxwell) or $\beta_1 = 0$ (scalar). Again, the Hamiltonian density is less than zero for modes with wavelengths sufficiently long ($k < e^{-3|\eta|} m$), so the effective theory is valid.

2.6 Maxwell and Scalar Theories

We have shown that the only version of the æther theory (2.12) for which the Hamiltonian is bounded below is the timelike sigma-model theory $\mathcal{L}_K = -(1/2)(\partial_\mu A_\nu)(\partial^\mu A^\nu)$,

corresponding to the choices $\beta_1 = \beta_*$, $\beta_4 = 0$, with the fixed-norm condition imposed by a Lagrange multiplier constraint. (Here and below, we rescale the field to canonically normalize the kinetic terms.) However, when we looked for explicit instabilities in the form of tachyons or ghosts in the last two sections, we found two other models for which such pathologies are absent: the Maxwell Lagrangian

$$\mathcal{L}_K = -\frac{1}{4}F_{\mu\nu}F^{\mu\nu}, \quad (2.91)$$

corresponding to $\beta_* = 0 = \beta_4$, and the scalar Lagrangian

$$\mathcal{L}_K = \frac{1}{2}(\partial_\mu A^\mu)^2, \quad (2.92)$$

corresponding to $\beta_1 = 0 = \beta_4$. In both of these cases, we found that the Hamiltonian is unbounded below,⁴ but a configuration with a small positive energy does not appear to run away into an unbounded region of phase space characterized by large negative and positive balancing contributions to the total energy.

These two models are also distinguished in another way: there are fewer than three propagating degrees of freedom at first order in perturbations in the Maxwell and scalar Lagrangian cases, while there are three in all others. This is closely tied to the absence of perturbative instabilities; the ultimate cause of those instabilities can be traced to the difficulty in making all of the degrees of freedom simultaneously well behaved. The drop in number of degrees of freedom stems from the fact that A_0 lacks time derivatives in the Maxwell Lagrangian and that the A_i lack time derivatives in the scalar Lagrangian. In other words, some of the vector components are themselves Lagrange multipliers in these special cases.

Only two perturbative degrees of freedom—the spin-1 modes—propagate in the Maxwell case (cf. (2.73)-(2.74) when $\beta_* = 0 = \beta_4$). The “mode” in (2.74) is a gauge

⁴Boundedness of the Hamiltonian was considered in [44].

degree of freedom; at first order in perturbations the Lagrangian has a gaugelike symmetry under $\delta A_\mu \rightarrow \delta A_\mu + \partial_\mu \phi(x)$ where $\bar{A}^\mu \partial_\mu \phi = 0$. As expected of a gauge degree of freedom, the spin-0 mode has zero energy and does not propagate. Meanwhile, the spin-1 perturbations propagate as well-behaved plane waves and have positive energy. We note that the Dirac method for counting degrees of freedom in constrained dynamical systems implies that there are *three* degrees of freedom [41].⁵ The additional degree of freedom, not apparent at the linear level, could conceivably cause an instability; this mode does not propagate because it is gaugelike at the linear level, but there is no gauge symmetry in the full theory.

In the scalar case, there are no propagating spin-1 degrees of freedom. The spin-0 degree of freedom has a nontrivial dispersion relation but no energy density (cf. (2.73)-(2.74), (2.86), and (2.89) when $\beta_1 = 0 = \beta_4$) at leading order in the perturbations. Essentially, the fixed-norm constraint is incompatible with what would be a single propagating scalar mode in this model; the theory is still dynamical, but perturbation theory fails to capture its dynamical content.

Each of these models displays some idiosyncratic features, which we now consider in turn.

2.6.1 Maxwell Action

The equation of motion for the Maxwell Lagrangian with a fixed-norm constraint is

$$\partial_\mu F^{\mu\nu} = -2\lambda A^\nu. \quad (2.93)$$

Setting $A_\mu A^\mu = \mp m^2$, the Lagrange multiplier is given by

$$\lambda = \pm \frac{1}{2m^2} A_\nu \partial_\mu F^{\mu\nu}. \quad (2.94)$$

⁵For a discussion of constrained dynamical systems see [45].

For timelike æther fields, the sign of λ is preserved along timelike trajectories since, when the kinetic term takes the special Maxwell form, there is a conserved current (in addition to energy-momentum density) due to the Bianchi identity⁶:

$$0 = \partial_\nu(\partial_\mu F^{\mu\nu}) = -2\partial_\nu(\lambda A^\nu). \quad (2.95)$$

In particular, the condition that $\lambda = 0$ is conserved along timelike A^ν [12, 41]. In the presence of interactions, this will continue to be true only if the coupling to external sources takes the form of an interaction with a conserved current, $A_\mu J^\mu$ with $\partial_\mu J^\mu = 0$.

If we take the timelike Maxwell theory coupled to a conserved current and restrict to initial data satisfying $\lambda = 0$ at every point in space, the theory reduces precisely to Maxwell electrodynamics—not only in the equation of motion, but also in the energy-momentum tensor. We can therefore be confident that this theory, restricted to this subset of initial data, is perfectly well behaved, simply because it is identical to conventional electromagnetism in a nonlinear gauge [46, 42, 47].

In the case of a spacelike vector expectation value, there is an explicit obstruction to finding smooth time evolution for generic initial data. In this case, the constraint equations are

$$-A_0^2 + A_i A_i = m^2 \quad \text{and} \quad \partial_i \partial^i A_0 - \partial_0 \partial_i A^i = -2\lambda A_0. \quad (2.96)$$

Suppose spatially homogeneous initial conditions for the A_i are given. Without loss of generality, we can align axes such that

$$A_\mu(t_0) = (A_0(t_0), 0, 0, A_3(t_0)), \quad (2.97)$$

⁶If $\lambda > 0$ initially, then it must pass through $\lambda = 0$ to reach $\lambda < 0$ —but $\lambda = 0$ is conserved along timelike trajectories, so λ can at best stop at $\lambda = 0$.

where $-A_0^2 + A_3^2 = m^2$. If $A_i A_i \neq m^2$, the equations of motion are

$$\partial_\mu F^\mu{}_\nu = 0. \quad (2.98)$$

The $\nu = 3$ equation reads

$$\partial_\mu F^\mu{}_3 = -\frac{\partial^2 A_3}{\partial t^2} = 0, \quad (2.99)$$

whose solutions are given by

$$A_3(t) = A_3(t_0) + C(t - t_0), \quad (2.100)$$

where C is determined by initial conditions. A_0 is determined by the fixed-norm constraint $A_0 = \pm\sqrt{A_3^2 - m^2}$. If $C \neq 0$, A_0 will eventually evolve to zero. Beyond this point, A_3 keeps decreasing, and the fixed-norm condition requires that A_0 be imaginary, which is unacceptable since A_μ is a real-valued vector field. Note that this never happens in the timelike case, as there always exists some real A_0 that satisfies the constraint for any value of A_3 . The problem is that A_3 evolves into the ball $A_i^2 < m^2$, which is catastrophic for the spacelike, but not the timelike, case. An analogous problem arises even when the Lagrange multiplier constraint is replaced by a smooth potential.

It is possible that this obstruction to a well-defined evolution will be regulated by terms of higher order in the effective field theory. Using the fixed-norm constraint and solving for A_0 , the derivative is

$$\partial_\mu A_0 = \frac{A_i}{\sqrt{A_j A_j - m^2}} \partial_\mu A_i. \quad (2.101)$$

As $A_j A_j$ approaches m^2 , with finite derivatives of the spatial components, the derivative of the A_0 component becomes unbounded. If higher-order terms in the effective action have time derivatives of the component A_0 , these terms could become relevant

to the vector field's dynamical evolution, indicating that we have left the realm of validity of the low-energy effective field theory we are considering.

We are left with the question of how to interpret the timelike Maxwell theory with initial data for which $\lambda \neq 0$. If we restrict our attention to initial data for which $\lambda < 0$ everywhere, then the evolution of the A_i would be determined and the Hamiltonian would be positive. We have

$$H = \frac{1}{2} \int d^3x \left(\frac{1}{2} F_{ij}^2 + (\partial_0 A_i)^2 - (\partial_i A_0)^2 \right) \quad (2.102)$$

$$= \frac{1}{2} \int d^3x \left(\frac{1}{2} F_{ij}^2 + F_{0i} F_{0i} - 2(\partial_i A_0) F_{i0} \right) \quad (2.103)$$

$$= \frac{1}{2} \int d^3x \left(\frac{1}{2} F_{ij}^2 + F_{0i} F_{0i} + 2A_0 \partial_i F_{i0} \right) \quad (2.104)$$

$$= \frac{1}{2} \int d^3x \left(\frac{1}{2} F_{ij}^2 + F_{0i} F_{0i} - 4\lambda A_0^2 \right), \quad (2.105)$$

which is manifestly positive when $\lambda < 0$. However, it is not clear why we should be restricted to this form of initial data, nor whether even this restriction is enough to ensure stability beyond perturbation theory.

The status of this model in both the spacelike and timelike cases remains unclear. However, there are indications of further problems. For the spacelike case, Peloso *et. al.* find a linear instability for perturbations with wave numbers on the order of the Hubble parameter in an exponentially expanding cosmology [48, 14]. For the timelike case, Seifert found a gravitational instability in the presence of a spherically symmetric source [49].

2.6.2 Scalar Action

The equation of motion for the scalar Lagrangian with a fixed-norm constraint is

$$\partial^\nu \partial_\mu A^\mu = 2\lambda A^\nu. \quad (2.106)$$

Using the fixed-norm constraint ($A_\mu A^\mu = \mp m^2$), we can solve for the Lagrange multiplier field,

$$\lambda = \mp \frac{1}{2m^2} A_\nu \partial^\nu \partial_\mu A^\mu. \quad (2.107)$$

In contrast with the Maxwell theory, in the scalar theory it is the timelike case for which we can demonstrate obstacles to smooth evolution, while the spacelike case is less clear. (The Hamiltonian is bounded below, but there are no perturbative instabilities or known obstacles to smooth evolution.)

When the vector field is timelike, we have four constraint equations in the scalar case,

$$A_0^2 - A_i A_i = m^2 \quad \text{and} \quad \partial_i (\partial_\mu A^\mu) = 2\lambda A_i. \quad (2.108)$$

Suppose we give homogeneous initial conditions such that $A_0(t_0) > m$. Align axes such that,

$$A_\mu(t_0) = (A_0(t_0), 0, 0, A_3(t_0)), \quad (2.109)$$

where $A_3(t_0)^2 = A_0(t_0)^2 - m^2$. Note that, since $A_3(t_0) \neq 0$, we have that $\lambda = 0$ from the $\nu = 3$ equation of motion. The $\nu = 0$ equation of motion therefore gives,

$$\frac{d^2 A_0}{dt^2} = 0. \quad (2.110)$$

We see that the timelike component of the vector field has the time evolution,

$$A_0(t) = A_0(t_0) + C(t - t_0). \quad (2.111)$$

For generic homogeneous initial conditions, $C \neq 0$. In this case, A_0 will not have a smooth time evolution since A_0 will saturate the fixed-norm constraint, and beyond this point A_0 will continue to decrease in magnitude. To satisfy the fixed-norm constraint, the spatial components of the vector field A_i would need to be imaginary,

which is unacceptable since A_μ is a real-valued vector field. This problem never occurs for the spacelike case since there always exist real values of A_i that satisfy the constraint for any A_0 .

Again, it is possible that this obstruction to a well-defined evolution will be regulated by terms of higher order in the effective field theory. The time derivative of A_3 is

$$\partial_\mu A_3 = \frac{A_0}{\sqrt{A_0 A_0 - m^2}} \partial_\mu A_0. \quad (2.112)$$

As $A_0 A_0$ approaches m^2 , with finite derivatives of A_0 , the derivative of the spatial component A_3 becomes unbounded. If higher-order terms in the effective action have time derivatives of the components A_i , these terms could become relevant to the vector field's dynamical evolution, indicating that we have left the realm of validity of the low-energy effective field theory we are considering.

Whether or not a theory with a scalar kinetic term and fixed expectation value is viable remains uncertain.

2.7 Conclusions

In this chapter, we addressed the issue of stability in theories in which Lorentz invariance is spontaneously broken by a dynamical fixed-norm vector field with an action

$$S = \int d^4x \left(-\frac{1}{2} \beta_1 F_{\mu\nu} F^{\mu\nu} - \beta_* (\partial_\mu A^\mu)^2 - \beta_4 \frac{A^\mu A^\nu}{m^2} (\partial_\mu A_\rho) (\partial_\nu A^\rho) + \lambda (A^\mu A_\mu \pm m^2) \right), \quad (2.113)$$

where λ is a Lagrange multiplier that strictly enforces the fixed-norm constraint. In the spirit of effective field theory, we limited our attention to only kinetic terms that are quadratic in derivatives, and took care to ensure that our discussion applies to regimes in which an effective field theory expansion is valid.

We examined the boundedness of the Hamiltonian of the theory and showed that,

for generic choices of kinetic term, the Hamiltonian is unbounded from below. Thus for a generic kinetic term, we have shown that a constant fixed-norm background is not the true vacuum of the theory. The only exception is the timelike sigma-model Lagrangian ($\beta_1 = \beta_*$, $\beta_4 = 0$ and $A^\mu A_\mu = -m^2$), in which case the Hamiltonian is positive-definite, ensuring stability. However, if the vector field instead acquires its vacuum expectation value by minimizing a smooth potential, we demonstrated (as was done previously in [30]) that the theory is plagued by the existence of a tachyonic ghost, and the Hamiltonian is unbounded from below. The timelike fixed-norm sigma-model theory nevertheless serves as a viable starting point for phenomenological investigations of Lorentz invariance; we explore some of this phenomenology in the next chapter.

We next examined the dispersion relations and energies of first-order perturbations about constant background configurations. We showed that, in addition to the sigma-model case, there are only two other choices of kinetic term for which perturbations have non-negative energies and do not grow exponentially in any frame: the Maxwell ($\beta_* = \beta_4 = 0$) and scalar ($\beta_1 = \beta_4 = 0$) Lagrangians. In either case, the theory has fewer than three propagating degrees of freedom at the linear level, as some of the vector components in the action lack time derivatives and act as additional Lagrange multipliers. A subset of the phase space for the Maxwell theory with a timelike æther field is well defined and stable, but is identical to ordinary electromagnetism. For the Maxwell theory with a spacelike æther field, or the scalar theory with a timelike field, we can find explicit obstructions to smooth time evolution. It remains unclear whether the timelike Maxwell theory or the spacelike scalar theory can exhibit true violation of Lorentz invariance while remaining well behaved.

2.A Appendix: Solutions to the Linearized Equations of Motion

We start by finding the solution to the equations of motion, linearized about a time-like, fixed-norm background, A_μ . Then, showing fewer details, we find the solutions to the equations of motion linearized about a spacelike background. Finally, we put the solutions in both cases into the compact form of (2.139)-(2.141). Our results agree with the solutions for Goldstone modes found in [43].

The equations of motion for a timelike (+) or spacelike (−) vector field are (2.16),

$$Q_\mu \equiv \left(\eta_{\mu\nu} \pm \frac{A_\mu A_\nu}{m^2} \right) (\beta_1 \partial_\rho \partial^\rho A^\nu + (\beta_* - \beta_1) \partial^\nu \partial_\rho A^\rho + \beta_4 G^\nu) = 0, \quad (2.114)$$

where G^ν is defined in (2.14) and $A^\mu Q_\mu = 0$ identically.

Timelike background. Consider perturbations about an arbitrary, constant (in space and time) timelike background $A_\mu = \bar{A}_\mu$ that satisfies the constraint: $\bar{A}_\mu \bar{A}^\mu = -m^2$. Define perturbations by $A_\mu = \bar{A}_\mu + \delta A_\mu$. Then, to first order in these perturbations, $\bar{A}^\mu Q_\mu = 0$ identically, and $\eta^{\mu\nu} \bar{A}_\mu \delta A_\nu = 0$ by the constraint. We can define a basis set of four Lorentz 4-vectors n^α , with components

$$n_\mu^0 = \bar{A}_\mu / m, \quad n_\mu^i; \quad i \in \{1, 2, 3\}, \quad (2.115)$$

such that

$$\eta^{\mu\nu} n_\mu^\alpha n_\nu^\beta = \eta^{\alpha\beta}. \quad (2.116)$$

The independent perturbations are $\delta a^\alpha \equiv \eta^{\mu\nu} n_\mu^\alpha \delta A_\nu$ for $\alpha = 1, 2, 3$. (δa^0 is zero at first order in perturbations due to the constraint.) It is then clear that there are three independent equations of motion at first order in perturbations (assuming the

constraint) for the three independent perturbations,

$$\delta Q^i \equiv n_\nu^i (\beta_1 \partial_\rho \partial^\rho \delta A^\nu + (\beta_* - \beta_1) \partial^\nu \partial_\rho \delta A^\rho + \beta_4 n_\mu^0 n_\rho^0 \partial^\mu \partial^\rho \delta A^\nu) = 0, \quad (2.117)$$

where $i \in \{1, 2, 3\}$. We look for plane wave solutions for the δA :

$$\delta A_\mu = \int d^4 k q_\mu(k) e^{ik_\nu x^\nu}. \quad (2.118)$$

Since $\eta^{\mu\nu} n_\mu^0 \delta A_\nu = 0$, at first order,

$$q_\mu = c_j n_\mu^j \quad \text{where} \quad j \in \{1, 2, 3\}. \quad (2.119)$$

The equations of motion become the algebraic equations:

$$0 = (\beta_1 k_\rho k^\rho n_\nu^i n^{j\nu} + (\beta_* - \beta_1) n_\nu^i k^\nu n_\mu^j k^\mu + \beta_4 n_\mu^0 n_\rho^0 k^\mu k^\rho n_\nu^i n^{j\nu}) c_j \quad (2.120)$$

$$= (\beta_1 k_\rho k^\rho \delta^{ij} + (\beta_* - \beta_1) n_\nu^i k^\nu n_\mu^j k^\mu + \beta_4 n_\mu^0 n_\rho^0 k^\mu k^\rho \delta^{ij}) c_j \quad (2.121)$$

$$\equiv M^{ij} c_j. \quad (2.122)$$

The three independent solutions to these equations are given by setting an eigenvalue of the matrix M to zero and setting c_i to the corresponding eigenvector. Setting an eigenvalue of M equal to zero gives a dispersion relation,

$$\beta_1 k_\rho k^\rho + \beta_4 (n_\mu^0 k^\mu)^2 = 0, \quad (2.123)$$

with two linearly independent eigenvectors,

$$(e_2)_i = \epsilon_{2ij} n_\mu^j k^\mu \quad ; \quad (e_3)_i = \epsilon_{3ij} n_\mu^j k^\mu. \quad (2.124)$$

The second eigenvalue of M gives the dispersion relation,

$$\beta_* k_\rho k^\rho + (\beta_* - \beta_1 + \beta_4)(n_\mu^0 k^\mu)^2 = 0, \quad (2.125)$$

with corresponding eigenvector,

$$c_i = n_\mu^i k^\mu. \quad (2.126)$$

Spacelike background. The first-order linearized equations of motion about a spacelike background are

$$\delta Q^a \equiv n_\nu^a (\beta_1 \partial_\rho \partial^\rho \delta A^\nu + (\beta_* - \beta_1) \partial^\nu \partial_\rho \delta A^\rho + \beta_4 n_\mu^3 n_\rho^3 \partial^\mu \partial^\rho \delta A^\nu) = 0 \quad (2.127)$$

where $a \in \{0, 1, 2\}$ and where, similarly to the timelike case, we have defined the set of four Lorentz 4-vectors, n_μ^α , to be

$$n_\mu^3 = \bar{A}_\mu / m \quad \text{and} \quad n_\mu^a; \quad a \in \{0, 1, 2\} \quad (2.128)$$

such that

$$\eta^{\mu\nu} n_\mu^\alpha n_\nu^\beta = \eta^{\alpha\beta}. \quad (2.129)$$

The independent perturbations are $\delta a^\alpha \equiv \eta^{\mu\nu} n_\mu^\alpha \delta A_\nu$ for $\alpha = 0, 1, 2$. (δa^3 is zero at first order in perturbations due to the constraint.)

Again we look for plane wave solutions of the form in (2.118). But now, since $\eta^{\mu\nu} n_\mu^3 \delta A_\nu = 0$, at first order,

$$q_\mu = c_a n_\mu^a \quad \text{where} \quad a \in \{0, 1, 2\}. \quad (2.130)$$

The equations of motion become the algebraic equations:

$$= (\beta_1 k_\rho k^\rho n_\nu^a n^{b\nu} + (\beta_* - \beta_1) n_\nu^a k^\nu n_\mu^b k^\mu + \beta_4 n_\mu^3 n_\rho^3 k^\mu k^\rho n_\nu^a n^{b\nu}) c_b \quad (2.131)$$

$$= (\beta_1 k_\rho k^\rho \eta^{ab} + (\beta_* - \beta_1) n_\nu^a k^\nu n_\mu^b k^\mu + \beta_4 n_\mu^3 n_\rho^3 k^\mu k^\rho \eta^{ab}) c_b \quad (2.132)$$

$$\equiv M^{ab} c_b \quad a, b \in \{0, 1, 2\}. \quad (2.133)$$

Two independent solutions correspond to the dispersion relation ($a \in \{0, 1, 2\}$)

$$\beta_1 k_\rho k^\rho + \beta_4 (n_\mu^3 k^\mu)^2 = 0, \quad (2.134)$$

with corresponding eigenmodes

$$(e_1)_a = \epsilon_{a1b3} n_\mu^b k^\mu \quad ; \quad (e_2)_a = \epsilon_{ab23} n_\mu^b k^\mu. \quad (2.135)$$

The third solution corresponds to the dispersion relation

$$\beta_* k_\rho k^\rho - (\beta_* - \beta_1 - \beta_4) (n_\mu^3 k^\mu)^2 = 0, \quad (2.136)$$

with corresponding eigenmode

$$c_a = \eta_{ab} n_\mu^b k^\mu. \quad (2.137)$$

General expression. We can express the solutions in the timelike and space-like cases in a compact form by using the orthonormality of the n_μ^α , (2.116), along with (2.115), (2.128), and the fact that⁷

$$\epsilon_{\alpha\beta\rho\sigma} n_\mu^\alpha n_\nu^\beta = \epsilon_{\mu\nu\alpha\beta} n_\rho^\alpha n_\sigma^\beta. \quad (2.138)$$

⁷This follows from the invariance of the Levi-Civita tensor,

$$\epsilon_{\alpha\beta\gamma\delta} n_\mu^\alpha n_\nu^\beta n_\rho^\gamma n_\sigma^\delta = \epsilon_{\mu\nu\rho\sigma}$$

plus orthonormality, (2.116).

Then plugging (2.119) and (2.130) into (2.118) yields the solutions

$$\delta A_\mu = \int d^4k q_\mu(k) e^{ik_\nu x^\nu}, \quad (2.139)$$

where either

$$q_\mu(k) = i\alpha^\nu k^\rho \frac{\bar{A}^\sigma}{m} \epsilon_{\mu\nu\rho\sigma} \quad \text{and} \quad \beta_1 k_\rho k^\rho + \beta_4 \left(\frac{\bar{A}_\mu k^\mu}{m} \right)^2 = 0 \quad \text{and} \quad \alpha^\nu \bar{A}_\nu = 0, \quad (2.140)$$

where α^ν are real-valued constants, or

$$q_\mu = i\alpha \left(\eta_{\mu\nu} \pm \frac{\bar{A}_\mu \bar{A}_\nu}{m^2} \right) k^\nu \quad \text{and} \quad \beta_* k_\rho k^\rho \pm (\beta_* - \beta_1 \pm \beta_4) \left(\frac{\bar{A}_\mu k^\mu}{m} \right)^2 = 0, \quad (2.141)$$

where α is a real-valued constant. The reality of the α 's follows from the condition, $q_\mu(k) = q_\mu^*(-k)$, that holds if and only if δA_μ in (2.118) is real. In (2.141), the “+” sign corresponds to the timelike background and the “−” sign to a spacelike background.

Chapter 3

Sigma-Model Æther

Theories of low-energy Lorentz violation by a fixed-norm “æther” vector field with two-derivative kinetic terms have a globally bounded Hamiltonian and are perturbatively stable only if the vector is timelike and the kinetic term in the action takes the form of a sigma model. Here we investigate the phenomenological properties of this theory. We first consider the propagation of modes in the presence of gravity, and show that there is a unique choice of curvature coupling that leads to a theory without superluminal modes. Experimental constraints on this theory come from a number of sources, and we examine bounds in a two-dimensional parameter space. We then consider the cosmological evolution of the æther, arguing that the vector will naturally evolve to be orthogonal to constant-density hypersurfaces in a Friedmann-Robertson-Walker cosmology. Finally, we examine cosmological evolution in the presence of an extra compact dimension of space, concluding that a vector can maintain a constant projection along the extra dimension in an expanding universe only when the expansion is exponential.

The contents of this chapter were written in collaboration with Sean Carroll, Tim Dulaney, and Heywood Tam and have been published in [2].

3.1 Introduction

Models of fixed-norm vector fields, sometimes called “æther” theories, serve a useful purpose as a phenomenological framework in which to investigate violations of Lorentz invariance at low energies [20, 21, 12, 22, 23, 24, 25]. For a recent review, see [13]. In the previous chapter (and in [1]) we argue that almost all such models are plagued by instabilities. For related work on stability in æther theories, see [29, 39, 44, 30, 27, 41, 48, 28].

There is one version of the æther theory that is stable under small perturbations and in which the Hamiltonian is globally bounded when only two-derivative terms are included in the action. This model is defined by a kinetic Lagrange density of the form

$$\mathcal{L}_\sigma^{\text{kinetic}} = -\frac{1}{2}(\nabla_\mu A_\nu)(\nabla^\mu A^\nu), \quad (3.1)$$

where A_μ is a dynamical timelike four-vector æther field. (The spacelike version has an unbounded Hamiltonian, and is unstable.) We refer to the theory defined by this action as “sigma-model æther,” due to its resemblance to a theory of scalar fields propagating on a fixed manifold with an internal metric, familiar from studies of spontaneous symmetry breaking. The æther theory is not identical to such a sigma model—in particular in curved space where covariant derivatives act on the vector—but the nomenclature is convenient.

Even though this theory is stable, it has an important drawback. It is conventional in æther models to give the vector field an expectation value by means of a Lagrange multiplier, which enforces the fixed-norm constraint

$$A_\mu A^\mu = -m^2. \quad (3.2)$$

We take m^2 to be positive and use a metric signature $(-+++)$, so that this defines

a timelike vector field. Despite the convenience of this formulation, it seems likely that a more complete version of the theory would arise as a limit of a theory in which the expectation value is fixed by minimizing a smooth potential of the form $V(A_\mu) = \xi(A_\mu A^\mu + m^2)^2$. As we showed in [1], any such theory would be plagued by ghosts and tachyons. As far as we can tell, therefore, the sigma-model æther theory cannot be derived from models with a smooth potential.

Nevertheless, as it is the only example of a Lorentz-violating æther theory that we are sure is globally well behaved, examining the dynamics and experimental constraints on this model is worthwhile. We undertake such an investigation in this chapter.

First we examine the degrees of freedom in this theory, taking into account the mixing with the gravitational field. There are three different massless modes, of spins 0, 1, and 2 in the æther rest frame.¹ Demanding that none of the modes propagate faster than light fixes a unique value for the coupling of the vector field to the Ricci tensor. We use experimental constraints on the preferred frame parameters $\alpha_{1,2}$ in the Parameterized Post-Newtonian (PPN) expansion to limit the magnitude of the vacuum expectation value, m . The spin-2 mode can propagate subluminally for some values of the vector field/Ricci tensor coupling; in such cases, very tight restrictions on the vacuum expectation value, m , due to limits from vacuum Čerenkov radiation of gravitons come into play.

Finally, we consider the cosmological evolution of the vector field in two different backgrounds. We study the evolution of the timelike vector field in a flat Friedmann-Robertson-Walker (FRW) universe and find that the vector field tends to align to be orthogonal to constant density hypersurfaces. In a background consisting of a timelike dimension, three expanding spatial dimensions, and one compact (nonexpanding)

¹The lack of rotational symmetry in frames other than the æther rest frame make classification of modes by spin in such frames impossible. But the æther rest frame has rotational symmetry, which allows for the spin classification with respect to this frame.

extra spatial dimension, we find that the vector field can evolve to have a non-zero projection in the direction of the compact extra dimension if the large dimensions are de Sitterlike. We take this as evidence that a timelike vector field with the Lagrangian that satisfies the aforementioned theoretical and experimental constraints would not lead to any significant departure from isotropy.

3.2 Excitations in the Presence of Gravity

We would like to understand the experimental constraints on, and cosmological evolution of, the sigma-model æther theory. For both of these questions, it is important to consider the effects of gravity. But whereas the flat-space model with a kinetic Lagrangian of the form (3.1) is unique, in curved space there is the possibility of an explicit coupling to curvature. The full action we consider is

$$S = \int d^4x \sqrt{-g} \left[\frac{1}{16\pi G} R - \frac{1}{2} (\nabla_\mu A_\nu)(\nabla^\mu A^\nu) + \frac{\alpha}{2} R_{\mu\nu} A^\mu A^\nu + \frac{\lambda}{2} (A_\mu A^\mu + m^2) \right]. \quad (3.3)$$

Here, λ is the Lagrange multiplier that enforces the fixed-norm constraint (3.2), α is a dimensionless coupling, $R_{\mu\nu}$ is the Ricci tensor and R is the curvature scalar. Note that, given the fixed-norm constraint, there are no other scalar operators that could be formed solely from A_μ and the Riemann tensor $R^\rho{}_{\sigma\mu\nu}$. By integrating by parts and using $R_{\mu\nu} A^\mu A^\nu = A^\nu [\nabla_\mu, \nabla_\nu] A^\mu$, this curvature coupling could equivalently be written purely in terms of covariant derivatives of A_μ ; the form (3.3) has the advantage of emphasizing that the new term has no effects in flat spacetime.

In [1] we showed that the sigma-model æther theory was stable in the presence of small perturbations in flat spacetime; the possibility of mixing with gravitons implies that we should check once more in curved spacetime. The equations of motion for

the vector field are

$$-\nabla_\mu \nabla^\mu A^\nu = \lambda A^\nu + \alpha R^{\mu\nu} A_\mu, \quad (3.4)$$

along with the fixed norm constraint from the equation of motion for λ . Assuming the fixed norm constraint, the equations of motion can be written in the form

$$\left(g^{\sigma\nu} + \frac{1}{m^2} A^\sigma A^\nu\right) (\nabla_\rho \nabla^\rho A_\sigma + \alpha R_{\rho\sigma} A^\rho) = 0. \quad (3.5)$$

The tensor $(g^{\sigma\nu} + A_\rho A_\nu/m^2)$ acts to take what would be the equation of motion in the absence of the constraint, and project it into the hyperplane orthogonal to A_μ .

The Einstein-æther system has a total of five degrees of freedom, all of which propagate as massless fields: one spin-2 graviton, one spin-1 excitation and one spin-0 excitation. Each of these dispersion relations can be written (in the short-wavelength limit) in frame-invariant notation as

$$k_\mu k^\mu = \left(\frac{1-v^2}{v^2}\right) \left(\frac{\bar{A}_\mu k^\mu}{m}\right)^2, \quad (3.6)$$

where v is the phase velocity in the æther rest frame. The squared phase velocities of the gravity-æther modes are [24]

$$v_2^2 = \frac{1}{1 - 8\pi G m^2 (1 + \alpha)} \approx 1 + 8\pi G m^2 (1 + \alpha) \quad (\text{spin-2}) \quad (3.7)$$

$$v_1^2 = \frac{2 - 8\pi G m^2 (1 + \alpha)(1 - \alpha)}{2(1 - 8\pi G m^2 (1 + \alpha))} \approx 1 + 4\pi G m^2 (1 + \alpha)^2 \quad (\text{spin-1}) \quad (3.8)$$

$$v_0^2 = \frac{2 - 8\pi G m^2}{(1 - 8\pi G m^2 (1 + \alpha))(2 + 8\pi G m^2 (1 - 2\alpha))} \approx 1 + 16\pi G m^2 \alpha \quad (\text{spin-0}) \quad (3.9)$$

where G is the gravitational constant appearing in Einstein's action. The approximate equalities hold assuming $8\pi G m^2 \ll 1$.²

²The relationship between the parameters in Eq. (3.3) (α , m^2) and those in Ref. [24] (c_1 , c_2 , c_3 , c_4)

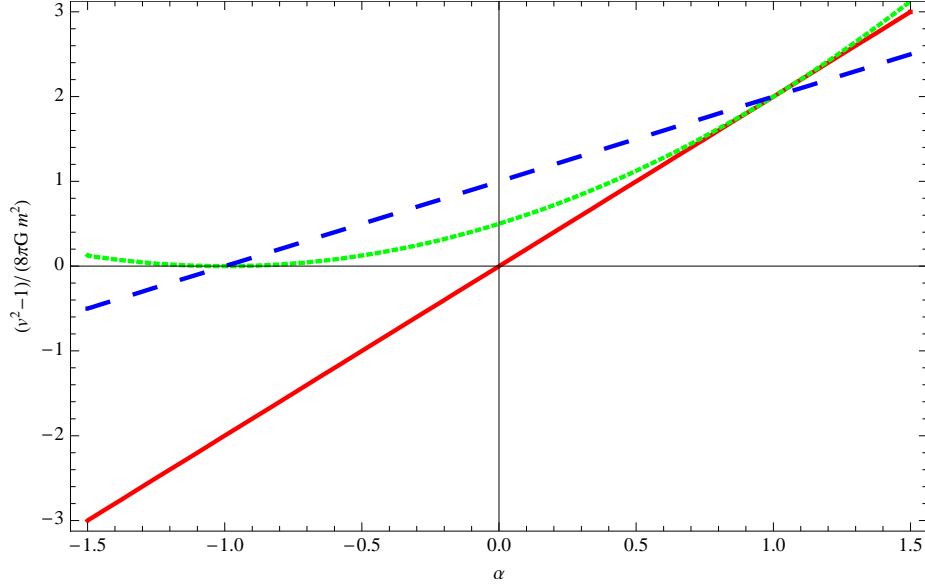


Figure 3.1: Æther rest frame mode phase velocities squared, v^2 , minus the speed of light in units of $8\pi G m^2$ as a function of α . The solid (red) line corresponds to spin-0, the small dashed (green) to spin-1, and the large dashed (blue) to spin-2. Only for $\alpha = -1$ do none of the modes propagate faster than light ($v^2 - 1 > 0$).

These squared mode phase velocities minus the squared speed of light are plotted in Fig. 3.1 as a function of α . It is clear that the only value of α for which none of the modes propagate superluminally ($v^2 > 1$) is

$$\alpha = -1. \quad (3.11)$$

We therefore have a *unique* version of a Lorentz-violating æther theory for which the Hamiltonian is bounded below (in flat space) and that is free of superluminal modes when coupled to gravity: the sigma-model kinetic term with an expectation value fixed by a Lagrange-multiplier constraint and a coupling to curvature of the form in (3.3) with $\alpha = -1$. In what follows, we will generally allow α to remain as a free parameter when considering experimental limits, keeping in mind that models with

is:

$$c_1 = 8\pi G m^2, \quad -c_2 = c_3 = \alpha 8\pi G m^2, \quad c_4 = 0. \quad (3.10)$$

$\alpha \neq -1$ are plagued by superluminal modes. We will find that the experimental limits on m are actually weakest when $\alpha = -1$.

Before moving on, however, we should note that the existence of superluminal phase velocities does not constitute *prima facie* evidence that the theory is ill behaved. There are two reasons for suspecting that superluminal propagation is bad. First, in [1], we showed that such models were associated with perturbative instabilities: there is always a frame in which small perturbations grow exponentially with time. Second, acausal propagation around a closed loop in spacetime could potentially occur if the background æther field were not constant through space [23, 30]. But in the presence of gravity, these arguments are not decisive. There now exists a scale beyond which we expect the theory to break down: namely, length scales on the order of M_{pl}^{-1} . Perhaps there is some length scale involved in boosting to a frame where the instability is apparent (or, equivalently, in approaching a trajectory that is a closed timelike curve) that is order M_{pl}^{-1} .

Again, in a background flat spacetime with a background timelike æther field $\bar{A}_\mu = \text{constant}$, the dispersion relations have the generic form

$$(v^{-2} - 1)(t^\mu k_\mu)^2 = k_\mu k^\mu, \quad (3.12)$$

where $t_\mu = \bar{A}_\mu/m$ characterizes the 4-velocity of the preferred rest frame. The velocity v^2 is given by Eqs. (3.7)-(3.9). In a boosted frame, where $t^\mu = (-\cosh \eta, \sinh \eta \hat{n})$, the frequency is given by

$$\frac{\omega}{|\vec{k}|} = \frac{-(1 - v^{-2}) \sinh \eta \cosh \eta (\hat{k} \cdot \hat{n}) \pm \sqrt{1 - (1 - v^{-2})(\cosh^2 \eta - \sinh^2 \eta (\hat{n} \cdot \hat{k})^2)}}{1 - (1 - v^{-2}) \cosh^2 \eta}. \quad (3.13)$$

Let us parameterize the boost in the standard way as

$$\cosh^2 \eta = \frac{1}{1 - \beta^2}, \quad 0 \leq \beta^2 < 1. \quad (3.14)$$

Then

$$\frac{\omega}{|\vec{k}|} = \frac{-(1 - v^{-2})\beta(\hat{k} \cdot \hat{n}) \pm \sqrt{1 - \beta^2} \sqrt{v^{-2} - \beta^2 + \beta^2(1 - v^{-2})(\hat{n} \cdot \hat{k})^2}}{v^{-2} - \beta^2}. \quad (3.15)$$

There is a pole in the frequency at $\beta^2 = v^{-2}$. The pole is physical if $v > 1$ and, (in the limit as $\hat{n} \cdot \hat{k} \rightarrow 0$) as β passes through the pole ($\beta^2 \rightarrow \beta^2 > v^{-2}$), the frequency acquires a nonzero imaginary part, which corresponds to growing mode amplitudes. (The frequency becomes imaginary at some $\beta^2 < 1$ as long as $\hat{n} \cdot \hat{k} \neq 1$.) The timescale on which the mode grows is set by $1/Im(\omega)$. In frames with a boost factor greater than the inverse rest-frame mode speed, $\beta > v^{-1}$, the timescale on which mode amplitudes grow is maximal for modes with wave vectors perpendicular to the boost direction ($\hat{n} \cdot \hat{k} = 0$) and is given by

$$T_{MAX}(\beta) = \frac{1}{|Im(\omega)|} = |\vec{k}|^{-1} \frac{\sqrt{\beta^2 - v^{-2}}}{\sqrt{1 - \beta^2}} \quad \text{when} \quad v^2 > 1. \quad (3.16)$$

We generically expect the linearized gravity analysis that led to the propagation speeds in Eqs. (3.6)-(3.9) to be valid for wave vectors that are much greater in magnitude than the energy scale set by other energy density in the space-time—generally, the Hubble scale, H . Thus the analysis makes sense for $|\vec{k}|^{-1} \ll H^{-1}$ and (as long as $1 - \beta^2$ is not infinitesimal) there will be instabilities on timescales less than the inverse Hubble scale and (unless $\beta^2 - v^{-2}$ is infinitesimal) greater than M_{Pl}^{-1} .

Thus, not only could superluminal propagation speeds lead to closed timelike curves and violations of causality, but the existence of instabilities on an unremarkable range of less-than-Hubble-radius timescales in boosted frames indicates that such

superluminal propagation speeds lead to instabilities. If $v > 1$, it appears as if instabilities can be accessed without crossing some scale threshold beyond which we'd expect the model to break down.

3.3 Experimental Constraints

We now apply existing experimental limits to the sigma-model æther theory, keeping for the moment α as well as m^2 as free parameters. Direct coupling of the æther field to Standard Model fields fits into the framework of the “Lorentz-violating extension” of the Standard Model considered in Ref. [21]. Such couplings are very tightly constrained by various experiments (for a discussion of experimental constraints, see Ref. [31]). The relevant limit from gravitational Čerenkov radiation in [30] translates to³

$$-8\pi G m^2(1 + \alpha) < 1 \times 10^{-15}. \quad (3.17)$$

Limits on PPN parameters give the strongest constraints on α and m^2 when $\alpha \approx -1$ (since the constraint in Eq. (3.17) is automatically satisfied). The preferred frame parameters must satisfy $|\alpha_1| < 10^{-4}$ and $|\alpha_2| < 10^{-7}$ [32]. We have the limits [13]

$$|\alpha_1| \approx |4\alpha^2(8\pi G_N m^2)| < 10^{-4} \quad \text{and} \quad |\alpha_2| \approx |(\alpha + 1)(8\pi G_N m^2)| < 10^{-7}, \quad (3.18)$$

where G_N is the gravitational constant as measured in our solar system or table-top experiments. This gravitational constant is related to the parameter in the action G

³Ref. [30] uses the same parameters as in [24, 13], thus the translation between our parameters and the parameters used in [24, 13, 30] is as stated in (3.10).

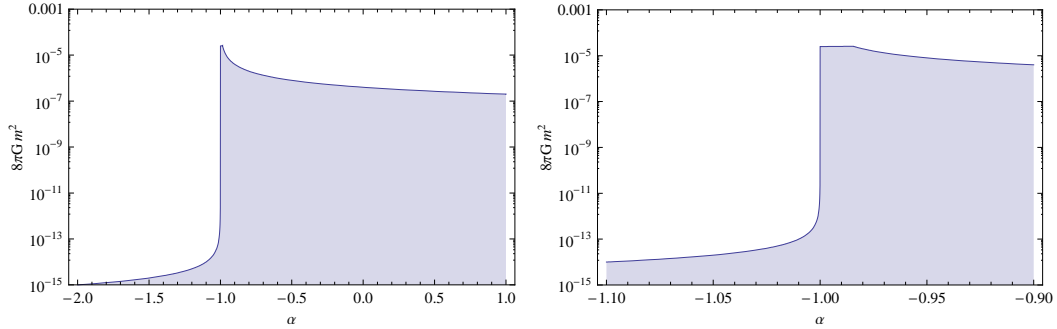


Figure 3.2: Parameter space allowed (shaded region) by constraints from Čerenkov radiation and PPN. The strongest constraint in the $\alpha < -1$ region is from Eq. (3.17), and for most of the $\alpha > -1$ region the strongest constraint is from the second inequality in Eq. (3.18). The plot on the right is a blowup of the small range of α for which the first constraint in Eq. (3.18) is strongest—when $\alpha = -1$ to within a couple of parts in one hundred.

by [23]

$$G_N = \frac{G}{1 - 4\pi G m^2}. \quad (3.19)$$

If we require that all modes have phase speeds v that satisfy $v^2 \leq 1$, then we must have $\alpha = -1$ and

$$8\pi G_N m^2 < 10^{-4} \quad (\alpha = -1). \quad (3.20)$$

All relevant constraints (allowing modes to have larger than unity phase velocities) are summarized in Fig. 3.2. Constraints from Big Bang Nucleosynthesis [23] are significantly weaker than the PPN and Čerenkov constraint above.

3.4 Cosmological Evolution

We now turn to the evolution of the sigma-model æther field in a cosmological background. It is usually assumed in the literature that the æther preferred frame coincides with the cosmological rest frame—*i.e.*, that in Robertson-Walker coordinates, a timelike æther field has zero spatial components, or a spacelike æther field has zero time component. Under this assumption, there has been some analysis of cosmolog-

ical evolution in the presence of æther fields [6, 27, 50, 51]. Cosmological alignment in a de Sitter background was considered in [52]. Evolution of vector field perturbations in a more general context, including the effect on primordial power spectra, was considered in [25, 53].

Here, we relax the aforementioned assumption. We determine the dynamical evolution of the æther alignment with respect to constant density hypersurfaces of flat FRW backgrounds, assuming that the æther field has a negligible effect on the form of the background geometry. We will show that a homogeneous timelike vector field tends to align in the presence of a homogeneous cosmological fluid such that its rest frame coincides with the rest frame of the cosmological fluid.

Take the background spacetime to be that of a flat FRW cosmology,

$$ds^2 = -dt^2 + a(t)^2(dx^2 + dy^2 + dz^2). \quad (3.21)$$

We take the equation state of the cosmological fluid to be $p_{fluid} = w\rho_{fluid}$. The Friedmann equation then implies

$$a(t) = t^{2/3(1+w)} \quad (3.22)$$

for $w \neq -1$, and

$$a(t) = e^{Ht}, \quad H = \text{constant} \quad (3.23)$$

for $w = -1$. We assume that m^2/M_P^2 is small, so that the backreaction of the vector field on the FRW geometry will be small, and the evolution of the vector field will be well approximated by its evolution in the FRW background.

Suppose the vector field is homogeneous. This is a reasonable assumption given that the background spacetime is homogeneous and therefore should only affect the time evolution of the vector field. We may use the rotational invariance of the FRW

background to choose coordinates such that the x -axis is aligned with the spatial part of the vector field. Then, without loss of generality, $A_0 = m \cosh(\phi(t))$ and $A_x = ma(t) \sinh(\phi(t))$. In this case the equations of motion reduce to,

$$\phi''(t) + 3H(t)\phi'(t) + [H^2(t) + \alpha H'(t)] \sinh(2\phi(t)) = 0, \quad (3.24)$$

where $H(t) = a'(t)/a(t)$. Expanding to first order in the angle ϕ , for $w \neq -1$ we have

$$\phi'' + \left[\frac{2}{(1+w)t} \right] \phi' + \left[\frac{8 - 12\alpha(1+w)}{9(1+w)^2 t^2} \right] \phi = 0. \quad (3.25)$$

It is a simple exercise to show that ϕ behaves as a damped oscillator for all $-1 < w < 1$ and $\alpha < \frac{2}{3(1+w)}$. For the case of a constant Hubble parameter ($w = -1$),

$$\phi(t) = Ae^{-Ht} + Be^{-2Ht}. \quad (3.26)$$

One can see even for large $\phi(t)$ that $|\phi(t)|$ generically decreases when $-1 < w < 1$ and $\alpha < \frac{2}{3(1+w)}$ because, since $\sinh(\phi) = -\sinh(-\phi)$, the essential features of the full equation mirror those of the linearized equation.

We conclude that a timelike vector field will generically tend to align to be purely timelike in the rest frame of the cosmological fluid, thereby restoring isotropy of the cosmological background. We do not examine the case of a spacelike æther field, since that is perturbatively unstable.

3.5 Extra Dimensions

Consider now the evolution of the vector field in a background spacetime with metric

$$ds^2 = -dt^2 + a(t)^2(dx^2 + dy^2 + dz^2) + dr^2. \quad (3.27)$$

This metric is the local distance measure for a spacetime in which the infinite spatial dimensions expand as a usual flat FRW metric, for general equation of state parameter w as discussed in the previous section, and a compact extra dimension with coordinate r does not expand. A scenario in which a spacelike æther is aligned completely along the compact fifth extra dimension was considered in [54].

The equations of motion are once again

$$(g^{\sigma\nu} + A^\sigma A^\nu / m^2)(\nabla_\rho \nabla^\rho A_\sigma + \alpha R_{\rho\sigma} A^\rho) = 0 \quad (3.28)$$

and $A_\mu A^\mu = -m^2$. Consider homogeneous configurations where, without loss of generality,

$$A_0 = m \cosh \phi(t), \quad A_x = a(t)m \sinh \phi(t) \cos \theta(t), \quad A_y = A_z = 0, \\ \text{and} \quad A_r = m \sinh \phi(t) \sin \theta(t). \quad (3.29)$$

The $\nu = 0$ equation of motion (Eq. (3.28)) reads

$$\left[\frac{1}{2}(5 - \cos 2\theta)(H^2(1 + \alpha) + \alpha H') - 2\alpha H^2 \cos^2 \theta - (\theta')^2 \right] \sinh 2\phi + 6H\phi' + 2\phi'' = 0. \quad (3.30)$$

When $\theta'^2 \ll H^2$, we can treat θ as being essentially constant and then the above equation determines the evolution of ϕ . Numerical simulations indicate that ϕ decays to zero, whatever the value of θ , if $-1 < \alpha < \frac{2}{3(1+w)}$. One can see the decay of ϕ (given the bounds on α) explicitly by expanding about $\phi = 0$ and $\theta = \text{constant}$ when ϕ is small.

If H is constant (*i.e.* the non-compact dimensions are de Sitterlike) and the vector field is aligned entirely along the timelike dimension and the compact dimension (so

$\theta = \pi/2$), then the equation of motion for $\phi(t)$ is

$$\phi''(t) + 3H\phi'(t) + \frac{3}{2}(1 + \alpha)H^2 \sinh(2\phi(t)) = 0, \quad (3.31)$$

the solution to which is

$$\phi(t) = A_+ e^{-\alpha_+ Ht/2} + A_- e^{-\alpha_- Ht/2}, \quad (3.32)$$

where

$$\alpha_{\pm} = 3 \left(1 \pm \sqrt{1 - \frac{4}{3}(1 + \alpha)} \right), \quad (3.33)$$

when $|\phi(t)| \ll 1$. If $1 + \alpha > 0$ then ϕ decays to zero. If $\alpha = -1$, ϕ decays to a (generically nonzero) constant, and ϕ can grow with time if $\alpha < -1$. It is interesting to see that, for the case where no perturbative modes propagate superluminally—the case where $\alpha = -1$ —the fixed-norm vector field can evolve during a de Sitter expansion phase so that it has a nonzero component in the compact fifth dimension while otherwise aligning so that isotropy is restored in the rest frame of the cosmological fluid. However, when the Universe enters a phase of expansion where $a(t) = t^{2/3(1+w)}$ and w is strictly greater than -1 (and less than 1), then the component of the vector field in the fifth dimension will decay away.

3.6 Conclusions

We investigated the dynamics of and limits on parameters in a theory with a fixed-norm timelike vector field whose kinetic term takes the form of a sigma model. We argued in the previous chapter that such sigma-model theories are the only æther models with two-derivative kinetic terms and a fixed-norm vector field for which the Hamiltonian is bounded below.

In the presence of gravity, the action for sigma-model æther is

$$S_A = \int d^4x \sqrt{-g} \left[\frac{1}{16\pi G} R - \frac{1}{2} (\nabla_\mu A_\nu) (\nabla^\mu A^\nu) + \frac{\alpha}{2} R_{\mu\nu} A^\mu A^\nu + \frac{\lambda}{2} (A_\mu A^\mu + m^2) \right]. \quad (3.34)$$

We showed that the five massless degrees of freedom in the linearized theory will not propagate faster than light only if $\alpha = -1$, and we argued that faster-than-light degrees of freedom generically lead to instabilities on less-than-Hubble-length timescales. In the special case $\alpha = -1$, the vacuum expectation value m^2 must be less than about $10^{-4} M_p^2$, where M_p is the Planck mass, in order to comply with limits on the PPN preferred frame parameter α_2 . Relaxing the $\alpha = -1$ assumption, we summarized the strongest limits on the parameters $\{\alpha, m\}$ (from gravitational Čerenkov radiation and the PPN preferred frame parameters) in Fig. 3.2.

We also showed that the æther field tends to dynamically align such that it is orthogonal to constant density hypersurfaces for the theoretically and experimentally relevant portion of the parameter space. The dynamics forces the rest frame of the æther and that of the perfect fluid dominating the cosmological evolution to coincide. Finally, we showed that the dynamics allows for the possibility of a non-zero spatial component in a non-expanding fifth dimension during a de Sitter era. Even a spatial component in a non-expanding fifth dimension will decay away during non-de Sitter eras, *e.g.*, in a matter- or radiation-dominated universe. We take this as evidence that æther fields with well-behaved semi-classical dynamics will not lead to any significant departure from isotropy.

Chapter 4

Primordial Perturbations from Anisotropic Inflation

We examine cosmological perturbations in a dynamical theory of inflation in which an abelian gauge field couples directly to the inflaton, breaking conformal invariance. When the coupling between the gauge field and the inflaton takes a specific form, inflation becomes anisotropic and anisotropy can persist throughout inflation, avoiding Wald’s no-hair theorem. After discussing scenarios in which anisotropy can persist during inflation, we calculate the dominant effects of a small persistent anisotropy on the primordial gravitational wave and curvature perturbation power spectra using the “in-in” formalism of perturbation theory. We find that the primordial power spectra of cosmological perturbations gain significant direction dependence and that the fractional direction dependence of the tensor power spectrum is suppressed in comparison to that of the scalar power spectrum.

The contents of this chapter were written in collaboration with Tim Dulaney and have been published in [3].

4.1 Introduction

Inflation gives a compelling explanation of the flatness, homogeneity, and isotropy of our Universe on large scales. It also generically predicts a nearly scale-invariant

spectrum of density perturbations, which is consistent with our observations of the cosmic microwave background (CMB) and of structure formation. Because of these successes, the inflationary paradigm has dominated very early Universe cosmology in recent years.

In this chapter we focus on the prediction of isotropy from inflation. The no-hair theorem of inflation states, roughly speaking, that an initially expanding, homogeneous universe with positive cosmological constant, Λ , and matter satisfying the dominant energy condition will become indistinguishable from a universe with de Sitter geometry on a time scale of $\sqrt{3/\Lambda}$ [10]. Because of the no-hair theorem, isotropy is generally taken as a prediction of inflation.

But there could be ways around the no-hair theorem. For example, models with spacelike vector fields that get vacuum expectation values can lead to a preferred direction during inflation, evading the no-hair theorem because the vector field stress-energy tensor does not satisfy the dominant (or even the weak) energy condition [6]. However, such “æther” models have been shown to be unstable [27, 14, 1].

Recently, another model has been shown to support a persistent anisotropy during inflation [7]. In this model, there is a nonminimal coupling between a $U(1)$ gauge field and the inflaton, essentially leading to a time-dependent $U(1)$ charge during inflation:

$$S = \int d^4x \sqrt{-g} \left[\frac{R}{2\kappa^2} - \frac{1}{2}(\partial_\mu \phi)(\partial^\mu \phi) - V(\phi) - \frac{f^2(\phi)}{4} F_{\mu\nu} F^{\mu\nu} \right]. \quad (4.1)$$

Here, the $U(1)$ field strength, $F_{\mu\nu}$, may or may not be the electromagnetic field strength. When the coupling, $f(\phi)$, between the inflaton, ϕ , and the $U(1)$ field takes a particular form and there exists a nonzero homogeneous $U(1)$ seed field, an anisotropy persists throughout inflation even though the space-time is undergoing nearly exponential expansion. More specifically, the “electric” field contributes non-negligible extra negative pressure in the direction in which it points, which causes

space-time to expand more slowly in that direction.

The model avoids the no-hair theorem by having (1) expansion that is not purely exponential and (2) a coupling between the inflaton and other matter. The mechanism for evasion of the no-hair theorem shows up in our results in the following ways: (A) all modifications to power spectra associated with the anisotropy go to zero when slow-roll parameters vanish and (B) isotropic dynamics is quickly restored if the inflaton-dependent coupling that breaks conformal invariance goes to a constant (as is the case at the end of inflation, when the inflaton field relaxes to the minimum of its potential).

All of the standard energy conditions are satisfied in this model, which means it should not be plagued by stability issues as in æther models. The model does, however, suffer from the standard fine-tuning problems of single field inflation. Nevertheless, to our knowledge this model could be the first consistent model of inflation that evades the no-hair theorem and includes anisotropy at a significant level. It is therefore interesting to investigate whether the model is truly consistent and to investigate its potential astrophysical signatures.

To that end, in this chapter we consider gauge-invariant cosmological perturbations in this anisotropic inflation model. We consider and discuss a model generalized from that of [7], and extend their formula for the relation between the anisotropic expansion parameter and the slow-roll parameter to include arbitrary forms of the inflaton potential. We also present the dominant effect of the anisotropy on the power spectra of tensor, vector and scalar perturbation correlations at the end of inflation.

Our main conclusions are the following:

- The power spectra for gravitational wave and curvature perturbations can develop dramatic direction dependence for very small values of the anisotropy parameter¹ if the parameter is nearly constant for a large period of inflation.

¹The anisotropy parameter is basically the fractional difference between the rate of expansion in

- The main cause of direction-dependence of the power spectra is a coupling between the $U(1)$ vector degrees of freedom to both tensor and scalar degrees of freedom through the anisotropic background. These interactions significantly affect the power spectra of modes after horizon crossing.
- The ratio of the fractional direction-dependent change in the gravitational wave power spectrum over that of the curvature perturbation power spectrum is nearly equal to the tensor-to-scalar ratio. In particular, the curvature perturbation power spectrum has much stronger direction dependence than the gravitational wave power spectrum.
- For a given scale, the tensor and scalar power in modes with wave vector perpendicular to the preferred direction is greater than the power in modes with wave vector parallel to the preferred direction.²
- There is no indication that the anisotropic inflation model is unstable. (*E.g.*, there are no ghosts.) This should be unsurprising since the stress-energy tensor for matter in the model satisfies the dominant energy condition.

Many have studied inflationary scenarios with actions similar to (4.1), interpreting $F_{\mu\nu}$ as the standard model electromagnetic field strength, in the context of explaining the existence of large-scale magnetic fields in the Universe. Initially Parker [55] and then Turner and Widrow [56] showed that magnetic fields produced in an inflationary Universe are “uninterestingly small” (*i.e.*, too small to possibly account for the observed large-scale magnetic fields in the Universe) unless the conformal invariance of the electromagnetic field is broken. The generation of seed magnetic fields starting from the action in (4.1) and a particular $f(\phi)$ was considered in [57] and more recently in [58]. Generic predictions for magnetic fields in a large class of models, of which

the preferred direction and that of a perpendicular direction.

²*I.e.*, the parameter g_* (see equation (4.39)), as defined in [6], that characterizes the direction-dependence of the power spectrum due to a preferred direction is *negative*.

the model we consider here is an example, were presented by Bamba, *et. al.* [59]; the particular realization of the model we consider in this chapter is what these authors refer to as the “weak coupling case”. Magnetogenesis, including the backreaction due to electromagnetic fields, in the inflationary scenario we consider here was considered in [60]. For a review of the generation of magnetic fields during inflation in a more general context see, for example, [61].

More recently, the effect of vector fields during inflation has been studied in the context of their effects on the curvature perturbation power spectrum. A “vector curvaton” scenario, in which a vector field with time-varying mass and Maxwell-type kinetic coupling term contributes to the curvature power spectrum, was found in [62] to allow significant anisotropic contributions to the curvature spectrum and bispectrum if the vector field remains light until the end of inflation. A similar massless vector curvaton scenario was considered in [63] and again the possibility of significant anisotropic contributions was found.³ The anisotropic contribution of vector field perturbations to primordial curvature perturbation correlations in various inflationary scenarios was also considered in [25, 51, 64, 65, 66, 67]. Perturbations of what correspond to our cross polarization gravitational wave degree of freedom were studied in [68], but in a scenario in which a second scalar field, uncoupled to the $U(1)$ field and the scalar field that couples to the $U(1)$ field, causes a transition back to isotropic expansion before the end of inflation.

This chapter is organized as follows. In §4.2, we introduce the model. In §4.3, we discuss our philosophy and methods for calculating and analyzing primordial perturbation spectra. Finally, in §4.4 and §4.5 we calculate the primordial perturbation spectra and briefly discuss stability. We summarize our conclusions in §4.6.

³Both studies employed the δN formalism in calculating the curvature perturbation power spectra.

4.2 Model and Background Solution

We consider a space-time governed by the following action [7]:

$$S = \int d^4x \sqrt{-g} \left[\frac{R}{2\kappa^2} - \frac{1}{2}(\partial_\mu \phi)(\partial^\mu \phi) - V(\phi) - \frac{f^2(\phi)}{4} F_{\mu\nu} F^{\mu\nu} \right], \quad (4.2)$$

where $g = \det(g_{\mu\nu})$, R is the Ricci scalar, ϕ is the inflaton, and $F_{\mu\nu} = \partial_\mu A_\nu - \partial_\nu A_\mu$ is a $U(1)$ gauge field strength. For convenience, we'll refer to the $U(1)$ field as the “electromagnetic” (EM) field, even though it need not be the standard model EM field. Here we've defined

$$\kappa^2 \equiv 8\pi G = 1/M_{\text{Planck}}^2. \quad (4.3)$$

We assume that the background is homogeneous, and that there is a nonzero homogeneous electric field.⁴ We orient coordinates such that $F_{ij} = F_{\eta y} = F_{\eta z} = 0$ and $F_{\eta x} \neq 0$. One could just as easily have chosen to consider a homogeneous magnetic field. This choice does not change the form of the background stress tensor, and we expect the results of this chapter to apply in the magnetic field case as well. However, allowing for both electric and magnetic fields of arbitrary relative alignment is beyond the scope of this chapter.

The background space-time is Bianchi I and the metric can be written in the following form by appropriate choice of coordinate axes:⁵

$$ds^2 = a(\eta)^2 \left(-d\eta^2 + \gamma_{ij}(\eta) dx^i dx^j \right), \quad (4.4)$$

⁴At least we assume that the “electric” field was aligned in our causal patch. We will not consider the effects of regions with differing directions of alignment of the electric field.

⁵The form is chosen so that the spatial metric has unit determinant (and therefore scaling or translating $\beta(\eta)$ does not affect the spatial volume element).

where⁶

$$\gamma_{xx} = e^{-4\beta(\eta)}, \quad \gamma_{yy} = \gamma_{zz} = e^{2\beta(\eta)} \quad \text{and} \quad \gamma_{ij} = 0 \quad \text{for all } i \neq j. \quad (4.5)$$

Since g is independent of β , the scale factor, a , completely characterizes the space-time volume. For convenience we define α to be the logarithm of the scale factor, so

$$a = e^\alpha. \quad (4.6)$$

In parametrizing the metric, we've used the conventions of [69]. The solution to the background electromagnetic field equation of motion is then [7],

$$F_{\eta x} = p_A \frac{e^{-4\beta(\eta)}}{f^2(\bar{\phi})}, \quad (4.7)$$

where p_A is an integration constant of mass dimension two and a prime indicates a derivative with respect to conformal time η . In these coordinates, Einstein's equations take the form [7]

$$\alpha'^2 = \beta'^2 + \frac{\kappa^2}{3} \left[\frac{\phi'^2}{2} + e^{2\alpha} V(\bar{\phi}) + \frac{p_A^2 e^{-2\alpha-4\beta}}{2f^2(\bar{\phi})} \right], \quad (4.8)$$

$$\alpha'' = -2\alpha'^2 + \kappa^2 e^{2\alpha} V(\bar{\phi}) + \frac{p_A^2 \kappa^2 e^{-2\alpha-4\beta}}{6f^2(\bar{\phi})}, \quad (4.9)$$

$$\beta'' = -2\alpha'\beta' + \frac{p_A^2 \kappa^2 e^{-2\alpha-4\beta}}{3f^2(\bar{\phi})}. \quad (4.10)$$

Given Einstein's equations above, the equation of motion for ϕ is redundant.⁷

It was shown that inflation can occur for suitable initial conditions such that the Universe is initially expanding, and that the energy density of the vector field will remain almost constant with respect to the inflaton energy density if $f(\phi) \propto$

⁶An equivalent ansatz would have been: $ds^2 = -dt^2 + a_{\parallel}(t)^2 dx^2 + a_{\perp}(t)^2 (dy^2 + dz^2)$.

⁷Recall that Einstein's equations and the matter field equations are related through the conservation equation, $\nabla_{\mu} T_{\nu}^{\mu} = 0$, where T_{ν}^{μ} is the matter stress-energy tensor.

$e^{-2\alpha}$ [7]. (Recall that if there's no inflaton-electromagnetic coupling, the ratio of electromagnetic energy density to inflaton energy density decays as a^{-4} .) Let us briefly show how this can occur.

If expansion is nearly exponential (in cosmic time), then the “slow-roll” parameters,

$$\epsilon \equiv -\frac{\partial_t H}{H^2} = \frac{\alpha'^2 - \alpha''}{\alpha'^2} \quad (4.11)$$

$$\delta \equiv \frac{\partial_t^2 H}{2H\partial_t H} \quad (4.12)$$

are very small compared to one and as usual, $H \equiv \frac{\partial_t a}{a}$.⁸ Higher derivatives of H must, of course, also be small if expansion is nearly exponential.

The field equations (4.8), (4.9) and (4.10), can be cast in the following form:

$$\hat{\rho}_A \equiv \frac{\kappa^2 p_A^2 e^{-4\beta}}{2a^2 f^2(\bar{\phi}) \alpha'^2} = \frac{3}{2} \left(3\Sigma - \epsilon\Sigma + \frac{\Sigma'}{\alpha'} \right) \quad (4.14)$$

$$\hat{\rho}_\phi \equiv \frac{a^2 \kappa^2 V(\bar{\phi})}{\alpha'^2} = 3 - \epsilon - \frac{3}{2}\Sigma + \frac{\epsilon}{2}\Sigma - \frac{\Sigma'}{2\alpha'} = 3 - \epsilon - \frac{1}{3}\hat{\rho}_A \quad (4.15)$$

$$\frac{\kappa^2 \bar{\phi}'^2}{\alpha'^2} = 2\epsilon - 6\Sigma + 2\epsilon\Sigma - 6\Sigma^2 - 2\frac{\Sigma'}{\alpha'} = 2\epsilon - \frac{4}{3}\hat{\rho}_A - 6\Sigma^2 \quad (4.16)$$

$$\text{where } \Sigma \equiv \beta'/\alpha'. \quad (4.17)$$

The quantities $\hat{\rho}_\phi$ and $\hat{\rho}_A$ are dimensionless energy densities, normalized by the Hubble scale squared times the Planck mass squared.

In standard single field inflation with an inflaton potential V , for example, one finds from the field equations that $\frac{\kappa\phi'}{\alpha'} \sim \sqrt{\epsilon}$, so that if expansion is nearly exponential, then the inflaton must be slowly rolling. Taking derivatives of the above equations in the isotropic case, one can find expressions for derivatives of V in terms of slow-roll

⁸Note that

$$\frac{\epsilon'}{\alpha'} = 2\epsilon(\epsilon + \delta). \quad (4.13)$$

parameters—thus yielding requirements of a potential that can give rise to inflation.

From (4.15) and (4.14) one finds

$$\frac{\hat{\rho}'_\phi}{\hat{\rho}_\phi \alpha'} = \frac{\partial_\phi V}{\kappa V} \frac{\kappa \bar{\phi}'}{\alpha'} + 2\epsilon = \frac{-\frac{\epsilon'}{\alpha'} - \frac{1}{3} \frac{\hat{\rho}'_A}{\alpha'}}{3 - \epsilon - \frac{1}{3} \hat{\rho}_A} \quad (4.18)$$

$$\frac{\hat{\rho}'_A}{\hat{\rho}_A \alpha'} = -4 - 2 \frac{\partial_\phi f}{\kappa f} \frac{\kappa \bar{\phi}'}{\alpha'} + 2\epsilon - 4\Sigma = \frac{2\frac{\Sigma'}{\alpha'} + \dots}{3\Sigma - \epsilon\Sigma + \frac{\Sigma'}{\alpha'}} \quad (4.19)$$

where $\dots \sim \mathcal{O}(\Sigma \frac{\epsilon'}{\alpha'}, \epsilon \frac{\Sigma'}{\alpha'}, \frac{\Sigma''}{\alpha'^2})$.

We can glean a fair bit of information from equations (4.14) - (4.19) without much effort. First, what if expansion were purely exponential so that $\delta = \epsilon = 0$? From (4.16) we can immediately see that $\hat{\rho}_A$ and Σ had better then also be zero based simply on the fact that $\frac{\kappa^2 \bar{\phi}'^2}{\alpha'^2}$, $\hat{\rho}_A$, and Σ^2 are positive. This could be seen as confirmation of the no-hair theorem; anisotropy can exist only if expansion is *not* purely exponential.⁹ Similarly, if ϵ is small, then $\hat{\rho}_A$ and Σ had also better be small. In particular, even in small field models of inflation where typically $\epsilon \ll \delta \ll 1$, the anisotropy parameters Σ and $\hat{\rho}_A$ must be order ϵ or smaller. Second, from (4.18) we see that $\hat{\rho}_\phi$ is nearly constant with respect to the Hubble parameter if ϵ and Σ are small. Also from (4.18) we see that

$$\frac{\partial_\phi V}{\kappa V} \frac{\kappa \bar{\phi}'}{\alpha'} = -2\epsilon + \mathcal{O}(\epsilon'/\alpha') + \dots \quad (4.21)$$

Third, from (4.19), if ϵ and Σ are small, we see that $\hat{\rho}_A$ decreases rapidly with respect to the Hubble parameter *unless*

$$\frac{f'}{f\alpha'} \lesssim -2 \quad (4.22)$$

⁹A more direct confirmation of the no-hair theorem comes from supposing $\phi' = 0$ (and, for simplicity, $\epsilon \ll 1$) so that $V(\phi)$ functions as a cosmological constant. Then from (4.16) and (4.15)

$$\frac{d \log \hat{\rho}_A}{dt} \approx -4 \frac{d}{dt} \alpha \approx -4\kappa \sqrt{\frac{V(\phi)}{3}}. \quad (4.20)$$

So $\hat{\rho}_A$, and thus by (4.14) also ϵ and Σ , go to zero on the time scale promised by the no-hair theorem.

or equivalently unless

$$\frac{\partial_\phi f}{\kappa f} \lesssim -2/\left(\frac{\kappa \bar{\phi}'}{\alpha'}\right). \quad (4.23)$$

Now since

$$\left(\frac{\partial_\phi V}{\kappa V}\right)^{-1} \sim \pm \sqrt{1/2\epsilon} \sqrt{1 - 3\Sigma/\epsilon + \dots} \sim -\left(\frac{\kappa \bar{\phi}'}{\alpha'}\right)^{-1} \quad (4.24)$$

a ready choice for the coupling function, f , if one wants the energy density of the electromagnetic field (and thus the anisotropy) not to decay rapidly with respect to the inflaton energy density, is thus

$$f(\phi) = \exp \left\{ 2c\kappa \int \left(\frac{\partial_\phi V}{\kappa V}\right)^{-1} d\phi \right\} \quad (4.25)$$

where c is an order one constant. This is the coupling function motivated and examined in [7]. Let's suppose the coupling function is of this exact form, so

$$\frac{\hat{\rho}'_A}{\hat{\rho}_A \alpha'} = -4 - 4c \left(\frac{\kappa \bar{\phi}'}{\alpha'}\right)^2 \left(\frac{\partial_\phi V}{\kappa V} \frac{\kappa \bar{\phi}'}{\alpha'}\right)^{-1} + 2\epsilon - 4\Sigma \quad (4.26)$$

$$= -4 - 4c(2\epsilon - 6\Sigma + \dots)(-2\epsilon + \mathcal{O}(\epsilon'/\alpha') + \dots)^{-1} + 2\epsilon - 4\Sigma \quad (4.27)$$

$$= (c-1)4 - 4(3c)\frac{\Sigma}{\epsilon} + \dots \quad (4.28)$$

Suppose initially that $\Sigma \ll \epsilon$. If $c < 1$ then $\hat{\rho}_A$ decreases along with Σ as long as ϵ is small. Anisotropy is wiped out (albeit much more slowly than in the case where $f(\phi) = 1$). If $c > 1$, then $\hat{\rho}_A$ initially increases, as does Σ (see (4.14)). The derivative of the electromagnetic field energy density will thus approach zero, $\frac{\hat{\rho}'_A}{\hat{\rho}_A \alpha'} \longrightarrow 0$, and so $\hat{\rho}_A$ and Σ will become nearly constant for a time. If Σ is initially greater than $\frac{(c-1)}{3c}\epsilon$, then $\hat{\rho}_A$ and Σ will initially decrease, ϕ will climb its potential, and then it will fall back down (slowly) after Σ has approached a constant [7].

From (4.14) one can see that if Σ is approximately constant then Σ must be

positive. So when the space-time undergoes anisotropic expansion in this model (and Σ is nearly constant) the preferred direction expands more slowly than the perpendicular directions.

When (4.25) holds, we can find an expression for Σ in terms of the slow-roll parameter during the period in which it is nearly constant. Assuming

$$\mathcal{O}(\epsilon) \approx \mathcal{O}(\delta), \quad c - 1 > \mathcal{O}(\epsilon), \quad \Sigma \lesssim \mathcal{O}(\epsilon), \quad \frac{\Sigma'}{\alpha'} \lesssim \mathcal{O}(\epsilon\Sigma), \quad \left(\frac{\Sigma'}{\alpha'}\right)' / \alpha' \lesssim \mathcal{O}(\epsilon^2\Sigma) \quad (4.29)$$

we can set the two different expressions for $\partial_\phi V/V$ derived from equations (4.18) and (4.19) equal to each other. Using this method we find

$$\Sigma \equiv \frac{\beta'}{\alpha'} = \frac{c-1}{3c}\epsilon + \frac{1+c-4c^2}{18c^2}\epsilon^2 + \frac{1-2c-4c^2}{18c^2}\epsilon\delta + \dots \quad \text{assuming } c-1 > \mathcal{O}(\epsilon). \quad (4.30)$$

The authors of [7] derived this expression to first order in ϵ for the particular potential $V = \frac{1}{2}m^2\phi^2$ and argued that Σ generically tracks the slow-roll parameter for general potentials. We find that the expression (4.30) actually holds for any potential V in a slow-roll regime ($\epsilon, \delta \ll 1$).

As $c \rightarrow 1$, the story is a bit different. For example, if $c = 1$, looking back to equations (4.26) - (4.28) one finds that $\hat{\rho}_A$, if it is initially greater in magnitude than $\mathcal{O}(\epsilon^2)$, decreases until it's on the order of ϵ^2 , and then stays nearly constant. From numerical studies it appears that if $\hat{\rho}_A$ is initially much greater in magnitude than $\mathcal{O}(\epsilon^2)$, then it will rapidly settle to a value much smaller than $\mathcal{O}(\epsilon^2)$. If the magnitude of $\hat{\rho}_A$ is initially on the order of ϵ^2 or less, then it will stay very nearly constant until the end of inflation. An example with $c = 1$ is provided in Fig. 4.1.

The trick of this model is to choose $f(\phi)$, given $V(\phi)$, such that the electromagnetic field energy density does not decay rapidly with respect to the inflaton energy density

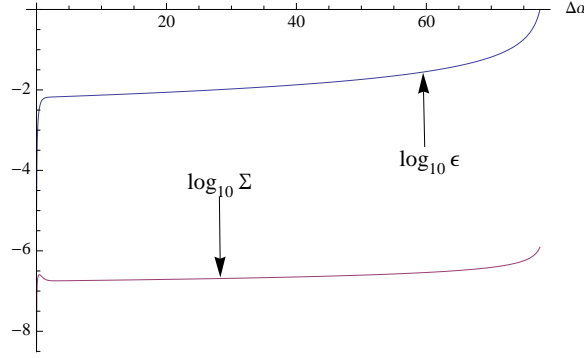


Figure 4.1: Log plot of Σ and ϵ as a function of e -foldings ($\Delta\alpha = \alpha - \alpha_0$) during inflation. The plot was generated with the potential $V = \frac{1}{2}m^2\phi^2$ and coupling function $f(\phi) = \exp\left[\frac{\kappa^2\phi^2}{2}\right]$. The initial conditions were $\phi_0 = 17.5/\kappa$, $\phi'_0 = 0$, $\alpha_0 = -75$, $\beta_0 = 0$ and $\beta'_0 = 0$. The constants m and p_A were chosen so that initially $\rho_A/\rho_\phi \approx 10^{-6}$. Notice that Σ very quickly settles to a value that is somewhat smaller than the square of the slow-roll parameter ϵ .

during inflation. We saw above that a choice guaranteed to work is

$$f(\phi) \approx \exp\left\{2\kappa \int \left(\frac{\partial_\phi V}{\kappa V}\right)^{-1} d\phi\right\}. \quad (4.31)$$

For example, if $V(\phi) \propto \phi^n$, then $f(\phi) \approx \exp[\kappa^2\phi^2/n]$. What if we were to choose instead, say, $f(\phi) \approx \exp[\lambda\kappa\phi]$? Then we would have

$$\frac{\hat{\rho}'_A}{\hat{\rho}_A\alpha'} = -4 - 2\lambda\frac{\kappa\bar{\phi}'}{\alpha'} + 2\epsilon - 4\Sigma. \quad (4.32)$$

If λ is order one, then the anisotropy will rapidly decay. However, if λ were large enough in magnitude then the anisotropy could persist for a good portion of inflation.

In our analysis, we will use only the background equations of motion, leaving $f(\phi)$ and $V(\phi)$ generic. We will then be interested in scenarios in which anisotropy can persist over several e -folds—scenarios in which $\frac{f'}{f\alpha'} = -2 + \mathcal{O}(\epsilon)$ and where $\hat{\rho}_A \approx 9\Sigma/2$ is approximately constant. We saw that consistency of the background equations and a slow-roll scenario dictates that $\hat{\rho}_A$ must be order ϵ or smaller. We also discussed specific examples of functions, $f(\phi)$, that can lead to such scenarios (assuming, oth-

erwise, a slow-roll scenario, $\epsilon, \delta \ll 1$). In order to calculate primordial power spectra, we will use the “in-in” formalism of perturbation theory, assuming

- $\epsilon \ll 1, \delta \ll 1$
- $\hat{\rho}_A \approx 9\Sigma/2 \lesssim \mathcal{O}(\epsilon)$
- $\hat{\rho}'_A/(\hat{\rho}_A\alpha') \lesssim \mathcal{O}(\epsilon)$.

4.3 Perturbations: Setup and Strategy

Our goal is to examine whether the background described in the previous section (slightly generalized from the space-time of [7]) is perturbatively stable, and to examine its signature at the level of primordial perturbation spectra.

We have calculated the quadratic action for dynamical modes in terms of the gauge-invariant variables defined in appendix 4.A. We calculated the action to quadratic order in perturbations starting with the form of the second order Einstein-Hilbert action given in appendix 4.B, and a similar expression for the quadratic-order matter action. We worked in Newtonian gauge and used a differential geometry package in *Mathematica* to massage the quadratic action into the (relatively) simple, manifestly gauge-invariant form presented in §4.4 and §4.5.

Regarding perturbative stability of the background, we find that there are no ghosts (fields with wrong-sign kinetic terms), and no other indication of instability at the quadratic level. Here, we take “perturbative stability” to mean that dimensionless combinations of fields assumed to be much less than one in the perturbative expansion of the action remain small. We find that such small quantities do indeed stay small.

In the remainder of this section we describe how we set up the calculation and analysis of perturbation spectra; we describe the physical scenario, the expression for expectation values in the “in-in” formalism, the definitions for the relevant degrees of freedom, and, finally, the current bound on a preferred direction during inflation. In §4.4 and §4.5 we calculate power spectra and briefly discuss stability.

4.3.1 Physical Scenario

Perturbations from inflation are usually assumed to be generated in the following way [70]:

- Quantum mechanical perturbative modes are in their ground state throughout inflation. So the vacuum expectation value of individual modes is zero, though the variance is generally nonzero.
- The normalization of the ground states is such that when the modes are well within the horizon, the canonically normalized¹⁰ fields, ϕ , obey a simple harmonic oscillator equation and satisfy the canonical commutation relations.¹¹
- As modes cross the horizon, their correlations are “frozen in” and translate into classical perturbations that lead to, for example, density perturbations that seed the formation of structure in the Universe and lead to temperature anisotropies of the cosmic microwave background radiation.

We shall assume the same, with one complication. We assume the quantity, $\Sigma \equiv \beta'/\alpha'$, which characterizes the deviation from isotropy, is nonzero so that expansion of the background space-time is slightly anisotropic, and modes that corresponded

¹⁰In conformal time, the kinetic term for a canonically normalized field, ϕ , in the quadratic action takes the form $\frac{1}{2}\phi'^2$.

¹¹Specifically,

$$[\partial_\eta \phi(\eta, \vec{x}), \phi(\eta, \vec{y})] = -i\hbar \delta^3(\vec{x} - \vec{y}) \quad (4.33)$$

where η is conformal time.

to scalar, vector, and tensor degrees of freedom in the isotropic background are now coupled. (Several scenarios in which this can occur were discussed in §4.2.) Because of the coupling of modes, the amplitudes of tensor, vector, and scalar perturbations are not separately conserved outside the horizon. As the inflaton decays at the end of inflation, the dynamics becomes isotropic again, and tensor, scalar, and vector modes decouple. At this point, superhorizon perturbations should be frozen in. We are therefore interested in the correlations of perturbations at the end of inflation. Especially if the $U(1)$ field in our model were interpreted as the electromagnetic field, the details of the reheating process at the end of inflation could also be important in calculating the direction dependence of CMB power spectra. In this chapter, however, we will only examine the effects of the gauge field on curvature and gravitational wave power spectra until just before reheating.

4.3.2 Correlations Using “in-in” Formalism

Because in the context of cosmological perturbations as described above we know only the quantum “in” states and we’re interested in expectation values evaluated at a particular time, we use the “in-in” formalism of perturbation theory (see *e.g.*, [15]). We separate our Hamiltonian into a free portion H_0 and an interacting portion H_I . The interaction-picture (free) fields’ evolution is determined by the free Hamiltonian. The expectation value for a general operator X at (conformal) time η can be written as

$$\begin{aligned} \langle X(\eta) \rangle = & \langle X^I(\eta) \rangle + i \int^\eta d\eta' \langle [H_I(\eta'), X^I(\eta)] \rangle \\ & + (i)^2 \int^\eta d\eta' \int^{\eta'} d\eta'' \langle [H_I(\eta'), [H_I(\eta''), X^I(\eta)]] \rangle + \dots \end{aligned} \quad (4.34)$$

where the ellipsis denotes terms with more powers of H_I and where X^I is the interaction-picture operator.

It should be noted that corrections of quadratic (or higher) order in the interaction Hamiltonian can lead to ambiguities when the details of the contour integration are not carefully considered [71]. We will work only to linear order in H_I , and therefore we need not worry about such ambiguities.

4.3.3 Decomposition of Perturbations

Since the background space-time is homogeneous, we decompose our perturbations into Fourier modes

$$\delta(x^i, \eta) = \int \frac{d^3k}{(2\pi)^3} e^{ik_j x^j} \delta(k_i, \eta). \quad (4.35)$$

We analyze perturbations about an anisotropic background. Since the background is anisotropic and thus there is no $SO(3)$ symmetry, perturbations cannot be decomposed into spin-0, spin-1, and spin-2 degrees of freedom and analyzed separately. We instead decompose gauge-invariant perturbations according to their transformation properties in the isotropic limit. (See appendix 4.A.)

There are five dynamical degrees of freedom in our model, corresponding to

- one scalar degree of freedom, r (spin-0 in isotropic limit),¹²
- two electromagnetic vector degrees of freedom, δA^+ and δA^- (spin-1 in isotropic limit),
- and two metric tensor degrees of freedom, E^+ and E^\times (spin-2 in isotropic limit).

In order to analyze the relevant dynamical perturbative degrees of freedom in our scenario, we derived the quadratic action in terms of the gauge-invariant variables of appendix 4.A. Then we eliminated the nondynamical degrees of freedom by using constraint equations derived from the action. Finally, we canonically normalized the degrees of freedom that correspond to the dynamical “free” fields in the limit

¹²See (4.138) in appendix 4.A.

as $\beta'/\alpha' \rightarrow 0$. Within the “in-in” formalism of perturbation theory, we take the interaction-picture fields to be those governed by the dynamics in the $\beta'/\alpha' = 0$ limit.

The quadratic action separates into two uncoupled pieces according to a residual symmetry under parity transformations. (See appendix 4.A.) The “odd” sector has two degrees of freedom, E^\times and δA^- . The “even” sector has three degrees of freedom, E^+ , δA^+ , and r . The fields E^+ , E^\times , and r correspond to fields that are conserved outside the horizon during isotropic inflation. Here r is a Mukhanov-Sasaki variable, equal to minus the curvature perturbation, $-\zeta$, as defined in, *e.g.*, [72], in a gauge with spatially flat slicing. We will therefore refer to r as the curvature perturbation.

4.3.4 Canonically Normalized Variables

The canonically normalized fields in each sector (“even” and “odd”, respectively) are given by

$$\begin{aligned} \hat{A}^+ &= f(\bar{\phi}) \delta A^+ & \hat{A}^- &= f(\bar{\phi}) \delta A^- \\ \hat{h}^+ &= a(\eta) E^+ / \kappa & \hat{h}^\times &= a(\eta) E^\times / \kappa \\ \hat{r} &= z(\eta) r \end{aligned} \quad \text{and} \quad (4.36)$$

where

$$z(\eta) \equiv a(\eta) \frac{\bar{\phi}'}{\alpha'}. \quad (4.37)$$

The fields on the right-hand sides of equations (4.36) are defined in appendix 4.A. As mentioned above, in the isotropic limit E^+ , E^- and r are conserved outside the horizon. The other important fact about the fields above is that the perturbative expansion of the action is valid when

$$E^+, E^\times, \frac{|\vec{k}|}{\bar{F}_{\eta x}} \delta A^+, \frac{|\vec{k}|}{\bar{F}_{\eta x}} \delta A^-, r \ll 1. \quad (4.38)$$

4.3.5 Comparison with Data

A formalism for finding signatures of a generic primordial preferred direction in the CMB has been developed [6, 68]. In [6] a small direction-dependent contribution to the primordial curvature power spectrum is parametrized by g_* where

$$P(\vec{k}) = P_0(k)(1 + g_* (\hat{n} \cdot \hat{k})^2) \quad (4.39)$$

and where \hat{n} is some preferred direction in the sky. It is postulated that g_* will be approximately independent of the scale for modes of astrophysical interest and that parity is still conserved. Parity conservation guarantees the absence of terms with odd powers of $(\hat{n} \cdot \hat{k})$. Contributions proportional to higher powers of $(\hat{n} \cdot \hat{k})^2$ are assumed to be negligible.

Using this formalism, a nonzero value for g_* was found using 5-year WMAP data at the nine sigma level [73]. The central value found for g_* is 0.29 for a preferred direction very close to the ecliptic pole. Since the WMAP scanning strategy is tied to the ecliptic plane, this strongly suggests that the nonzero value of g_* is due to some systematic effect [74, 73]. Still, we may reasonably take from the analysis in [73] an upper bound for g_* of

$$|g_*| < 0.3. \quad (4.40)$$

In [75] it is estimated that Planck will be sensitive to values of $|g_*|$ as small as 0.02.

Obviously, the gravitational wave power spectrum has not yet been measured, so there is no limit on the analogous parameter, $g_{*\text{grav}}$, for the gravitational wave power spectrum.

4.4 Perturbations: Odd Sector

As described in §4.3.3, the quadratic action separates into two uncoupled pieces according to a residual symmetry under parity transformations. We’ll therefore analyze the two “sectors”—which we refer to as “odd” and “even” for reasons discussed in appendix 4.A—in different sections. We start in this section by analyzing the odd sector¹³ because it is less complicated than the even sector, having only two coupled degrees of freedom (a tensor and a vector degree of freedom) instead of three degrees of freedom as in the even sector. The even sector, which includes the curvature perturbation, contains the most interesting physics; analyzing the odd sector is valuable for extracting $g_{*\text{grav}}$ and as a warm-up for the analysis of the even sector.

In this section we present the action for the odd sector to quadratic order in gauge-invariant perturbation variables. Then we argue that the form of the action implies that the background is classically stable. Next we diagonalize the kinetic term in the action by defining new perturbation variables in terms of which the kinetic term in the action is canonically normalized. This diagonalization allows us to identify the fields that should be quantized. The Hamiltonian derived from the diagonal form of the action is then separated into a “free” part and an “interacting” part, and “in-in” perturbation theory is used to find the autocorrelations (power spectra) and cross correlations of the vector and tensor degrees of freedom (see (4.36)) in terms of the preferred direction and the background quantities H and Σ . The most interesting result in this section is the tensor perturbation power spectrum, given in (4.80).

¹³Our odd sector corresponds to the $2d$ -vector sector analyzed numerically in [68].

In the odd sector, the action takes the form

$$\begin{aligned}
S^{\text{odd}} = \int d\eta \int \frac{d^3k}{(2\pi)^3} & \left(\frac{1}{2} \hat{h}^{\times*'} \hat{h}^{\times'} + \frac{1}{2} \hat{A}^{-*'} \hat{A}^{-'} \right. \\
& - \frac{1}{2} \hat{h}^{\times*} \hat{h}^{\times} \left(k^2 - \frac{a''}{a} - 4\hat{\rho}_A \alpha'^2/3 + \frac{1}{2} \Delta_{\vec{k}} \alpha'^2 \left(2\hat{\rho}_A/3 + 6\Sigma^2 - \frac{3}{2} \Delta_{\vec{k}} \Sigma^2 \right) \right) \\
& - \frac{1}{2} \hat{A}^{-*} \hat{A}^{-} \left(k^2 - \frac{f''}{f} + 2\Sigma \alpha' \frac{f'}{f} + \alpha'^2 (2\hat{\rho}_A - 2\Sigma + 2\Delta_{\vec{k}} \hat{\rho}_A/3 - \Sigma^2) \right) \\
& \left. + \left(i\psi'_{\vec{k}} \hat{h}^{\times*} \hat{A}^{-} \left(\frac{f'}{f} + \alpha' \Sigma + \Delta_{\vec{k}} \alpha' \Sigma \right) - i\psi'_{\vec{k}} \hat{h}^{\times*} \hat{A}^{-'} + \text{h.c.} \right) \right) \quad (4.41)
\end{aligned}$$

where

$$k^2 \equiv \gamma^{ij} k_i k_j = k_1^2 e^{4\beta} + k_2^2 e^{-2\beta}, \quad (4.42)$$

$$\Delta_{\vec{k}} \equiv \frac{k^{2'}}{k^2 \beta'} = \frac{4k_1^2 e^{4\beta} - 2k_2^2 e^{-2\beta}}{k_1^2 e^{4\beta} + k_2^2 e^{-2\beta}}, \quad (4.43)$$

$$\frac{\psi'_{\vec{k}}}{\alpha'} \equiv \frac{k_2 e^{-\beta}}{\sqrt{k^2}} \sqrt{\hat{\rho}_A}, \quad (4.44)$$

and f' denotes the derivative of $f(\bar{\phi}(\eta))$ with respect to conformal time. Without loss of generality we have set $k_3 = 0$ and we have taken the preferred direction (the direction along which the background electric field points) to be \hat{x}^1 .

By inspection we can see that \hat{h}^{\times} and \hat{A}^{-} decouple when the wave vector is parallel to the preferred direction (so $k_2 = 0$). This decoupling should be expected due to the enhanced rotational symmetry about the wave vector in this case.

4.4.1 Preliminary Look at Stability

By design, the kinetic terms are canonically normalized. And in the short wavelength limit ($k \gg aH$), the action simplifies to that of two uncoupled harmonic oscillators; there's no indication of instability in the short wavelength limit.

Let's consider the case where $k_2 = 0$ so the wave vector corresponding to a mode points in the preferred direction. In this case, $\psi'_{\vec{k}} = 0$ and $\Delta_{\vec{k}} = 4$. By inspection,

one sees that the cross-terms vanish. More explicitly,

$$S^{\text{odd}} \xrightarrow{k_2 \rightarrow 0} \int d\eta \int \frac{d^3 k}{(2\pi)^3} \left(\frac{1}{2} \hat{h}^{\times*'} \hat{h}^{\times'} + \frac{1}{2} \hat{A}^{-*'} \hat{A}^{-'} - \frac{1}{2} \hat{h}^{\times*} \hat{h}^{\times} \left(k^2 - \frac{a''}{a} \right) - \frac{1}{2} \hat{A}^{-*} \hat{A}^{-} \left(k^2 - \frac{f''}{f} + 2\Sigma \alpha' \frac{f'}{f} + \alpha'^2 (14\hat{\rho}_A/3 - 2\Sigma - \Sigma^2) \right) \right). \quad (4.45)$$

When $k_2 \rightarrow 0$ the action for \hat{h}^\times takes the same form as in the isotropic case. Though the effective mass for \hat{h}^\times is not real for all time (so naively, there's a tachyon), the important point is that \hat{h}^\times/a , which we assumed to be much less than one in our perturbative expansion of the metric (see (4.38)), oscillates with decaying amplitude before horizon crossing, and then remains constant or decays after horizon crossing. In other words, $\hat{h}^\times \sim aE^\times$ never increases faster than a , which is consistent with the perturbative expansion. Similarly, given that $2\Sigma\alpha'\frac{f'}{f} + \alpha'^2(14\hat{\rho}_A/3 - 2\Sigma - \Sigma^2) \ll \frac{f''}{f}$, the long wavelength solution for \hat{A}^- is approximately, $\hat{A}^- \approx C_1 f + C_2 f \int \frac{d\eta}{f^2}$. Now given that $f \approx a^{-2} \approx H^2 \eta^2$, one can see that $\frac{|\vec{k}|}{F_{\eta x}} \delta A^- \sim (C_1 + \frac{C_2}{H} a^3) a^{-4}$ (which is decaying) in the long wavelength limit. So clearly the perturbative expansion of the action remains valid when $k_2 = 0$.

Now let's consider a wave vector that's antiparallel to the preferred direction, so $k_1 = 0$. In this case, $\psi'_k = \sqrt{\hat{\rho}_A} \alpha'$ and $\Delta_k = -2$. Then the effective mass squared for \hat{h}^\times becomes

$$m_{\text{eff}}^2 = k^2 - \frac{a''}{a} - \alpha'^2 (2\hat{\rho}_A + 9\Sigma^2). \quad (4.46)$$

Compared to the isotropic case, the effective mass squared for \hat{h}^\times receives an additional negative contribution. This suggests that \hat{h}^\times will grow slightly faster than a outside the horizon. The situation is, of course, complicated by the coupling to \hat{A}^- , but all extra terms in the action when $k_1 = 0$ compared to the terms present when $k_2 = 0$ are small. This suggests that any possible growth of the perturbative fields in this case will be very moderate and does not represent an instability. This reasoning

will be checked by calculating the power spectra of perturbative fields; we can check that the magnitudes of power spectra do not grow rapidly in time.

The same situation occurs in the even sector; perturbations clearly do not grow when $k_2 = 0$ and all extra terms in the action when $k_1 = 0$ compared to the terms present when $k_2 = 0$ are small.

4.4.2 Diagonalized Action

In general, the canonical quantization of a theory can only proceed once the kinetic interactions have been diagonalized. Usually the diagonalization is accomplished by some constant field redefinition. In our case, we need a time-dependent field redefinition because the “coefficients” in the kinetic portions of the action are not constant. (See appendix 4.C.)

The kinetic terms can be diagonalized by performing a time-dependent unitary rotation

$$\begin{pmatrix} \hat{h}^\times \\ \hat{A}^- \end{pmatrix} = \begin{pmatrix} \cos \psi_{\vec{k}}(\eta) & -i \sin \psi_{\vec{k}}(\eta) \\ -i \sin \psi_{\vec{k}}(\eta) & \cos \psi_{\vec{k}}(\eta) \end{pmatrix} \begin{pmatrix} U_1 \\ U_2 \end{pmatrix}. \quad (4.47)$$

In terms of the rotated fields, U_i , the odd-sector action takes the form

$$S^{\text{odd}} = \int d\eta \int \frac{d^3 k}{(2\pi)^3} \left[\frac{1}{2} \begin{pmatrix} U'_1 \\ U'_2 \end{pmatrix}^\dagger \begin{pmatrix} U'_1 \\ U'_2 \end{pmatrix} - \frac{1}{2} \begin{pmatrix} U_1 \\ U_2 \end{pmatrix}^\dagger M \begin{pmatrix} U_1 \\ U_2 \end{pmatrix} \right] \quad (4.48)$$

where the Hermitian matrix M is defined

$$\begin{aligned}
M \equiv & \left(k^2 - \frac{1}{2} \left(\frac{a''}{a} + \frac{f''}{f} \right) + \Sigma \alpha'^2 \left(\frac{f'}{f \alpha'} - 1 - \frac{1}{2} \Sigma + \frac{3}{2} \Sigma \Delta_{\vec{k}} - \frac{3}{8} \Sigma \Delta_{\vec{k}}^2 \right) \right. \\
& \left. + \frac{1}{3} \hat{\rho}_A \alpha'^2 (3 + \Delta_{\vec{k}}) \right) \mathbb{I} \\
& + [\sin(2\psi_{\vec{k}}) \sigma_3 - \cos(2\psi_{\vec{k}}) \sigma_2] \left(\frac{\psi'_{\vec{k}}}{\alpha'} \right) \alpha'^2 \left(1 - \frac{f'}{f \alpha'} + \Sigma - \frac{3}{2} \Sigma \Delta_{\vec{k}} \right) \\
& + [\cos(2\psi_{\vec{k}}) \sigma_3 + \sin(2\psi_{\vec{k}}) \sigma_2] \left(\frac{1}{2} \left(\frac{f''}{f} - \frac{a''}{a} \right) \right. \\
& \left. - \Sigma \alpha'^2 \left(\frac{f'}{f \alpha'} - 1 - \frac{1}{2} \Sigma - \frac{3}{2} \Sigma \Delta_{\vec{k}} + \frac{3}{8} \Sigma \Delta_{\vec{k}}^2 \right) - \frac{1}{3} \hat{\rho}_A \alpha'^2 \left(5 + \frac{1}{2} \Delta_{\vec{k}} \right) \right) \quad (4.49)
\end{aligned}$$

and where \mathbb{I} is the 2×2 identity matrix and we have used the following convention for the Pauli matrices

$$\sigma_2 = \begin{pmatrix} 0 & -i \\ i & 0 \end{pmatrix} \quad \text{and} \quad \sigma_3 = \begin{pmatrix} 1 & 0 \\ 0 & -1 \end{pmatrix}. \quad (4.50)$$

Physical quantities should not depend on the initial value of $\psi_{\vec{k}}$. Indeed, we will see that correlations of \hat{h}^\times and \hat{A}^- at a time, η , calculated using the “in-in” formalism of perturbation theory, depend only on the change in $\psi_{\vec{k}}$ after horizon crossing.

4.4.3 Correlations Using Perturbation Theory

In order to calculate correlations, we use the “in-in” formalism of perturbation theory, taking the small parameters to be ϵ , δ , $\hat{\rho}_A$, and Σ . As discussed at the end of §4.2 we take

$$\epsilon = \frac{\alpha'^2 - \alpha''}{\alpha'^2} \ll 1, \quad \delta = \frac{\partial_t^2 H}{2H \partial_t H} \ll 1, \quad \hat{\rho}_A \approx 9\Sigma/2 \lesssim \mathcal{O}(\epsilon), \quad \frac{\hat{\rho}'_A}{\hat{\rho}_A \alpha'} \lesssim \mathcal{O}(\epsilon). \quad (4.51)$$

Given these assumptions and the background field equations (4.8) - (4.10) ,

$$\frac{f'}{f\alpha'} = -2 + \mathcal{O}(\epsilon), \quad \frac{f''}{f\alpha'^2} = 2 + \mathcal{O}(\epsilon) = \frac{a''}{a\alpha'^2} \quad \text{and} \quad \alpha' \approx -\frac{1}{\eta}. \quad (4.52)$$

We choose as our free Hamiltonian

$$H_0^{\text{odd}} \equiv \int \frac{d^3k}{(2\pi)^3} \left[\frac{1}{2} \begin{pmatrix} U'_1 \\ U'_2 \end{pmatrix}^\dagger \begin{pmatrix} U'_1 \\ U'_2 \end{pmatrix} + \frac{1}{2} \begin{pmatrix} U_1 \\ U_2 \end{pmatrix}^\dagger M^{(0)} \begin{pmatrix} U_1 \\ U_2 \end{pmatrix} \right] \quad (4.53)$$

where

$$M^{(0)} \equiv \left(\gamma^{ij}(\eta_0) k_i k_j - \frac{2}{\eta^2} \right) \mathbb{I}. \quad (4.54)$$

The interaction-picture fields then obey the following equations:

$$\frac{d^2 U_i^I}{d\eta^2} + \left(\gamma^{ij}(\eta_0) k_i k_j - \frac{2}{\eta^2} \right) U_i^I = 0. \quad (4.55)$$

Each of these fields can be expanded in terms of time-independent creation and annihilation operators as,

$$\begin{aligned} U_i^I(\vec{x}, \eta) &= \int \frac{d^3k}{(2\pi)^3} e^{ik_j x^j} U_i^I(\vec{k}, \eta) \\ &= \int \frac{d^3k}{(2\pi)^3} \left(e^{ik_i x^i} \chi^{(0)}(k_{\eta_0}, \eta) \hat{a}_{\vec{k}}^i + e^{-ik_i x^i} \chi^{(0)*}(k_{\eta_0}, \eta) (\hat{a}_{\vec{k}}^i)^\dagger \right), \end{aligned} \quad (4.56)$$

where the canonically normalized mode functions are

$$\chi^{(0)}(k, \eta) = \frac{e^{-ik\eta}}{\sqrt{2k}} \left(1 - \frac{i}{k\eta} \right) \quad (4.57)$$

and where the commutation relations of the creation and annihilation operators are

$$\left[\hat{a}_{\vec{k}}^i, (\hat{a}_{\vec{q}}^j)^\dagger \right] = (2\pi)^3 \delta^{ij} \delta(\vec{k} - \vec{q}) \quad \text{and} \quad \left[\hat{a}_{\vec{k}}^i, \hat{a}_{\vec{q}}^j \right] = 0. \quad (4.58)$$

Here,

$$k_{\eta_0} \equiv \sqrt{\gamma^{ij}(\eta_0) k_i k_j}. \quad (4.59)$$

If we choose $\beta_0 = 0$ then $\gamma^{ij}(\eta_0) = \delta^{ij}$. But then if β changes during inflation, the coordinates at the end of inflation will not be isotropic. On the other hand, if we choose β_0 so that $\beta = 0$ at the end of inflation (when the dynamics returns to being isotropic), then the coordinates at the end of inflation will be isotropic. The latter choice is more convenient.

Using the results of the previous section and the form of the matrix M in (4.49), the interaction-picture Hamiltonian takes the form

$$H_I(\eta) = \int \frac{d^3 k}{(2\pi)^3} \left(\frac{1}{2} \begin{pmatrix} U_1^I \\ U_2^I \end{pmatrix}^\dagger M^{(1)} \begin{pmatrix} U_1^I \\ U_2^I \end{pmatrix} \right) \quad (4.60)$$

where

$$\begin{aligned} M^{(1)} &= M - M^{(0)} = f_1(\eta, \vec{k}) \mathbb{I} \\ &+ [\sin(2\psi_{\vec{k}}) \sigma_3 - \cos(2\psi_{\vec{k}}) \sigma_2] f_2(\eta, \hat{k}) + [\cos(2\psi_{\vec{k}}) \sigma_3 + \sin(2\psi_{\vec{k}}) \sigma_2] f_3(\eta, \hat{k}) \end{aligned} \quad (4.61)$$

and we have defined

$$\begin{aligned} f_1(\eta, \vec{k}) &\equiv (\gamma^{ij}(\eta) - \gamma^{ij}(\eta_0)) k_i k_j - \frac{1}{2} \left(\frac{a''}{a} + \frac{f''}{f} - \frac{4}{\eta^2} \right) \\ &+ \Sigma \alpha'^2 \left(\frac{f'}{f \alpha'} - 1 - \frac{1}{2} \Sigma + \frac{3}{2} \Sigma \Delta_{\vec{k}} - \frac{3}{8} \Sigma \Delta_{\vec{k}}^2 \right) + \frac{1}{3} \hat{\rho}_A \alpha'^2 (3 + \Delta_{\vec{k}}) \end{aligned} \quad (4.62)$$

$$f_2(\eta, \hat{k}) \equiv \left(\frac{\psi'_{\vec{k}}}{\alpha'} \right) \alpha'^2 \left(1 - \frac{f'}{f \alpha'} + \Sigma - \frac{3}{2} \Sigma \Delta_{\vec{k}} \right) \quad (4.63)$$

$$\begin{aligned} f_3(\eta, \hat{k}) &\equiv \frac{1}{2} \left(\frac{f''}{f} - \frac{a''}{a} \right) - \Sigma \alpha'^2 \left(\frac{f'}{f \alpha'} - 1 - \frac{1}{2} \Sigma - \frac{3}{2} \Sigma \Delta_{\vec{k}} + \frac{3}{8} \Sigma \Delta_{\vec{k}}^2 \right) \\ &- \frac{1}{3} \hat{\rho}_A \alpha'^2 \left(5 + \frac{1}{2} \Delta_{\vec{k}} \right). \end{aligned} \quad (4.64)$$

Our convention for the correlations of the fields will be

$$\langle U_i(\vec{k}, \eta) U_j(\vec{q}, \eta) \rangle = C_{ij}(\vec{k}, \eta) (2\pi)^3 \delta(\vec{k} + \vec{q}), \quad (4.65)$$

where the power spectra are the diagonal entries of the matrix C_{ij} . Using (4.34), the correlations can be written as

$$\langle U_i(\vec{p}, \eta) U_j(\vec{q}, \eta) \rangle = \langle U_i^I(\vec{p}, \eta) U_j^I(\vec{q}, \eta) \rangle + i \int^\eta d\eta' \langle [H_I(\eta'), U_i^I(\vec{p}, \eta) U_j^I(\vec{q}, \eta)] \rangle + \dots \quad (4.66)$$

More explicitly, the correlations take the form

$$C_{ij}(\vec{p}, \eta) = |\chi^{(0)}(p_{\eta_0}, \eta)|^2 \delta_{ij} + i \int^\eta d\eta' M_{ij}^{(1)}(\vec{p}, \eta') I_{p_{\eta_0}}(\eta', \eta) + \dots \quad (4.67)$$

where

$$I_p(\eta', \eta) = ((\chi^{(0)}(p, \eta') \chi^{(0)*}(p, \eta))^2 - (\chi^{(0)*}(p, \eta') \chi^{(0)}(p, \eta))^2). \quad (4.68)$$

It is clear from this formula that the zeroth-order power spectra of the fields U_i are isotropic and scale invariant and that the cross-correlation vanishes. Here it's convenient to define the function

$$\tilde{I}(p\eta', p\eta) \equiv ip^2 I_p(\eta', \eta) \quad (4.69)$$

where

$$\begin{aligned} \tilde{I}(x, y) = & \left(\frac{1}{2x^2y^2} - \frac{1}{2x^2} + \frac{2}{xy} - \frac{1}{2y^2} + \frac{1}{2} \right) \sin(2x - 2y) \\ & + \left(\frac{1}{x^2y} - \frac{1}{xy^2} + \frac{1}{x} - \frac{1}{y} \right) \cos(2x - 2y). \end{aligned} \quad (4.70)$$

Solving for the correlations of the variables \hat{h}^\times and \hat{A}^- in terms of the correlations

of the rotated variables U_i , we find

$$P_{\hat{h}^\times}(\vec{p}) = \cos^2 \psi_{\vec{p}} C_{11}(\vec{p}) + \sin^2 \psi_{\vec{p}} C_{22}(\vec{p}) + \frac{i}{2} \sin(2\psi_{\vec{p}})(C_{12}(\vec{p}) - C_{21}(\vec{p})) \quad (4.71)$$

$$P_{\hat{A}^-}(\vec{p}) = \sin^2 \psi_{\vec{p}} C_{11}(\vec{p}) + \cos^2 \psi_{\vec{p}} C_{22}(\vec{p}) - \frac{i}{2} \sin(2\psi_{\vec{p}})(C_{12}(\vec{p}) - C_{21}(\vec{p})) \quad (4.72)$$

$$\begin{aligned} C_{\hat{h}^\times \hat{A}^-}(\vec{p}) &= \cos^2 \psi_{\vec{p}} C_{12}(\vec{p}) + \sin^2 \psi_{\vec{p}} C_{21}(\vec{p}) + \frac{i}{2} \sin(2\psi_{\vec{p}})(C_{11}(\vec{p}) - C_{22}(\vec{p})) \\ &= -C_{\hat{A}^- \hat{h}^\times}(\vec{p}) \end{aligned} \quad (4.73)$$

where we have used the fact that $\psi_{-\vec{k}} = -\psi_{\vec{k}}$. All of the above correlations, and $\psi_{\vec{p}}$, are functions of time. It is understood that these expressions are evaluated at the end of inflation.

From here on, we will use the short hand notation

$$p = p_{\eta_0}. \quad (4.74)$$

Using (4.67) and the expression for $M^{(1)}$, the power spectra and correlations are

given more explicitly by,

$$\begin{aligned}
P_{\hat{h}\times}(\vec{p}, \eta) = & |\chi^{(0)}(p, \eta)|^2 + p^{-2} \left\{ \int^{\eta} f_1(\eta', \vec{p}) \tilde{I}(p\eta', p\eta) d\eta' \right. \\
& + \int^{\eta} \sin(2\psi_{\vec{p}}(\eta') - 2\psi_{\vec{p}}(\eta)) f_2(\eta', \hat{p}) \tilde{I}(p\eta', p\eta) d\eta' \\
& \left. + \int^{\eta} \cos(2\psi_{\vec{p}}(\eta') - 2\psi_{\vec{p}}(\eta)) f_3(\eta', \hat{p}) \tilde{I}(p\eta', p\eta) d\eta' \right\} + \dots \quad (4.75)
\end{aligned}$$

$$\begin{aligned}
P_{\hat{A}-}(\vec{p}, \eta) = & |\chi^{(0)}(p, \eta)|^2 + p^{-2} \left\{ \int^{\eta} f_1(\eta', \vec{p}) \tilde{I}(p\eta', p\eta) d\eta' \right. \\
& - \int^{\eta} \sin(2\psi_{\vec{p}}(\eta') - 2\psi_{\vec{p}}(\eta)) f_2(\eta', \hat{p}) \tilde{I}(p\eta', p\eta) d\eta' \\
& \left. - \int^{\eta} \cos(2\psi_{\vec{p}}(\eta') - 2\psi_{\vec{p}}(\eta)) f_3(\eta', \hat{p}) \tilde{I}(p\eta', p\eta) d\eta' \right\} + \dots \quad (4.76)
\end{aligned}$$

$$\begin{aligned}
C_{\hat{h}\times\hat{A}-}(\vec{p}, \eta) = & ip^{-2} \left\{ \int^{\eta} \cos(2\psi_{\vec{p}}(\eta') - 2\psi_{\vec{p}}(\eta)) f_2(\eta', \hat{p}) \tilde{I}(p\eta', p\eta) d\eta' \right. \\
& \left. - \int^{\eta} \sin(2\psi_{\vec{p}}(\eta') - 2\psi_{\vec{p}}(\eta)) f_3(\eta', \hat{p}) \tilde{I}(p\eta', p\eta) d\eta' \right\} + \dots = -C_{\hat{A}-\hat{h}\times}(\vec{p}, \eta). \quad (4.77)
\end{aligned}$$

It's clear from the expression above that the correlations are functions only of the change in the angle $\psi_{\vec{p}}$.

4.4.4 Discussion

We are interested primarily in *direction-dependent* modifications to the power spectra—*i.e.*, modifications of the power spectra that depend on the direction of the wave vector, not just its magnitude. Non-direction-dependent effects will modify spectral indices, but such effects cannot be disentangled experimentally as due to primordial anisotropy. In principle, one could use our method to calculate spectral indices and, for example, relate them to the size of the direction-dependent effects.

The largest direction-dependent contribution comes from the piece involving f_2 .

The contribution is given by

$$p^{-2} \left(\int^{\eta} \sin(2\psi_{\vec{p}}(\eta') - 2\psi_{\vec{p}}(\eta)) f_2(\eta', \hat{p}) \tilde{I}(p\eta', p\eta) d\eta' \right) \\ \approx -\frac{(aH)^2}{p^3} \left(\cos\left[2\frac{\psi'_{\vec{p}}}{\alpha'} \log(aH/p)\right] - 1 \right) \quad (4.78)$$

assuming $\frac{\psi'_{\vec{p}}}{\alpha'}$ is approximately constant throughout inflation, where we've used the fact that $\left(1 - \frac{f'}{f\alpha'}\right) \approx 3$ and the relevant integral is calculated in appendix 4.D. Modes of astrophysical interest crossed the horizon about sixty e -folds before the end of inflation, so for such modes, $\log(aH/p) \approx 60$.

When

$$f(\phi) = \exp \left\{ 2c\kappa \int \left(\frac{\partial_{\phi} V}{\kappa V} \right)^{-1} d\phi \right\}, \quad (4.79)$$

for $c-1 \sim \mathcal{O}(1)$ we found that $\hat{\rho}_A \approx \frac{3(c-1)}{2c}\epsilon$ during the anisotropic period of expansion. If the anisotropic period of expansion were to last all sixty e -folds before the end of inflation, then we should expect order one direction-dependent corrections to the gravitational wave power spectrum for inflationary scenarios in which $\sqrt{\epsilon} \gtrsim \frac{1}{60}$. Such values of ϵ can easily be realized in large-field inflationary models. This analytic result seems to confirm the numerical findings in [68].

Demanding that the direction-dependent effect on the gravitational wave power spectrum for modes of astrophysical interest is less than, say, about 30% would mean that the argument of the cosine function in (4.78) is small so that the cosine can be expanded in a Taylor series. In this case the power spectrum for \hat{h}^{\times} is approximately

$$P_{\hat{h}^{\times}}(\vec{p}, \eta) \approx \frac{(aH)^2}{2p^3} \left(1 + \left(2\frac{\psi'_{\vec{p}}}{\alpha'} \log(aH/p) \right)^2 \right) \\ \approx \frac{(aH)^2}{2p^3} \left(1 + 4\hat{\rho}_A (\log(aH/p))^2 (1 - (\hat{n} \cdot \hat{p})^2) \right). \quad (4.80)$$

where \hat{n} is the preferred direction. Thus we may identify

$$g_{*\text{grav}} \approx -4\hat{\rho}_A(\log(aH/p))^2 \approx -18\Sigma(\log(aH/p))^2. \quad (4.81)$$

Note that $g_{*\text{grav}}$ is nearly (though not exactly) scale invariant for modes of astrophysical interest.

Imposing a limit like $|g_{*\text{grav}}| < 0.3$ for modes of astrophysical interest corresponds to a limit on $\hat{\rho}_A$ like

$$\hat{\rho}_A|_{\text{average after horizon crossing}} \lesssim 10^{-4} \quad \text{when} \quad |g_{*\text{grav}}| < 0.3. \quad (4.82)$$

4.5 Perturbations: Even Sector

The even-sector action is much more complicated than that of the odd sector. This sector contains three dynamical degrees of freedom that, in the isotropic limit, transform as a scalar, vector and tensor under rotations. This sector is further complicated by additional nondynamical scalar variables.

As in the previous section, we begin in this section by diagonalizing the kinetic part of the quadratic action. This process is more complicated for the three dynamical degrees of freedom in this (even) sector than for the two of the odd sector, and the smallness of certain background quantities must be exploited; we eventually work in the limit $\hat{\rho}_A \ll \epsilon \ll 1$, which is confirmed to be a sensible limit at the end of the calculation. As in the odd-sector calculation, we quantize and use “in-in” perturbation theory to calculate power spectra and cross correlations of the scalar, vector, and tensor degrees of freedom. The most interesting results in this section are the scalar perturbation power spectrum (4.111) and corresponding value for g_* (4.112), and also the ratio of the direction-dependent correction to the scalar power spectrum over that of the tensor power spectrum (4.116).

Instead of presenting the entire quadratic action (as we did in (4.41) for the odd sector), here we present the action to lowest order in δ , ϵ , $\hat{\rho}_A$, and Σ . We expand the action assuming that $\hat{\rho}_A$, Σ , and $\hat{\rho}'_A/\hat{\rho}_A$ are order ϵ or smaller. For simplicity, we first present the action to lowest order before elimination of the auxiliary fields Φ and Ψ . (See appendix 4.A for the definitions of Φ and Ψ .) The action can be written

$$S^{\text{even}} = \int d\eta \int \frac{d^3k}{(2\pi)^3} [\mathbf{H}^\dagger \mathbf{M}_1 \mathbf{H} + \Phi^\dagger \mathbf{Q} \mathbf{H} + \mathbf{H}^\dagger \mathbf{Q}^\dagger \Phi + \Phi^\dagger \mathbf{M}_2 \Phi] \quad (4.83)$$

where the vectors \mathbf{H} and Φ are defined by

$$\mathbf{H} = \begin{pmatrix} \hat{h}^{+'} \\ \hat{A}^{+'} \\ \hat{r}' \\ \hat{h}^+ \\ \hat{A}^+ \\ \hat{r} \end{pmatrix} \quad \Phi = \begin{pmatrix} \Phi \\ \Psi \end{pmatrix} \quad (4.84)$$

and the matrices \mathbf{M}_1 , \mathbf{M}_2 , and \mathbf{Q} are given by

$$\mathbf{M}_1 = \begin{pmatrix} \frac{1}{2} & 0 & 0 & 0 & 0 & 0 \\ 0 & \frac{1}{2} & 0 & -i\psi'_k & 0 & -i2\sqrt{2}\frac{a}{\kappa z}\psi'_k \\ 0 & 0 & \frac{1}{2} & 0 & 0 & 0 \\ 0 & i\psi'_k & 0 & \alpha'^2 - \frac{k^2}{2} & 2i\psi'_k\alpha' & 2\sqrt{2}\frac{a}{\kappa z}\psi'^2_k \\ 0 & 0 & 0 & -2i\psi'_k\alpha' & \alpha'^2 - \frac{k^2}{2} & -i4\sqrt{2}\frac{a\alpha'}{\kappa z}\psi'_k \\ 0 & i2\sqrt{2}\frac{a}{\kappa z}\psi'_k & 0 & 2\sqrt{2}\frac{a}{\kappa z}\psi'^2_k & i4\sqrt{2}\frac{a\alpha'}{\kappa z}\psi'_k & \frac{1}{2}\frac{z''}{z} - \frac{k^2}{2} + 16\frac{a^2}{\kappa^2 z^2}\psi'^2_k - 8\frac{a^2\alpha'^2}{\kappa^2 z^2}\hat{\rho}_A \end{pmatrix} + \mathcal{O}(\epsilon), \quad (4.85)$$

$$\mathbf{M}_2 = \begin{pmatrix} \frac{a^2}{\kappa^2} \psi'_k{}^2 & -\frac{3a^2}{\kappa^2} (\psi'_k{}^2 + (2/3)\hat{\rho}_A \alpha'^2) - \frac{3}{2} z^2 \alpha'^2 \\ -\frac{3a^2}{\kappa^2} (\psi'_k{}^2 + (2/3)\hat{\rho}_A \alpha'^2) - \frac{3}{2} z^2 \alpha'^2 & \frac{9a^2}{\kappa^2} (\psi'_k{}^2 + (2/3)\hat{\rho}_A \alpha'^2) - \frac{\kappa^2 z^2}{a^2} + \frac{3z^2 \alpha'^2}{2} (1 + \frac{2z'}{\alpha' z}) \end{pmatrix} + \frac{a^2 k^2}{\kappa^2} \begin{pmatrix} 0 & -(1 - \frac{\Delta_{\vec{k}} \Sigma}{4}) \\ -(1 - \frac{\Delta_{\vec{k}} \Sigma}{4}) & (1 + \frac{\Delta_{\vec{k}} \Sigma}{2} - \frac{\kappa^2 z^2}{2a^2}) \end{pmatrix} + \mathcal{O}(\epsilon^2), \quad (4.86)$$

$$\mathbf{Q} = \begin{pmatrix} 0 & i \frac{a}{\sqrt{2}\kappa} \psi'_k & 0 & \sqrt{2} \frac{a}{\kappa} \psi'_k{}^2 & -i \frac{a}{\sqrt{2}\kappa} \psi'_k \alpha' & 4 \frac{a^2}{\kappa^2 z} \psi'_k{}^2 \\ 0 & 0 & 0 & -3\sqrt{2} \frac{a}{\kappa} \psi'_k{}^2 + \frac{ak^2 \xi}{4\sqrt{2}\kappa} (\Delta_{\vec{k}} - 4) & 0 & \frac{1}{2} k^2 z - 12 \frac{a^2}{\kappa^2 z} \psi'_k{}^2 \end{pmatrix} + \mathcal{O}(\epsilon^{3/2}), \quad (4.87)$$

and ψ'_k is as in (4.44). Note here the identity

$$\alpha'^2 (\Delta_{\vec{k}} - 4) \hat{\rho}_A = -4 \psi'_k{}^2. \quad (4.88)$$

Solving the (constraint) equations of motion derived by varying the action with respect to Φ and Ψ and plugging the constraint equations back into the action leads to the action in terms of the three dynamical fields:

$$S^{\text{even}} = \int d\eta \int \frac{d^3 k}{(2\pi)^3} [\mathbf{H}^\dagger (\mathbf{M}_1 - \mathbf{Q}^\dagger \mathbf{M}_2^{-1} \mathbf{Q}) \mathbf{H}]. \quad (4.89)$$

Keep in mind that ψ'_k is a direction-dependent quantity that varies from zero to plus or minus $\sqrt{\hat{\rho}_A}$, depending on the orientation of the wave vector with respect to

the preferred direction. The bottom right element of \mathbf{M}_1 , representing (minus) the effective mass for \hat{r} , is $\frac{1}{2}(\frac{z''}{z} - k^2)$ in the isotropic limit. So if, for example, $\hat{\rho}_A$ is order $\frac{\kappa^2 z^2}{a^2} = \mathcal{O}(\epsilon)$ then we should expect a very dramatic direction-dependent effect on the curvature perturbation power spectrum, because the direction-dependent term would be on the same order as the normal, isotropic term (at least in the long wavelength limit). In fact, assuming that taking into account the $\mathbf{Q}^\dagger \mathbf{M}_2^{-1} \mathbf{Q}$ correction to \mathbf{M}_1 and properly diagonalizing the kinetic term in the action would not weaken the direction-dependent effect on the power spectrum, we can get a rough limit on the average value of $\hat{\rho}_A/(\kappa^2 z^2/a^2)$ during inflation, after horizon crossing. Based on the argument of §4.3.5, we may take a 30% direction-dependent contribution to curvature perturbation power spectrum to be an upper limit. Noting that $\frac{z''}{z} = \alpha'^2(2 + \mathcal{O}(\epsilon, \delta))$, the 30% limit translates roughly to¹⁴

$$\left. \frac{\hat{\rho}_A a^2}{\kappa^2 z^2} \right|_{\text{average}} \approx \left. \frac{\hat{\rho}_A}{2\epsilon} \right|_{\text{average}} < 10^{-2} \quad (\text{approximate}). \quad (4.90)$$

Given phenomenological constraints, it is therefore most interesting to consider scenarios in which $\hat{\rho}_A \ll \epsilon$. Taking

$$\hat{\rho}_A \sim (9/2)\Sigma \ll \epsilon, \quad (4.91)$$

by inspection one can see that in the long wavelength limit

$$\mathbf{Q}^\dagger \mathbf{M}_2^{-1} \mathbf{Q} = \mathcal{O}(\hat{\rho}_A/\epsilon) \quad (4.92)$$

¹⁴The first equality can be seen from equations (4.16) and (4.37), given that $\hat{\rho}_A$ must be small compared to $\kappa^2 z^2/a^2$.

and

$$\mathbf{M}_1 = \begin{pmatrix} \frac{1}{2} & 0 & 0 & 0 & 0 & 0 \\ 0 & \frac{1}{2} & 0 & 0 & 0 & -i2\sqrt{2}\frac{a}{\kappa z}\psi'_k \\ 0 & 0 & \frac{1}{2} & 0 & 0 & 0 \\ 0 & 0 & 0 & \alpha'^2 - \frac{k^2}{2} & 0 & 0 \\ 0 & 0 & 0 & 0 & \alpha'^2 - \frac{k^2}{2} & -i4\sqrt{2}\frac{a\alpha'}{\kappa z}\psi'_k \\ 0 & i2\sqrt{2}\frac{a}{\kappa z}\psi'_k & 0 & 0 & i4\sqrt{2}\frac{a\alpha'}{\kappa z}\psi'_k & \frac{1}{2}\frac{z''}{z} - \frac{k^2}{2} \end{pmatrix} + \mathcal{O}(\epsilon, \hat{\rho}_A/\epsilon). \quad (4.93)$$

We will find, with a careful analysis in the $\hat{\rho}_A \ll \epsilon$ limit, that the actual constraint on $\hat{\rho}_A$ is much stronger than the approximate constraint in (4.90). Thus the $\hat{\rho}_A \ll \epsilon$ approximation is valid.

4.5.1 Diagonalizing the Action

Once again, the resulting kinetic terms are not diagonalized and canonical quantization cannot proceed. In the $\hat{\rho}_A \ll \epsilon \ll 1$ limit, the kinetic terms can be diagonalized by performing a time-dependent unitary rotation

$$\begin{pmatrix} \hat{r} \\ \hat{A}^+ \end{pmatrix} = \begin{pmatrix} \cos \theta'_k(\eta) & -i \sin \theta'_k(\eta) \\ -i \sin \theta'_k(\eta) & \cos \theta'_k(\eta) \end{pmatrix} \begin{pmatrix} U_1 \\ U_2 \end{pmatrix}, \quad (4.94)$$

where

$$\theta'_k(\eta) \equiv -2\sqrt{2}\frac{a}{\kappa z}\psi'_k = -2\sqrt{2}\frac{a}{\kappa z} \left(\frac{k_2 e^{-\beta}}{\sqrt{k^2}} \sqrt{\hat{\rho}_A} \alpha' \right) \quad (4.95)$$

and where ψ'_k is the rotation angle in the odd sector, given by (4.44). The rotation of \hat{r} and \hat{A}^+ occurs on a much faster timescale than that of \hat{h}^\times and \hat{A}^- since $\psi'_k = \mathcal{O}(\sqrt{\hat{\rho}_A})$ and $\theta'_k = \mathcal{O}(\sqrt{\hat{\rho}_A}/\epsilon)$.

In terms of these rotated fields the even action takes the form

$$S^{\text{even}} = \int d\eta \int \frac{d^3k}{(2\pi)^3} \left[\frac{1}{2} \hat{h}^{+*'} \hat{h}^{+*} - \frac{1}{2} (k^2 - 2\alpha'^2) \hat{h}^+ \hat{h}^{+*} \right. \\ \left. + \frac{1}{2} \begin{pmatrix} U'_1 \\ U'_2 \end{pmatrix}^\dagger \begin{pmatrix} U'_1 \\ U'_2 \end{pmatrix} - \frac{1}{2} \begin{pmatrix} U_1 \\ U_2 \end{pmatrix}^\dagger M \begin{pmatrix} U_1 \\ U_2 \end{pmatrix} + \dots \right] \quad (4.96)$$

where the Hermitian matrix M is defined

$$M \equiv (k^2 - 2\alpha'^2) \mathbb{I} + [\sin(2\theta_{\vec{k}}) \sigma_3 - \cos(2\theta_{\vec{k}}) \sigma_2] \left(3 \frac{\theta'_{\vec{k}}}{\alpha'} \right) \alpha'^2 \quad (4.97)$$

up to corrections of order ϵ , δ , and $\hat{\rho}_A/\epsilon$.¹⁵ We've used the same convention for Pauli matrices as in Eq. (4.50) and, again, \mathbb{I} is the 2×2 identity matrix.

4.5.2 Correlations Using Perturbation Theory

The analysis of correlations of dynamical fields in this sector will be very similar to that of the odd sector, up to minus signs and replacing $\psi_{\vec{k}}$ with $\theta_{\vec{k}}$. It should be noted that the largest direction-dependent corrections to correlations in the odd sector are order $\sqrt{\hat{\rho}_A}$, whereas here we're working to order $\sqrt{\hat{\rho}_A/\epsilon}$ assuming $\hat{\rho}_A \ll \epsilon$. It therefore should be unsurprising that the autocorrelation of the gravitational wave amplitude, \hat{h}^+ , has no anisotropic contribution at $\mathcal{O}(\sqrt{\hat{\rho}_A/\epsilon})$. The same can be said of the cross-correlation between \hat{h}^+ and \hat{A}^+ .

Considering now only terms up to order $\sqrt{\hat{\rho}_A/\epsilon}$ given $\hat{\rho}_A \ll \epsilon$, we choose as our

¹⁵ Recall that, *e.g.*, $z''/2z = \alpha'^2 + \mathcal{O}(\epsilon, \delta)$ and $z'/z = \alpha' + \mathcal{O}(\epsilon, \delta)$.

free Hamiltonian

$$H_0^{\text{even}} \equiv \int \frac{d^3k}{(2\pi)^3} \left[\frac{1}{2} \hat{h}^{+'} \hat{h}^{+*'} + \frac{1}{2} \begin{pmatrix} U_1' \\ U_2' \end{pmatrix}^\dagger \begin{pmatrix} U_1' \\ U_2' \end{pmatrix} + \frac{1}{2} \left(\gamma^{ij}(\eta_0) k_i k_j - \frac{2}{\eta^2} \right) \hat{h}^+ \hat{h}^{+*} \right. \\ \left. + \frac{1}{2} \begin{pmatrix} U_1 \\ U_2 \end{pmatrix}^\dagger M^{(0)} \begin{pmatrix} U_1 \\ U_2 \end{pmatrix} \right] \quad (4.98)$$

where

$$M^{(0)} \equiv \left(\gamma^{ij}(\eta_0) k_i k_j - \frac{2}{\eta^2} \right) \mathbb{I}. \quad (4.99)$$

The interaction-picture fields then obey the following equations:

$$\frac{d^2 U_i^I}{d\eta^2} + \left(\gamma^{ij}(\eta_0) k_i k_j - \frac{2}{\eta^2} \right) U_i^I = 0. \quad (4.100)$$

As in §4.4, the fields can be expanded into appropriately normalized mode functions and time-independent creation and annihilation operators. Dropping terms of order ϵ , $\hat{\rho}_A/\epsilon$, δ or higher (including terms with coefficients $(\gamma^{ij}(\eta) - \gamma^{ij}(\eta_0))k_i k_j$) the interaction-picture Hamiltonian takes the form

$$H_I(\eta) = \int \frac{d^3k}{(2\pi)^3} \left(\frac{1}{2} \begin{pmatrix} U_1^I \\ U_2^I \end{pmatrix}^\dagger M^{(1)} \begin{pmatrix} U_1^I \\ U_2^I \end{pmatrix} \right) \quad (4.101)$$

where

$$M^{(1)} = M - M^{(0)} = 3 \left[\sin(2\theta_{\vec{k}}) \sigma_3 - \cos(2\theta_{\vec{k}}) \sigma_2 \right] \left(\frac{\theta_{\vec{k}}'}{\alpha'} \right) \alpha'^2. \quad (4.102)$$

After computing correlations of the rotated variables using the “in-in” formalism, we can find the correlations of the unrotated variables using the equations analogous to equations (4.71) - (4.73).

The correlations are approximately given by

$$P_{\hat{r}}(\vec{p}, \eta) \approx |\chi^{(0)}(p, \eta)|^2 + p^{-2} \int^{\eta} \sin(2\theta_{\vec{p}}(\eta') - 2\theta_{\vec{p}}(\eta)) 3 \frac{\theta'_{\vec{p}}(\eta')}{\alpha'(\eta')} \alpha'^2(\eta') \tilde{I}(p\eta', p\eta) d\eta' \quad (4.103)$$

$$P_{\hat{A}+}(\vec{p}, \eta) \approx |\chi^{(0)}(p, \eta)|^2 - p^{-2} \int^{\eta} \sin(2\theta_{\vec{p}}(\eta') - 2\theta_{\vec{p}}(\eta)) 3 \frac{\theta'_{\vec{p}}(\eta')}{\alpha'(\eta')} \alpha'^2(\eta') \tilde{I}(p\eta', p\eta) d\eta' \quad (4.104)$$

$$\begin{aligned} C_{\hat{r}\hat{A}+}(\vec{p}, \eta) &\approx ip^{-2} \int^{\eta} \cos(2\theta_{\vec{p}}(\eta') - 2\theta_{\vec{p}}(\eta)) 3 \frac{\theta'_{\vec{p}}(\eta')}{\alpha'(\eta')} \alpha'^2(\eta') \tilde{I}(p\eta', p\eta) d\eta' \\ &\approx -C_{\hat{A}+\hat{r}}(\vec{p}, \eta). \end{aligned} \quad (4.105)$$

where \tilde{I} is defined in (4.70).

Assuming $\hat{\rho}_A$ and $\frac{\kappa\phi'}{\alpha'} = \frac{z}{\kappa a}$ are nearly constant during inflation, as in the scenarios we described in §4.2, then

$$\theta_{\vec{p}}(\eta) \approx \frac{\theta'_{\vec{p}}}{\alpha'} \alpha(\eta) \quad (4.106)$$

and we may estimate the relevant integral as in appendix 4.D. Then we see that

$$P_{\hat{r}}(\vec{p}, \eta) \approx \frac{(aH)^2}{2p^3} \left(1 - 2 \left(\cos \left(\left(2 \frac{\theta'_{\vec{p}}}{\alpha'} \right) \log(aH/p) \right) - 1 \right) \right), \quad (4.107)$$

$$P_{\hat{A}+}(\vec{p}, \eta) \approx \frac{(aH)^2}{2p^3} \left(1 + 2 \left(\cos \left(\left(2 \frac{\theta'_{\vec{p}}}{\alpha'} \right) \log(aH/p) \right) - 1 \right) \right), \quad (4.108)$$

$$C_{\hat{r}\hat{A}+}(\vec{p}, \eta) = -C_{\hat{A}+\hat{r}}(\vec{p}, \eta) \approx i \frac{(aH)^2}{p^3} \sin \left(\left(2 \frac{\theta'_{\vec{p}}}{\alpha'} \right) \log(aH/p) \right), \quad (4.109)$$

where $\frac{\theta'_{\vec{p}}}{\alpha'}$ should be taken as the average value after horizon crossing.

Now g_* , the parameter that characterizes the effect of a preferred direction on the CMB power spectrum, is roughly given by

$$|g_*| \approx -2 \left(\cos \left(\left(2 \frac{\theta'_{\vec{p}}}{\alpha'} \right) \log(aH/p) \right) - 1 \right) \Big|_{\max}. \quad (4.110)$$

The maximal value of $\frac{\theta'_p}{\alpha'}$ for a given wave vector is approximately $2\sqrt{\frac{\hat{\rho}_A}{\epsilon}}$. So even if $\hat{\rho}_A/\epsilon$ is, say, order 10^{-4} , the argument of the cosine in (4.110) could be significant for modes of astrophysical interest because for such modes $\log(aH/p) \approx 60$. It's then clear that $|g_*|$ could be order one even for very small values of Σ and $\hat{\rho}_A$.

Let's suppose that $\hat{\rho}_A$ is small enough to satisfy the $|g_*| < 0.3$ bound of §4.3.5. Then the cosine in (4.107) can be expanded in a Taylor series to give

$$P_{\hat{r}}(\vec{p}, \eta) \approx \frac{(aH)^2}{2p^3} \left(1 + 16 \frac{\hat{\rho}_A}{\epsilon} (\log(aH/p))^2 (1 - (\hat{n} \cdot \hat{p})^2) \right), \quad (4.111)$$

where \hat{n} is the preferred direction, and therefore

$$g_* \approx -16 \frac{\hat{\rho}_A}{\epsilon} \left(\log \left(\frac{aH}{p} \right) \right)^2 \approx -72 \frac{\Sigma}{\epsilon} \left(\log \left(\frac{aH}{p} \right) \right)^2. \quad (4.112)$$

Note that g_* is negative, as is $g_{*\text{grav}}$ (see equation (4.81)). A negative g_* means that, for a given scale, power is minimized in the preferred direction. We can understand this general feature in the following way: the pressure contributed by the background electric field slows the expansion of the direction along which the electric field points. In other words, expansion is slower along the preferred direction. Generically the power in primordial perturbations increases in proportion to the Hubble parameter squared; the faster the expansion, the more quickly quantum fluctuations are stretched into “classical” perturbations. Since the power of primordial perturbations increases with the Hubble parameter, squared, and since in our scenario the space-time is expanding most slowly in the preferred direction, we might expect that the power of perturbations with wave vectors parallel to the preferred direction will be smaller than the power of perturbations with wave vectors in any other direction. We predict that, generically, models in which a preferred direction expands more rapidly/slowly than other directions will lead to positive/negative values of g_* .

The limit $|g_*| < 0.3$ translates into a limit on the average value of $\frac{\hat{\rho}_A}{\epsilon}$ during

inflation (after horizon-crossing) for modes of astrophysical interest:

$$\left. \frac{\hat{\rho}_A}{\epsilon} \right|_{\text{average after horizon crossing}} < \frac{3}{160 (60)^2}. \quad (4.113)$$

Since $\hat{\rho}_A$ is assumed to be essentially constant during inflation (as is $\hat{\rho}_\phi$), the limit can be written,

$$\left. \frac{\hat{\rho}_A}{\hat{\rho}_\phi \epsilon} \right|_{\text{average after horizon crossing}} \lesssim 10^{-6}. \quad (4.114)$$

The measurement of g_* puts a very stringent constraint on the ratio of vector field energy density to the inflaton energy density. At the same time, we see that even a very small $U(1)$ gauge field energy density during inflation could lead to a significant direction-dependent effect on the curvature perturbation power spectrum.

Supposing that $\hat{\rho}_A \ll \epsilon$, as we've just seen must be the case in order to comply with observation, the ratio of the gravitational wave power spectrum (P_T) to the scalar power spectrum (P_S) is approximately^{16,17}

$$\frac{P_T}{P_S} = 4 \frac{P_{E^+} + P_{E^\times}}{P_r} \approx \frac{8P_{\hat{h}^\times}}{P_{\hat{r}}} \left(\frac{\kappa^2 z^2}{a^2} \right) \approx 16\epsilon. \quad (4.115)$$

This fact, in conjunction with (4.81) and (4.112), leads to the prediction

$$\frac{g_{*\text{grav}}}{g_*} \approx \frac{1}{64} \frac{P_T}{P_S}. \quad (4.116)$$

The direction-dependent effects of a small persistent anisotropy during inflation on the tensor power spectrum are suppressed with respect to the direction-dependent effects on the scalar power spectrum by a number of order the tensor-to-scalar ratio.

This is a consistency condition for the model, given the constraint from observation,

¹⁶In the last equality we used equations (4.16) and (4.37), given that $\hat{\rho}_A$ must be small compared to $\kappa^2 z^2 / a^2$.

¹⁷What are identified as tensor perturbations are the amplitudes of the transverse, traceless (TT) part of $\delta g_{ij} / a^2$. We defined $\delta g_{ij,TT} / a^2 = 2E_{ij}$, thus the extra factor of 2².

$$\hat{\rho}_A \ll \epsilon.$$

4.6 Conclusions

In this chapter, we considered gauge-invariant perturbations in a class of models with a persistent background anisotropy. After determining the quadratic action in terms of the dynamical fields, we computed the dominant direction-dependent effects of the background anisotropy on primordial power spectra.

We showed that even a very small persistent anisotropy (with the anisotropy parameter much smaller than the slow-roll parameter ϵ) can give rise to a dramatic direction-dependent effect on the primordial power spectra of dynamical fields. In an anisotropic background, the coupling between what reduce to the spin-1 and the spin-0 and spin-2 degrees of freedom in the isotropic case is extremely important. We showed that such couplings give rise to the dominant direction-dependent contributions to the primordial power spectra of tensor and scalar perturbations.

There has been a fair amount of work on vector fields with time-dependent couplings that are put in by hand, assuming exponential expansion. We found that the amount of anisotropy in power spectra are quite sensitive to the details of how nonexponential the expansion is, and how long the expansion lasts. Perhaps this sensitivity is unsurprising in light of the no-hair theorem.

We found that for a given scale $|\vec{k}|$, the curvature power, $P(\vec{k})$, is minimized when \vec{k} points along the preferred direction.¹⁸ We attribute this feature to the fact that, in the class of models we considered, the preferred direction is expanding more slowly than other directions.

We showed that anisotropic effects are more pronounced in the scalar power spectrum than in the tensor power spectra. In fact, we showed that the direction-

¹⁸In other words, we found that g_* is negative.

dependent effects on the tensor power spectrum are suppressed with respect to the direction-dependent effects on the scalar power spectrum by a number of order the tensor-to-scalar ratio. *A priori* one might have expected that the tensor power spectra and the scalar power spectrum would develop fractional direction dependence of the same magnitude. We find that this is not the case.

Finally, upon examination of the quadratic action for all dynamical degrees of freedom, we find no indication of instabilities in this model. This should not be surprising since the matter stress-energy satisfies the dominant energy condition.

We did not calculate the cross correlation between tensor and scalar perturbations. But one can see from the form of the quadratic action¹⁹ that such a nonzero, direction-dependent correlation should exist. The cross-correlation effect will be small compared to the direction-dependent effect on the curvature power spectrum, but it could be interesting.

4.A Appendix: Parametrization of Perturbations

In the following we use many of the same conventions and notation as in [69]. Since the background space-time is homogeneous, we decompose our perturbations into Fourier modes

$$\delta(x^i, \eta) = \int \frac{d^3k}{(2\pi)^3} e^{ik_j x^j} \delta(k_i, \eta). \quad (4.117)$$

For a given Fourier mode, characterized by the time-independent wave vector k_i , we form an orthonormal basis $\{e_i^1, e_i^2\}$ for the subspace perpendicular to the wave vector such that

$$\gamma^{ij} e_i^a e_j^b = \delta^{ab} \quad \text{and} \quad \gamma^{ij} e_i^a k_j = 0. \quad (4.118)$$

Here γ_{ij} is the spatial metric defined in (4.4). Such an orthonormal basis for the

¹⁹See equations (4.85) - (4.89).

spatial hypersurfaces is uniquely defined up to a spatial rotation about the wave vector k_i . To remain properly normalized with the above normalization condition, these basis vectors must be time dependent.

For definiteness, and without loss of generality, we will take wave vectors to be of the form $k_i = (k_1, k_2, 0)$. The basis vectors can then be written as

$$e_i^1 = \left(-\frac{e^{-3\beta}k_2}{\sqrt{k^2}}, \frac{e^{3\beta}k_1}{\sqrt{k^2}}, 0 \right) \quad \text{and} \quad e_j^2 = (0, 0, e^\beta), \quad (4.119)$$

where $\gamma^{ij}k_ik_j = k^2$.

It turns out that there always exists a choice of basis vectors e_i^1 and e_j^2 that results in the basis vectors having definite sign under what we will call

$$\text{k parity: } k_i \rightarrow -k_i. \quad (4.120)$$

Our basis (4.119) is such that under k parity, $e_i^a \rightarrow (-1)^a e_i^a$. Such a choice of basis is now unique up to discrete spatial rotations around the k_i axis by multiples of $\pi/2$.

We parametrize the most general perturbations about the background Bianchi I metric (4.4) in the standard way,

$$ds^2 = -a(\eta)^2 \left[(1 + 2A)d\eta^2 + 2B_id x^i dt + (\gamma_{ij}(\eta) + h_{ij})dx^i dx^j \right]. \quad (4.121)$$

Following [69],

$$B_i = \partial_i B + \bar{B}_i \quad (4.122)$$

$$h_{ij} = 2C \left(\gamma_{ij} + \frac{\sigma_{ij}}{\mathcal{H}} \right) + 2\partial_i \partial_j E + 2\partial_{(i} E_{j)} + 2E_{ij} \quad (4.123)$$

where $\sigma_{ij} = \frac{1}{2}\gamma'_{ij}$ and $\mathcal{H} = \alpha'$ and also,

$$\gamma^{ij}\partial_i\bar{B}_j = 0, \quad \gamma^{ij}\partial_i E_j = 0, \quad \gamma^{ij}\partial_i E_{jk} = 0 \quad \text{and} \quad \gamma^{ij}E_{ij} = 0. \quad (4.124)$$

We parametrize perturbations of the inflaton field and the electromagnetic field by $\delta\phi$ and $\delta F_{\mu\nu}$, respectively.

One can show that the following are $U(1)$ gauge and diffeomorphism invariant variables,

$$\Phi(k) = A + \frac{1}{a(\eta)} \left(a \left(B - \frac{(k^2 E)'}{k^2} \right) \right)', \quad (4.125)$$

$$\Psi(k) = -C - \frac{a'(\eta)}{a(\eta)} \left[B - \frac{(k^2 E)'}{k^2} \right], \quad (4.126)$$

$$\Phi^i(k) = \bar{B}^i - (E^i)', \quad (4.127)$$

$$E_{ij}, \quad (4.128)$$

$$\chi(k) = \delta\phi + \phi'(\eta) \left[B - \frac{(k^2 E)'}{k^2} \right], \quad (4.129)$$

$$\Phi_{ij}^F(k) = \delta F_{ij} + 2\bar{F}_{\eta[i} i k_{j]} \left[B - \frac{(k^2 E)'}{k^2} \right], \quad (4.130)$$

$$\Phi_i^F(k) = \delta F_{\eta i} - \gamma^{jk} \bar{F}_{\eta j} i k_i (i k_k E + E_k) + \left(\bar{F}_{\eta i} \left[B - \frac{(k^2 E)'}{k^2} \right] \right)'. \quad (4.131)$$

The perturbation in the gauge field can be decomposed along directions transverse and parallel to the spatial wave vector:

$$\delta A_i = (i\delta A^{(\perp,+)}(k, \eta))e_i^1 + (\delta A^{(\perp,-)}(k, \eta))e_i^2 + (i\delta A^{\parallel}(k, \eta))\hat{k}_i, \quad (4.132)$$

where the amplitudes $\delta A^{(\perp,\pm)}(k, \eta)$ are $U(1)$ gauge invariant.²⁰ In $A_0 = E = B = B_i = 0$ gauge the electromagnetic gauge fields $\delta A^{(\perp,\pm)}(k, \eta)$ are simply related to the

²⁰The factors of i accompanying some perturbations is to ensure that the relation $\delta^*(k, \eta) = \delta(-k, \eta)$ holds for all Fourier amplitudes.

gauge-invariant magnetic and electric field perturbations. In particular we may define

$$\delta A^+(k, \eta) \equiv \frac{i(e^1)^i k^j \Phi_{ij}^F}{k^2} \quad \text{and} \quad \delta A^-(k, \eta) \equiv -\frac{(e^2)^i k^j \Phi_{ij}^F}{k^2}, \quad (4.133)$$

where $\gamma^{ij} k_i k_j = k^2$ and where spatial indices are understood to be raised and lowered with the spatial metric, γ_{ij} . The dynamical, gauge-invariant dynamical electromagnetic variables are $\delta A^\pm(k, \eta)$ as defined above and are equal to $\delta A^{(\perp, \pm)}(k, \eta)$ as defined in (4.132) in $A_0 = E = B = B_i = 0$ gauge (a modified Newtonian gauge).

The tensor perturbations, E_{ij} are gauge invariant by construction. We will further decompose the tensor perturbations by constructing the two independent symmetric traceless tensors that are transverse to the wave vector k_i . We again follow [69] and define these tensors as

$$E_{ij} = E^+ \epsilon_{ij}^+ + i E^\times \epsilon_{ij}^\times, \quad (4.134)$$

$$\epsilon_{ij}^+ = \frac{e_i^1 e_j^1 - e_i^2 e_j^2}{\sqrt{2}}, \quad (4.135)$$

$$\epsilon_{ij}^\times = \frac{e_i^1 e_j^2 + e_i^2 e_j^1}{\sqrt{2}}. \quad (4.136)$$

We have chosen this normalization since

$$\gamma^{ik} \gamma^{jl} \epsilon_{ij}^\lambda \epsilon_{kl}^{\lambda'} = \delta^{\lambda\lambda'}. \quad (4.137)$$

Because we have chosen a basis with the property that, under k parity, $e_i^a \rightarrow (-1)^a e_i^a$ these tensors have k parity transformations $\epsilon_{ij}^+ \rightarrow +\epsilon_{ij}^+$ and $\epsilon_{ij}^\times \rightarrow -\epsilon_{ij}^\times$.

We will take the Mukhanov-Sasaki scalar variable (which is conserved outside the horizon in the isotropic limit) to be

$$r \equiv \frac{\alpha'}{\phi'} \chi + \Psi. \quad (4.138)$$

In a gauge with spatially flat slicing, this variable corresponds to minus the curvature perturbation, $-\zeta$, as defined, *e.g.*, in [72].

Some of the variables listed are not dynamical and must be removed from the action using constraint equations. There are a total of five dynamical variables in the theory. In the isotropic limit, these variables correspond to two electromagnetic perturbations, two tensor perturbations and one scalar perturbation. Furthermore, the action separates into uncoupled parts according to the transformation of fields under k parity: a piece including E^+ , δA^+ and r and one including E^\times and δA^- .

4.B Appendix: Quadratic Action and Einstein's Equations

Given a metric $g_{\mu\nu} = \bar{g}_{\mu\nu} + \delta g_{\mu\nu}$, the Einstein-Hilbert action to quadratic order in $\delta g_{\mu\nu}$ can be written as

$$\begin{aligned} \delta^{(2)} S_{EH} = \int d^4x \sqrt{-\bar{g}} \Big\{ & \frac{1}{4\kappa^2} \bar{g}^{\mu\nu} (\bar{\nabla}^\alpha \delta g_{\beta\mu}) (\bar{\nabla}^\beta \delta g_{\alpha\nu}) - \frac{1}{4\kappa^2} \bar{g}^{\mu\nu} (\bar{\nabla}^\alpha \delta g_{\mu\nu}) (\bar{\nabla}^\beta \delta g_{\alpha\beta}) \\ & + \frac{1}{8\kappa^2} \bar{g}^{\mu\nu} \bar{g}^{\rho\sigma} (\bar{\nabla}^\alpha \delta g_{\mu\nu}) (\bar{\nabla}_\alpha \delta g_{\rho\sigma}) - \frac{1}{8\kappa^2} \bar{g}^{\mu\nu} \bar{g}^{\rho\sigma} (\bar{\nabla}^\alpha \delta g_{\mu\rho}) (\bar{\nabla}_\alpha \delta g_{\nu\sigma}) \\ & + \frac{1}{2\kappa^2} \bar{R}^{\mu\nu} \bar{g}^{\rho\sigma} (\delta g_{\mu\rho}) (\delta g_{\nu\sigma}) - \frac{1}{4\kappa^2} \bar{R}^{\mu\nu} \bar{g}^{\rho\sigma} (\delta g_{\mu\nu}) (\delta g_{\rho\sigma}) + \frac{1}{8\kappa^2} \bar{R} (\bar{g}^{\mu\nu} \delta g_{\mu\nu})^2 \\ & - \frac{1}{8\kappa^2} \bar{R} \bar{g}^{\mu\nu} \bar{g}^{\rho\sigma} (\delta g_{\mu\rho} \delta g_{\nu\sigma}) \Big\} \quad (4.139) \end{aligned}$$

after dropping boundary terms. In the above equation, the covariant derivatives ($\bar{\nabla}$) are compatible with the background metric

$$\bar{\nabla}_\alpha \bar{g}_{\mu\nu} = 0. \quad (4.140)$$

We used this form of the action and our parameterization to compute Einstein's equations. In particular, the first-order change in the components Einstein tensor can

be written in the following way (in Newtonian gauge, where $E = B = B_i = 0$):

$$a^2 \delta G_\eta^\eta = -2\Delta\Psi + 6\mathcal{H}\Psi' - \left(\frac{\Psi}{\mathcal{H}}\right)' \sigma^2 + \frac{\sigma^{ij}}{\mathcal{H}} \partial_i \partial_j \Psi - \sigma_j^i \partial_i \Phi^j + (E_j^i)' \sigma_i^j + (6\mathcal{H}^2 - \sigma^2)\Phi - \frac{1}{2}(\sigma^2)' \frac{\Psi}{\mathcal{H}} \quad (4.141)$$

$$a^2 \delta G_i^\eta = -\sigma^2 \frac{\partial_i \Psi}{\mathcal{H}} + \sigma_i^j \partial_j \left(\Phi + \left(\frac{\Psi}{\mathcal{H}}\right)' \right) - 2\partial_i(\Psi' + \mathcal{H}\Phi) - \frac{1}{2}\Delta\gamma_{ij}\Phi^j - 2\sigma_k^j \partial_j E_i^k + \sigma_j^k \partial_i E_k^j + 3\sigma_i^j \partial_j \Psi + \frac{(\sigma_j^i)'}{\mathcal{H}} \partial_j \Psi \quad (4.142)$$

$$\begin{aligned} a^2 \delta G_j^i &= \delta_j^i [2\Psi'' + (2\mathcal{H}^2 + 4\mathcal{H}')\Phi + \Delta(\Phi - \Psi) + 2\mathcal{H}\Phi' + 4\mathcal{H}\Psi'] - \partial^i \partial_j (\Phi - \Psi) \\ &\quad - 2\frac{\sigma_k^{(i}}{\mathcal{H}} \partial_j) \partial^k \Psi + \sigma_j^i \left[-\mathcal{H} \left(\frac{\Psi'}{\mathcal{H}^2}\right)' + \left(\frac{\mathcal{H}'}{\mathcal{H}^2}\right)' \Psi + \frac{\Delta\Psi}{\mathcal{H}} - \Phi' \right] \\ &\quad + \delta_j^i \left[\sigma^2 (\Phi + (\Psi/\mathcal{H})') + \frac{\sigma^{kl}}{\mathcal{H}} \partial_k \partial_l \Psi \right] + (E_j^i)'' - \Delta E_j^i + 2\mathcal{H}(E_j^i)' - \sigma_k^l (E_l^k)' \delta_j^i \\ &\quad + \delta_j^i (\sigma_l^k \partial_k \Phi^l) - 2\mathcal{H}\gamma^{ik} \partial_{(k} \Phi_{j)} - \gamma^{ik} [\partial_{(k} \Phi_{j)}' - 2\sigma_{(k}^l \partial_{|l|} \Phi_{j)}] \\ &\quad + (\sigma_j^i)' \left[2\frac{\mathcal{H}'}{\mathcal{H}^2} \Psi - 2\frac{\Psi'}{\mathcal{H}} - 2(\Phi + \Psi) \right] + \sigma_j^i \left[2\frac{\mathcal{H}'}{\mathcal{H}} \Psi - 4\mathcal{H}\Phi \right] \\ &\quad + \frac{1}{2}\delta_j^i \frac{\sigma^{2'}}{\mathcal{H}} \Psi - \frac{(\sigma_j^i)''}{\mathcal{H}} \Psi + 4\mathcal{H} [\sigma_k^i E_j^k - \sigma_j^k E_k^i] + 2 [\sigma_k^i E_j^k - s_j^k E_k^i]' - 5\sigma_j^i \Psi' \\ &\quad + 2\mathcal{H} [\sigma_k^i \partial_j E^k - \sigma_j^k \partial_k E^i] + [(\sigma_k^i)' \partial_j E^k - (\sigma_j^k)' \partial_k E^i], \end{aligned} \quad (4.143)$$

where $'$ denotes derivatives with respect to conformal time and

$$\mathcal{H} = \frac{a'}{a}, \quad \sigma_{ij} = \frac{1}{2}\gamma'_{ij}. \quad (4.144)$$

In these equations, spatial indices are raised and lowered with γ_{ij} .

Our expressions (4.141) - (4.143) do not match those of [69]. In particular, the expression in [69] does not contain the gauge noninvariant terms on the last line in (4.143).²¹ We are confident that our expression is correct, in part because our Einstein tensor is gauge covariant while theirs is gauge invariant.

²¹Some of our manifestly gauge-invariant terms disagree with those of [69] as well.

4.C Appendix: Diagonalizing a Kinetic Term

Suppose a kinetic term takes the form

$$K = \frac{1}{2}X^{\dagger'}X' + X^{\dagger'}MX + X^{\dagger}M^{\dagger}X' \quad (4.145)$$

where X is a vector of fields and M is a time-dependent matrix. Diagonalizing the kinetic term requires a change of variables

$$X \longrightarrow VY, \quad (4.146)$$

where V is a time-dependent unitary matrix, such that

$$K \longrightarrow \frac{1}{2}Y^{\dagger'}Y' + \text{total derivative} + Y^{\dagger}QY \quad (4.147)$$

where Q is some Hermitian matrix. We can calculate directly that

$$K = \frac{1}{2}Y^{\dagger'}Y' + Y^{\dagger}\left(V^{\dagger'}V + V^{\dagger}(M^{\dagger} - M)V\right)Y' + \text{total derivative} + Y^{\dagger}QY. \quad (4.148)$$

The kinetic term is diagonalized by a unitary matrix V that satisfies

$$V^{\dagger'}V = -V^{\dagger}(M^{\dagger} - M)V \quad \text{or equivalently} \quad VV^{\dagger'} = M - M^{\dagger}. \quad (4.149)$$

If M were a time-independent matrix, then the kinetic term would be diagonalized by a constant unitary matrix V such that

$$V^{\dagger}(M - M^{\dagger})V = D \quad (4.150)$$

where D is a constant diagonal matrix.

4.D Appendix: Estimates of Integrals

In order to get a quantitative estimate of the effect of the anisotropic background on power spectra, we must estimate the integrals in (4.75) - (4.77). We may take $\hat{\rho}_A$, Σ , and the slow-roll parameters to be nearly constant. Then the relevant integrals are

$$p^{-2} \int^{\eta} \sin(2\psi_{\bar{p}}(\eta') - 2\psi_{\bar{p}}(\eta)) \alpha'(\eta')^2 \tilde{I}(p\eta', p\eta) d\eta',$$

$$p^{-2} \int^{\eta} \cos(2\psi_{\bar{p}}(\eta') - 2\psi_{\bar{p}}(\eta)) \alpha'(\eta')^2 \tilde{I}(p\eta', p\eta) d\eta' \quad (4.151)$$

$$\int^{\eta} (e^{2n\beta(\eta')} - e^{2n\beta(\eta_0)}) \tilde{I}(p\eta', p\eta) d\eta' \quad \text{and} \quad p^{-2} \int^{\eta} \alpha'(\eta')^2 \tilde{I}(p\eta', p\eta) d\eta' \quad (4.152)$$

where $\tilde{I}(x, y)$ was defined in (4.70) as

$$\tilde{I}(x, y) = \left(\frac{1}{2x^2y^2} - \frac{1}{2x^2} + \frac{2}{xy} - \frac{1}{2y^2} + \frac{1}{2} \right) \sin(2x - 2y)$$

$$+ \left(\frac{1}{x^2y} - \frac{1}{xy^2} + \frac{1}{x} - \frac{1}{y} \right) \cos(2x - 2y). \quad (4.153)$$

During slow-roll inflation,

$$\alpha'(\eta) = e^{\alpha(\eta)} H(\eta) \approx -\frac{1}{\eta} \quad (4.154)$$

$$\psi_{\bar{p}}(\eta') - \psi_{\bar{p}}(\eta) \approx (\alpha(\eta') - \alpha(\eta)) \frac{k_2 e^{-\beta_0}}{k_0} \sqrt{\hat{\rho}_A} \quad (4.155)$$

$$(e^{2n\beta(\eta')} - e^{2n\beta(\eta_0)}) \approx 2n\Sigma (\alpha(\eta') - \alpha(\eta_0)). \quad (4.156)$$

Let us define a new variable z by²²

$$-p\eta = e^{-z}. \quad (4.157)$$

²²This is just a convenient dimensionless variable and is not equal to $a\phi'/\alpha'$ as in (4.37).

From (4.154) it's clear that

$$e^z \approx \frac{aH}{p} \quad \text{and so} \quad z \approx \log(H/p) + \alpha. \quad (4.158)$$

We may thus rewrite the integrals (4.151) and (4.152) in terms of the variable z :

$$\begin{aligned} I_s &\equiv p^{-1} \int^{z_*} \sin \left(2 \frac{\psi'_{\vec{p}}}{\alpha'} (z - z_*) \right) \tilde{I}(-e^{-z}, -e^{-z_*}) e^z dz, \\ I_c &\equiv p^{-1} \int^{z_*} \cos \left(2 \frac{\psi'_{\vec{p}}}{\alpha'} (z - z_*) \right) \tilde{I}(-e^{-z}, -e^{-z_*}) e^z dz \end{aligned} \quad (4.159)$$

$$I_1 \equiv p^{-1} \int^{z_*} (z - z_0) \tilde{I}(-e^{-z}, -e^{-z_*}) e^{-z} dz, \quad I_2 \equiv p^{-1} \int^{z_*} \tilde{I}(-e^{-z}, -e^{-z_*}) e^z dz \quad (4.160)$$

where z_* is the value of z at the end of inflation and

$$\frac{\psi'_{\vec{p}}}{\alpha'} \equiv \frac{p_2 e^{-\beta_0}}{p} \sqrt{\hat{\rho}_A}. \quad (4.161)$$

The function

$$\tilde{I}(-e^{-z}, -e^{-z_*}) e^z \quad (4.162)$$

oscillates rapidly with growing amplitude for $z < 0$. See Fig. 4.2. For $z > 0$ and values of z_* on the order of tens, the function is well approximated by a constant

$$\tilde{I}(-e^{-z}, -e^{-z_*}) e^z \approx -\frac{2}{3} e^{2z_*} \quad 0 < z < z_*. \quad (4.163)$$

The constant can be found by expanding the function about $z_* = \infty$ and then about $z = \infty$.

The contribution of terms that go like I_1 will be subdominant compared to contributions from terms proportional to the other integrals²³, so we will not bother to

²³The contribution from I_1 can be important if inflation lasts a very long time — on the order of 10^3 e -folds.

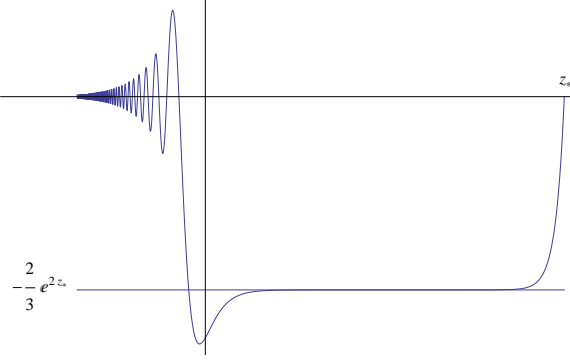


Figure 4.2: The function $e^z \tilde{I}(-e^z, -e^{-z_*})$ on a linear scale. The axes cross at the point $\{0, 0\}$. For $0 < z < z_*$ the function is well approximated by $-\frac{2}{3}e^{2z_*}$. The frequency of oscillation for $z < 0$ does not vary much as z_* increases—only the amplitude changes. The plot above was generated using $z_* = 15$.

calculate I_1 . Since the dominant contribution to the other integrals will occur when $z > 0$ (which corresponds to after horizon crossing) we may approximate the integrals by

$$I_s \approx -\frac{2}{3}e^{2z_*}p^{-1} \int_0^{z_*} \sin\left(2\frac{\psi'_{\vec{p}}}{\alpha'}(z - z_*)\right) dz = -\frac{2}{3}e^{2z_*}p^{-1} \left[\frac{2\psi'_{\vec{p}}}{\alpha'}\right]^{-1} \left(\cos\left[\frac{2\psi'_{\vec{p}}}{\alpha'}z_*\right] - 1\right), \quad (4.164)$$

$$I_c \approx -\frac{2}{3}e^{2z_*}p^{-1} \int_0^{z_*} \cos\left(2\frac{\psi'_{\vec{p}}}{\alpha'}(z - z_*)\right) dz = -\frac{2}{3}e^{2z_*}p^{-1} \left[\frac{2\psi'_{\vec{p}}}{\alpha'}\right]^{-1} \left(-\sin\left[\frac{2\psi'_{\vec{p}}}{\alpha'}z_*\right]\right) \quad (4.165)$$

$$I_2 = p^{-1} \int^{z_*} \tilde{I}(-e^{-z}, -e^{-z_*}) e^z dz \approx -\frac{2}{3}e^{2z_*}p^{-1}z_*. \quad (4.166)$$

Modes of astrophysical interest crossed the horizon about 60 e -folds—plus or minus a few—before the end of inflation. Such modes of astrophysical interest therefore correspond to $z_* \approx 60$.

Bibliography

- [1] S. M. Carroll, T. R. Dulaney, M. I. Gresham, and H. Tam, Phys. Rev. **D79**, 065011 (2009), arXiv:0812.1049.
- [2] S. M. Carroll, T. R. Dulaney, M. I. Gresham, and H. Tam, Phys. Rev. **D79**, 065012 (2009), arXiv:0812.1050.
- [3] T. R. Dulaney and M. I. Gresham, Phys. Rev. **D81**, 103532 (2010), arXiv:1001.2301.
- [4] D. Baumann and H. V. Peiris, Adv. Sci. Lett. **2**, 105 (2009), arXiv:0810.3022.
- [5] A. H. Guth, Phys. Rev. **D23**, 347 (1981).
- [6] L. Ackerman, S. M. Carroll, and M. B. Wise, Phys. Rev. **D75**, 083502 (2007), arXiv:astro-ph/0701357.
- [7] M.-a. Watanabe, S. Kanno, and J. Soda, Phys. Rev. Lett. **102**, 191302 (2009), arXiv:0902.2833.
- [8] V. F. Mukhanov, *Physical Foundations of Cosmology* (Cambridge University Press, Cambridge, UK, 2005).
- [9] S. Weinberg, *Cosmology* (Oxford University Press, 2008).
- [10] R. W. Wald, Phys. Rev. **D28**, 2118 (1983).
- [11] L. Bianchi, Soc. Ital. Sci. Mem. di Mat. **11** (1898).

- [12] T. Jacobson and D. Mattingly, Phys. Rev. **D64**, 024028 (2001), arXiv:gr-qc/0007031.
- [13] T. Jacobson, PoS **QG-PH**, 020 (2007), arXiv:0801.1547.
- [14] B. Himmetoglu, C. R. Contaldi, and M. Peloso, Phys. Rev. **D79**, 063517 (2009), arXiv:0812.1231.
- [15] S. Weinberg, Phys. Rev. **D72**, 043514 (2005), arXiv:hep-th/0506236.
- [16] S. Weinberg, Phys. Rev. **D67**, 123504 (2003), arXiv:astro-ph/0302326.
- [17] S. Weinberg, Phys. Rev. **D69**, 023503 (2004), arXiv:astro-ph/0306304.
- [18] C. M. Will and J. Nordtvedt, Kenneth, Astrophys. J. **177**, 757 (1972).
- [19] M. Gasperini, Class. Quant. Grav. **4**, 485 (1987).
- [20] V. A. Kostelecky and S. Samuel, Phys. Rev. **D40**, 1886 (1989).
- [21] D. Colladay and V. A. Kostelecky, Phys. Rev. **D58**, 116002 (1998), arXiv:hep-ph/9809521.
- [22] C. Eling and T. Jacobson, Phys. Rev. **D69**, 064005 (2004), arXiv:gr-qc/0310044.
- [23] S. M. Carroll and E. A. Lim, Phys. Rev. **D70**, 123525 (2004), arXiv:hep-th/0407149.
- [24] T. Jacobson and D. Mattingly, Phys. Rev. **D70**, 024003 (2004), arXiv:gr-qc/0402005.
- [25] E. A. Lim, Phys. Rev. **D71**, 063504 (2005), arXiv:astro-ph/0407437.
- [26] C. Eling, T. Jacobson, and D. Mattingly, (2004), arXiv:gr-qc/0410001.

- [27] T. R. Dulaney, M. I. Gresham, and M. B. Wise, Phys. Rev. **D77**, 083510 (2008), arXiv:0801.2950.
- [28] J. B. Jimenez and A. L. Maroto, JCAP **0902**, 025 (2009), arXiv:0811.0784.
- [29] V. A. Kostelecky and R. Lehnert, Phys. Rev. **D63**, 065008 (2001), arXiv:hep-th/0012060.
- [30] J. W. Elliott, G. D. Moore, and H. Stoica, JHEP **08**, 066 (2005), arXiv:hep-ph/0505211.
- [31] D. Mattingly, Living Rev. Rel. **8**, 5 (2005), arXiv:gr-qc/0502097.
- [32] C. M. Will, Living Rev. Rel. **9**, 3 (2005), arXiv:gr-qc/0510072.
- [33] N. Arkani-Hamed, H.-C. Cheng, M. A. Luty, and S. Mukohyama, JHEP **05**, 074 (2004), arXiv:hep-th/0312099.
- [34] N. Arkani-Hamed, H.-C. Cheng, M. A. Luty, S. Mukohyama, and T. Wiseman, JHEP **01**, 036 (2007), arXiv:hep-ph/0507120.
- [35] H.-C. Cheng, M. A. Luty, S. Mukohyama, and J. Thaler, JHEP **05**, 076 (2006), arXiv:hep-th/0603010.
- [36] S. M. Carroll, M. Hoffman, and M. Trodden, Phys. Rev. **D68**, 023509 (2003), arXiv:astro-ph/0301273.
- [37] S. L. Dubovsky and S. M. Sibiryakov, Phys. Lett. **B638**, 509 (2006), arXiv:hep-th/0603158.
- [38] C. Eling, B. Z. Foster, T. Jacobson, and A. C. Wall, Phys. Rev. **D75**, 101502 (2007), arXiv:hep-th/0702124.
- [39] V. A. Kostelecky, (2001), arXiv:hep-ph/0104227.

- [40] A. Adams, N. Arkani-Hamed, S. Dubovsky, A. Nicolis, and R. Rattazzi, JHEP **10**, 014 (2006), arXiv:hep-th/0602178.
- [41] R. Bluhm, N. L. Gagne, R. Potting, and A. Vrublevskis, Phys. Rev. **D77**, 125007 (2008), arXiv:0802.4071.
- [42] J. L. Chkareuli, C. D. Froggatt, and H. B. Nielsen, Nucl. Phys. **B821**, 65 (2009), arXiv:hep-th/0610186.
- [43] B. M. Gripaios, JHEP **10**, 069 (2004), arXiv:hep-th/0408127.
- [44] M. A. Clayton, (2001), arXiv:gr-qc/0104103.
- [45] M. Henneaux and C. Teitelboim, *Quantization of Gauge Systems* (Princeton University, Princeton, N.J., 1992).
- [46] Y. Nambu, Progr. Theoret. Phys. Suppl. Extra No. , 190 (1968).
- [47] R. Bluhm, S.-H. Fung, and V. A. Kostelecky, Phys. Rev. **D77**, 065020 (2008), arXiv:0712.4119.
- [48] B. Himmetoglu, C. R. Contaldi, and M. Peloso, Phys. Rev. Lett. **102**, 111301 (2009), arXiv:0809.2779.
- [49] M. D. Seifert, Phys. Rev. **D76**, 064002 (2007), arXiv:gr-qc/0703060.
- [50] T. R. Dulaney and M. I. Gresham, (2008), arXiv:0805.1078.
- [51] T. S. Koivisto and D. F. Mota, JCAP **0808**, 021 (2008), arXiv:0805.4229.
- [52] S. Kanno and J. Soda, Phys. Rev. **D74**, 063505 (2006), arXiv:hep-th/0604192.
- [53] B. Li, D. Fonseca Mota, and J. D. Barrow, Phys. Rev. **D77**, 024032 (2008), arXiv:0709.4581.
- [54] S. M. Carroll and H. Tam, Phys. Rev. **D78**, 044047 (2008), arXiv:0802.0521.

- [55] L. Parker, Phys. Rev. Lett. **21**, 562 (1968).
- [56] M. S. Turner and L. M. Widrow, Phys. Rev. **D37**, 2743 (1988).
- [57] B. Ratra, Astrophys. J. **391**, L1 (1992).
- [58] V. Demozzi, V. Mukhanov, and H. Rubinstein, JCAP **0908**, 025 (2009), arXiv:0907.1030.
- [59] K. Bamba, N. Ohta, and S. Tsujikawa, Phys. Rev. **D78**, 043524 (2008), arXiv:0805.3862.
- [60] S. Kanno, J. Soda, and M.-a. Watanabe, JCAP **0912**, 009 (2009), arXiv:0908.3509.
- [61] D. Grasso and H. R. Rubinstein, Phys. Rept. **348**, 163 (2001), arXiv:astro-ph/0009061.
- [62] K. Dimopoulos, M. Karciauskas, and J. M. Wagstaff, Phys. Lett. **B683**, 298 (2010), arXiv:0909.0475.
- [63] S. Yokoyama and J. Soda, JCAP **0808**, 005 (2008), arXiv:0805.4265.
- [64] A. Golovnev and V. Vanchurin, Phys. Rev. **D79**, 103524 (2009), arXiv:0903.2977.
- [65] K. Dimopoulos, M. Karciauskas, D. H. Lyth, and Y. Rodriguez, JCAP **0905**, 013 (2009), arXiv:0809.1055.
- [66] C. A. Valenzuela-Toledo, Y. Rodriguez, and D. H. Lyth, Phys. Rev. **D80**, 103519 (2009), arXiv:0909.4064.
- [67] C. A. Valenzuela-Toledo and Y. Rodriguez, Phys. Lett. **B685**, 120 (2010), arXiv:0910.4208.
- [68] B. Himmetoglu, JCAP **1003**, 023 (2010), arXiv:0910.3235.

- [69] T. S. Pereira, C. Pitrou, and J.-P. Uzan, JCAP **0709**, 006 (2007), arXiv:0707.0736.
- [70] V. F. Mukhanov, H. A. Feldman, and R. H. Brandenberger, Phys. Rept. **215**, 203 (1992).
- [71] P. Adshead, R. Easther, and E. A. Lim, Phys. Rev. **D79**, 063504 (2009), arXiv:0809.4008.
- [72] S. Dodelson, *Modern Cosmology* (Academic Pr., Amsterdam, Netherlands, 2003).
- [73] N. E. Groeneboom, L. Ackerman, I. K. Wehus, and H. K. Eriksen, (2009), arXiv:0911.0150.
- [74] D. Hanson and A. Lewis, Phys. Rev. **D80**, 063004 (2009), arXiv:0908.0963.
- [75] A. R. Pullen and M. Kamionkowski, Phys. Rev. **D76**, 103529 (2007), arXiv:0709.1144.